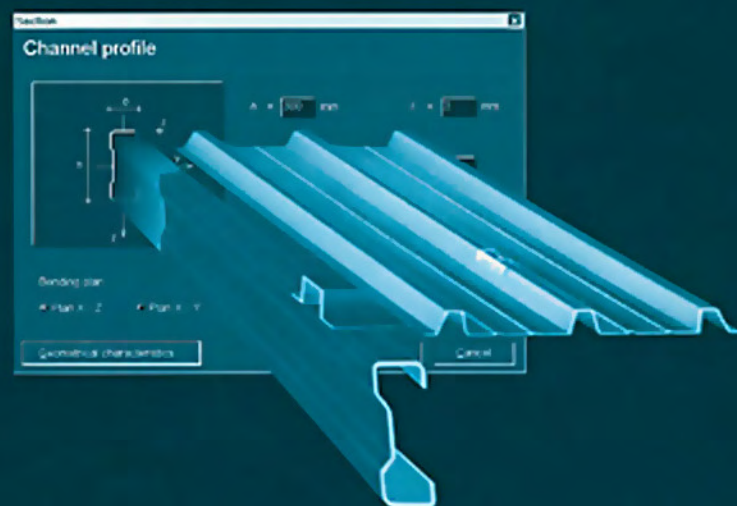


DESIGN OF
METALLIC COLD-FORMED
THIN-WALLED MEMBERS



A. GHERSI, R. LANDOLFO AND F. M. MAZZOLANI

FREE
design program
on CD-ROM

Also available as a printed book
see title verso for ISBN details

Design of Metallic Cold-formed Thin-walled Members

Design of Metallic Cold-formed Thin-walled Members

A.Gheresi, R.Landolfo and F.M.Mazzolani



London and New York

First published 2002 by Spon Press 11 New Fetter Lane, London EC4P 4EE

Simultaneously published in the USA and Canada by Spon Press 29 West 35th Street, New York,
NY 10001

Spon Press is an imprint of the Taylor & Francis Group

This edition published in the Taylor & Francis e-Library, 2005.

“To purchase your own copy of this or any of Taylor & Francis or Routledge’s collection of
thousands of eBooks please go to <http://www.ebookstore.tandf.co.uk/>.”

© 2002 A.Gherzi, R.Landolfo and F.M.Mazzolani

All rights reserved. No part of this book may be reprinted or reproduced or utilized in any form or
by any electronic, mechanical, or other means, now known or hereafter invented, including
photocopying and recording, or in any information storage or retrieval system, without permission
in writing from the publishers.

The publisher makes no representation, express or implied, with regard to the accuracy of the
information contained in this book and cannot accept any legal responsibility or liability for any
errors or omissions that may be made.

British Library Cataloguing in Publication Data A catalogue record for this book is available
from the British Library

Library of Congress Cataloging in Publication Data Gherzi, A. (Aurelio) Design of metallic cold-
formed thin-walled members/A.Gherzi, R.Landolfo, and F.M.Mazzolani. p. cm.

Includes bibliographical references and index.

1. Building, Iron and steel. 2. Aluminium construction, 3. Thin-walled structures. 4. Metals—Cold
working. I. Landolfo, R. (Raffaele) II. Mazzolani, Federico M. III. Title. TA684 .G49 2001
624.1'821—dc21
2001049083

ISBN 0-203-16451-2 Master e-book ISBN

ISBN 0-203-27848-8 (Adobe eReader Format)

ISBN 0-415-24437-4 (Print Edition)

Contents

<i>List of tables</i>	v
<i>List of symbols</i>	vi
<i>Preface</i>	xxi
1 General aspects	1
2 Codified design bases	24
3 Eurocode 3	44
4 Eurocode 9	63
5 AISI Specification	82
6 Comparison among codes	103
7 The ColdForm computer program	132
<i>References</i>	163
<i>Index</i>	167

List of tables

2.1	Different formulations for the plasticity factor η	32
2.2	Numerical coefficients for the buckling	42
3.1	Nominal values of basic yield strength $f_y b$ and ultimate tensile strength f_u (CEN, ENV 1993–1–3)	45
3.2	Reduction factor for doubly supported compression elements (CEN, ENV 1993–1–3, 1996)	45
3.3	Reduction factor for projecting compression elements (CEN, ENV 1993–1–3, 1996)	51
3.4	Imperfection factor α	61
4.1	Element classification	67
4.2	Values of β_1 , β_2 and β_3	68
4.3	(CEN, ENV 1999–1–1, 1998)	69
4.4	Parameters ω_1 , ω_2 and	71
4.5	Buckling factor for doubly supported compression elements (CEN, prENV 1999–1–3, 1999)	77
4.6	Shear buckling strength for webs with transverse stiffeners at supports (CEN, ENV 1999–1–1, 1999)	77
4.7	Values of the imperfection factors α and	80
5.1	(AISI, 1996)	85
7.1	Characteristics of materials defined inside the program	129

List of symbols

<i>Symbol</i>	<i>Cold form</i>	<i>Definition</i>	<i>Code</i>	<i>Units</i>
a		Buckling curve	EC3	
a_0		Buckling curve	EC3	
A	A	Area of the cross-section	EC3	L ²
			EC9	
A		Ratio of the effective over gross area in uniform compressed section		–
$A50$		Minimum elongation	EC9	%
A_e	Ae	Effective area of the cross-section	AISI	L ²
A_{eff}	Aeff	Effective area of the cross-section	EC3	L ²
$A_e l$		Area of the elastic zone	EC9	L ²
			EC3	
A_g	Ag	Gross area of the cross-section	EC3	L ²
			EC9	
A_n	An	Net area of the cross-section	EC3	L ²
			EC9	
			AISI	
$A_{pl,c}$		Area of the plastic compression zone	EC3	L ²
$A_{pl,t}$		Area of the plastic tension zone	EC3	L ²
A_s		Effective cross-sectional area of the stiffener	EC3	L ²
$A_{s, red}$		Reduced effective area of the stiffener	EC3	L ²
			EC9	
b		Buckling curve	EC3	
b	b	Effective width	AISI	L
b		Width	EC3	L
b		Width of flange	EC9	L
<i>Symbol</i>	<i>Cold form</i>	<i>Definition</i>	<i>Code</i>	<i>Units</i>
b_0		Width of flange contributing to shear lag	EC3	L

b_0		Flat width with one intermediate stiffener	AISI	L
b_0		Net width		L
b_1	b1	Effective width portion	AISI	L
b_1		Notional flat width portion	EC3	L
b_1		Width portion	EC9	L
b_2	b2	Effective width portion	AISI	L
b_2		Notional flat width portion	EC3	L
b_2		Width portion	EC9	L
b_e		Effective design width of element	AISI	L
b_{e1}	be1	Effective width portion	EC3	L
b_{e2}	be2	Effective width portion	EC3	L
b_{eff}	beff	Effective width	EC3	L
b_p	bP	Notional flat width	EC3	L
			EC9	
$b_{p,1}$		Notional flat width portion	EC9	L
$b_{p,2}$		Notional flat width portion	EC9	L
$b_{p,ad}$		Notional flat width of the adjacent element	EC3	L
$b_{p,c}$		Effective width compression portion	EC3	L
b_s		Notional flat width portion	EC9	L
B_c		Term for determining the tensile yield point of corners	AISI	–
c		Buckling curve	EC3	
C		Ratio of corner area to total cross-sectional area	AISI	–
C_2		Coefficient	AISI	–
C_m		End moment coefficient in interaction formula	AISI	–
C_{mx}	Cmy	End moment coefficient in interaction formula	AISI	–
C_{my}	Cmx	End moment coefficient in interaction formula	AISI	–
C_θ		Rotational spring stiffness	EC3	F
$C_{\theta,1}$		Rotational spring stiffness	EC3	F
			EC9	
$C_{\theta,2}$		Rotational spring stiffness	EC3	F
			EC9	
<i>Symbol</i>	<i>Cold form</i>	<i>Definition</i>	<i>Code</i>	<i>Units</i>

d		Depth of a web element	EC9	L
d_s		Reduced effective width of stiffener	AISI	L
d'_s		Actual effective width of stiffener	AISI	L
D		Overall depth of lip	AISI	L
e_N		Shift of the centroidal axis	EC3	L
			EC9	
$e_{N,y}$	eny	Shift of the y centroidal axis	EC3	L
			EC9	
$e_{N,z}$	enz	Shift of the z centroidal axis	EC3	L
			EC9	
E		Initial elastic modulus		FL ⁻²
E		Modulus of elasticity	EC3	FL ⁻²
			EC9	
			AISI	
E_s		Secant elastic modulus		FL ⁻²
E_t		Tangent elastic modulus		FL ⁻²
f		Stress in the element	AISI	FL ⁻²
$f_{0.2}$	f0	0.2% proof stress	EC9	FL ⁻²
f_{0w}		Reduced value of the material strength	EC9	FL ⁻²
f_1		Stress along edges	EC3	FL ⁻²
f_2		Stress along edges	EC3	FL ⁻²
f_{bv}	fbv	Shear buckling strength	EC3	FL ⁻²
			EC9	
f_t		Ultimate tensile strength		FL ⁻²
f_y		Maximum strength (f_{ya} if the section is fully effective; f_{yb} otherwise)	EC3	FL ⁻²
f_y		Yield stress	EC3	FL ⁻²
f_{ya}	fya	Average yield strength	EC3	FL ⁻²
f_{yb}	fyb	Basic yield strength	EC3	FL ⁻²
			EC9	
f_{e0}		Conventional elastic limit		FL ⁻²
	F	Concentric force		F
F_e	Fe	Elastic buckling stress	AISI	FL ⁻²

F_n	F _n	Nominal buckling stress	AISI	FL ⁻²
F_u		Minimum ultimate tensile strength	AISI	FL ⁻²
F_u		Virgin ultimate strength	AISI	F ⁻²
F_y	F _y	Design yield stress	AISI	FL ⁻²
F_y		Minimum basic yield strength	AISI	FL ⁻²
<i>Symbol</i>	<i>Cold form</i>	<i>Definition</i>	<i>Code</i>	<i>Units</i>
F_y		Virgin yield strength	AISI	FL ⁻²
F_{ya}	F _{ya}	Full-section tensile yield strength	AISI	FL ⁻²
F_{yc}		Average tensile yield strength of corners	AISI	FL ⁻²
F_{yf}		Average tensile yield strength of flat	AISI	FL ⁻²
g		Stress gradient coefficient	EC9	–
G_{el}		Centroid of the elastic zone	EC3	
G_{ep}		Null strain point	EC3	
$G_{pl,c}$		Centroid of the plastic compression zone	EC3	
$G_{pl,t}$		Centroid of the plastic tension zone	EC3	
h	h	Depth of the flat portion of the web measured along the plane of the web	AISI	L
h		Height of the cross-section		L
h		Height of web		L
h_w	hw	Web height between the midlines of the flanges	EC3	L
			EC9	
i	I	Radius of gyration of the gross section	EC3	L
			EC9	
I		Moment of inertia of the gross section		L ⁴
I_a		Adequate moment of inertia of the stiffener so that each component element will behave as a stiffened element	AISI	L ⁴
I_{eff}		Moment of inertia of the effective section		L ⁴
I_{el}		Second moment of area of the elastic zone	EC3	L ⁴
I_s		Effective second moment of area of the stiffener	EC3	L ⁴
			EC9	
I_s		Moment of inertia of full section of the stiffener about its own centroidal axis parallel to the element to be stiffened	AISI	L ⁴
I_x		Moments of inertia of the full unreduced section about the x axis	AISI	L ⁴

<i>Symbol</i>	<i>Cold form</i>	<i>Definition</i>	<i>Code</i>	<i>Units</i>
I_x	Ix	Moment of inertia of the gross section about the x axis	EC3 EC9	L^4
I_y		Moment of inertia of the full unreduced section about the y axis	AISI	L^4
I_y	Iy	Moment of inertia of the gross section about the y axis	EC3 EC9	L^4
k		Numerical coefficient function of the ratio r/t		–
k		Numerical coefficient that depends on the type of forming	EC3	–
k	k	Plate buckling coefficient	AISI	–
k_a		Plate buckling coefficient	AISI	–
k_L		Local buckling coefficient		–
$K_{L,av}$		Weighted average factor		–
$k_{L,f}$		Buckling coefficient compressed flange		–
$K_{L,min}$		Stress reduction factor		–
$k_{L,w}$		Buckling coefficient compressed web		–
k_u		Plate buckling coefficient	AISI	–
k_v	kv	Shear buckling coefficient	AISI	–
k_y	kappay	Factor	EC3 EC9	–
k_z	kappaz	Factor	EC3 EC9	–
k_σ	k sigma	Local buckling coefficient	EC3 EC9	–
K		Effective length factor	AISI	–
K		Spring stiffness	EC3 EC9	FL^{-2}
K_x		Effective length factor for buckling about the x axis	AISI	–
K_y		Effective length factor for buckling about the y axis	AISI	–
l	l	Length		L
L		Length		L
L		Buckling length for flexural buckling	EC3	L

			EC9	
L		Unbraced length of member	AISI	L
<i>Symbol</i>	<i>Cold form</i>	<i>Definition</i>	<i>Code</i>	<i>Units</i>
L_x		Actual unbraced lengths for bending about the x axis	AISI	L
L_y		Actual unbraced lengths for bending about the y axis	AISI	L
m		Term for determining the tensile yield point of corners	AISI	–
M	M	Bending moment		FL
M	M	Required flexural strength	AISI	FL
$M_{0,2}$		Conventional elastic moment		FL
$M_{b,red}$		Reduced design moment resistance with respect to lateral torsional buckling		FL
M_{cr}		Elastic lateral buckling moment of the gross section		FL
$M_{c,Rd}$	Mc,Rd	Design moment resistance of a cross-section	EC3	FL
			EC9	
$M_{cy,Rd}$	Mcy,Rd	Design bending moment about y	EC3	FL
$M_{cz,Rd}$	Mc z ,Rd	Design bending moment about z	EC3	FL
M_d		Reduced design moment		FL
$M_{d,1}$		Reduced design moment according to reduced thickness approach		FL
$M_{d,2}$		Reduced design moment according to effective width approach		FL
$M_{d,3}$		Reduced design moment according to reduced stress approach with $K_{L,min}$		FL
$M_{d,4}$		Reduced design moment according to reduced stress approach with $K_{L,av}$		FL
	Mmax	Design bending moment strength		FL
	Mmax,y	Design bending moment strength about y axis		FL
	Mmax,yt	Design bending moment strength about y axis determined using the gross, unreduced cross-section properties		FL
	Mmax,z	Design bending moment strength about z axis		FL
				FL
	Mmax,z t	Design bending moment strength about z axis determined using the gross, unreduced cross-section properties		FL
<i>Symbol</i>	<i>Cold</i>	<i>Definition</i>	<i>Code</i>	<i>Units</i>

<i>form</i>				
<i>Symbol</i>	<i>Cold form</i>	<i>Definition</i>	<i>Code</i>	<i>Units</i>
M_n	Mn	Nominal flexural strength	AISI	FL
M_{nx}		Nominal flexural strengths about the x centroidal axes	AISI	FL
M_{nxt}		Nominal flexural strengths about the x centroidal axes determined using the gross, unreduced cross-section properties	AISI	FL
M_{ny}		Nominal flexural strengths about the y centroidal axes	AISI	FL
M_{nyt}		Nominal flexural strengths about the y centroidal axes determined using the gross, unreduced cross-section properties	AISI	FL
M_{sd}	MSd	Bending moment	EC3 EC9	FL
M_x	My	Required flexural strength with respect to the x centroidal axes	AISI	FL
M_x	My	Required flexural strength with respect to the x centroidal axes of the effective section determined for the required compressive axial strength alone	AISI	FL
M_y	Mz	Required flexural strength with respect to y centroidal axes	AISI	FL
M_y	Mz	Required flexural strengths with respect to the y centroidal axes of the effective section determined for the required compressive axial strength alone	AISI	FL
M_y		Yielding moment of the gross section		FL
$M_{y,red}$		Reduced yielding moment		FL
$M_{y,sd}$	My,Sd	Bending moments about the y - y axis	EC3 EC9	FL
$M_{z,sd}$	Mz,Sd	Bending moments about the z axis	EC3 EC9	FL
n		Hardening parameter of the material		–
n		Number of bends in the cross-section with an internal radius $r \leq t$	EC3	–
N	N	Axial force		F
$N_{b,Rd}$	Nb,Rd	Design buckling resistance for axial compression	EC3 EC9	F
$N_{c,Rd}$	Nc,Rd	Design compression resistance of a cross-section	EC3 EC9	F
N_{sd}	NSd	Axial force	EC3 EC9	F

$N_{t,Rd}$	Nt,Rd	Design tension resistance of a cross-section	EC3 EC9	F
N_u		Ultimate axial strength		F
N_y		Yielding axial force		F
N_y		Yielding axial force for the gross section prevented from buckling		F
$N_{y,red}$		Reduced axial force which takes into account yielding local and global buckling		F
p		Numerical coefficient		
	P	Weight per unit length		FL ⁻¹
P	P	Required compressive axial strength	AISI	F
	Pmax	Design compressive axial strength		F
P_n	Pn	Nominal axial strength	AISI	F
P_{Ex}		Elastic buckling strength about the x axes	AISI	F
P_{Ey}		Elastic buckling strength about the y axes	AISI	F
P_{no}		Nominal axial strength of member	AISI	F
q		Numerical coefficient		–
r	r	Internal radius	EC3 EC9	L
r		Radius		L
r	i	Radius of gyration of the full unreduced section	AISI	L
R	r	Inside bend radius	AISI	L
R		Required strength	AISI	
R_n		Nominal strength	AISI	
S_e	Se	Effective section modulus	AISI	L ³
s_w	sw	Slant height of the largest plane element in the web	EC3 EC9	L
S		Material constant	AISI	–
<i>Symbol</i>	<i>Cold form</i>	<i>Definition</i>	<i>Code</i>	<i>Units</i>
S_{fxt}		Elastic section modulus of the full unreduced section for the extreme tension fibre about the x axis	AISI	L ³
S_{fyt}		Elastic section modulus of the full unreduced section for the extreme tension fibre about the y axis	AISI	L ³

t		Sheet thickness	AISI	L
t		Thickness	EC3	L
			EC9	
			AISI	
t		Web thickness	AISI	L
t_{eff}	teff	Effective thickness	EC9	L
$t_{eff,1}$		Effective thickness portion	EC9	L
$t_{eff,2}$		Effective thickness portion	EC9	L
t_f		Flange thickness		L
t_r		Reduced thickness		L
t_{red}		Reduced thickness	EC3	L
$t\omega$		Web thickness		L
T	T	Required tensile axial strength	AISI	F
	Tmax	Design tensile strength		F
T_n	Tn	Nominal tensile strength	AISI	F
u		Unit load	EC3	FL ⁻¹
			EC9	
V	V	Required shear strength	AISI	F
V	V	Shear	EC3	F
			EC9	
$V_{b,Rd}$	Vb,Rd	Shear buckling resistance	EC3	F
			EC9	
	Vmax	Design shear strength		F
V_n	Vn	Nominal shear strength	AISI	F
$V_{pl,Rd}$	Vpl,Rd	Plastic shear resistance	EC3	F
			EC9	
V_{Sd}		Shear force	EC3	F
			EC9	
$V_{o,Rd}$	Vw,Rd	Design shear resistance	EC3	F
			EC9	
w	w	Flat width	AISI	L
W		Section modulus		L ³

<i>Symbol</i>	<i>Cold form</i>	<i>Definition</i>	<i>Code</i>	<i>Units</i>
W_{eff}	Weff	Effective section modulus	EC3 EC9	L^3
$W_{eff,b}$		Section modulus of the effective cross-section according to effective width approach		L^3
$W_{eff,t}$		Section modulus of the effective cross-section according to reduced thickness approach		L^3
$W_{eff,y}$		Effective section modulus for the maximum compressive stress in a cross-section that is subject only to bending moment about the z axes	EC3 EC9	L^3
$W_{eff,z}$		Effective section modulus for the maximum compressive stress in a cross-section that is subject only to bending moment about the y axes	EC3 EC9	L^3
W_{el}		Gross elastic section modulus	EC3	L^3
W_g		Section modulus of gross section		L^3
$W_{pp,eff}$		Effective partially plastic section modulus	EC3 EC9	L^3
W_y	Wy	Section modulus about the y axis	EC3 EC9	L^3
W_z	Wz	Section modulus about the z axis	EC3 EC9	L^3
x	x	Axes	EC3 EC9	
y	y	Axes	EC3 EC9	
y		Coordinate		L
y_1		Distances from the neutral axis to most severely stressed fibres in a beam		L
y_2		Distances from the neutral axis to the compression flange element in a beam		L
<i>Symbol</i>	<i>Cold form</i>	<i>Definition</i>	<i>Code</i>	<i>Units</i>
z	z	Axes	EC3 EC9	
z		Coordinate	EC3	L

α		Coefficient	EC3	–
α	alpha	Imperfection factor	EC3	–
			EC9	
α		Parameter	EC9	–
α_{LT}		Imperfection factor in lateral-torsional buckling		–
α_x	alphax	Magnification factor	AISI	–
α_y	alphay	Magnification factor	AISI	–
α_y		Shape factor	EC9	–
α_z		Shape factor	EC9	–
β		Slenderness parameter	EC9	–
β_1		Limit slenderness parameter	EC9	–
β_2		Limit slenderness parameter	EC9	–
β_3		Limit slenderness parameter	EC9	–
β_A	betaA	Reduction factor	EC3	–
$\beta_{M,y}$	betaMy	Equivalent uniform moment factor	EC3	–
$\beta_{M,z}$	betaMz	for buckling about the y axis Equivalent uniform moment factor for buckling about the z axis	EC3	–
β_ω		Coefficient		–
X		Curvature		L ⁻¹
X		Reduction coefficient for the flexural buckling of the stiffener	EC3	–
X		Reduction coefficient in flexural buckling of members in compression		–
X	chi	Reduction factor for buckling resistance	EC3	–
			EC9	
X		Slope of the strain diagram	EC3	L ⁻¹
$X_{0.2}$		Curvature corresponding to strain $f_{0.2}/E$		L ⁻¹
X_{LT}		Reduction factor in lateral-torsional buckling		–
X_{min}	chi min	Lesser of the reduction factors for buckling about the y and z axis	EC3	–
			EC9	–
<i>Symbol</i>	<i>Cold form</i>	<i>Definition</i>	<i>Code</i>	<i>Units</i>
δ		Deflection of the stiffener		L
$\Delta M_{y,Sd}$		Additional moments due to possible shifts of the centroidal	EC3	FL

		axes in the y direction	EC9	
$\Delta M_{z,Sd}$		Additional moments due to possible shifts of the centroidal axes in the Z direction	EC3 EC9	FL
e		Material constant	EC3 EC9	–
ε		Strain		–
ε_0		0.2% proof stress corresponding residual deformation	EC9	–
ε_y		Strain corresponding to the yield limit	EC3	–
ϕ		Parameter	EC9	–
ϕ		Resistance factor	AISI	–
ϕ	phi	Slope of the web relative to the flanges	EC3 EC9	–
ϕ_b		Resistance factor for bending strength	AISI	–
ϕ_c		Resistance factor for concentrically loaded compression member	AISI	–
ϕ_{LT}		Parameter		–
ϕ_t		Resistance factor for tension member	AISI	–
ϕ_v		Resistance factor for shear strength	AISI	–
γ_0		Exponent	EC9	–
γ_m		Partial safety factor		–
γ_M		Partial safety factor	EC3	–
γ_{M0}	gamma M0	Partial safety factor for yielding	EC3	–
			EC9	
γ_{M1}	gamma M1	Partial safety factor for buckling	EC3	–
			EC9	
γ_{M2}	gamma M2	Partial safety factor for net section	EC3	–
			EC9	
η		Coefficient	EC9	–
η		Plasticity factor		–
η_0		Exponent	EC9	–
<i>Symbol</i>	<i>Cold form</i>	<i>Definition</i>	<i>Code</i>	<i>Units</i>

λ	lambda	Flexural buckling slenderness	EC3 EC9	L
λ		Geometrical slenderness in flexural buckling of columns		L
λ	lambda	Slenderness factor	AISI	–
$\bar{\lambda}$		Relative slenderness	EC3	–
$\bar{\lambda}$	lambda bar	Relative slenderness for flexural buckling about a given axis	EC3 EC9	–
$\bar{\lambda}_0$		Normalized slenderness		–
$\bar{\lambda}_0$		Imperfection factor	EC9	–
λ_1		Flexural buckling slenderness	EC3 EC9	L
$\bar{\lambda}_{lim}$		Parameter	EC9	–
λ_c		Slenderness factor	AISI	–
λ_{LT}		Geometrical slenderness ratio in lateral-torsional buckling		–
λ_p		Plate slenderness		–
$\bar{\lambda}_p$	lambdaP	Relative plate slenderness	EC3 EC9	–
$\bar{\lambda}_{p,red}$	lambdaP red	Relative reduced plate slenderness	EC3 EC9	–
$\bar{\lambda}_s$		Relative slenderness of the stiffener	EC9	–
$\bar{\lambda}_w$	lambdaw	Relative web slenderness	EC3 EC9	–
μ_y	muy	Coefficient	EC3	–
M_z	muz	Coefficient	EC3	–
ν		Poisson's ratio	EC3 EC9	–
θ		Angle between an element and its edge stiffener	AISI	–
ρ	rho	Reduction factor	EC3 EC9	–

AISI

σ	sigma	Normal stress		FL ⁻²
$\bar{\sigma}$		Normalized normal stress		–
σ_1		Normal stress along edges		FL ⁻²
σ_2		Normal stress along edges		FL ⁻²
σ_c		Buckling strength of aluminium plate		FL ⁻²
$\sigma_{com,Ed}$		Largest compressive stress	EC3 EC9	FL ⁻²

<i>Symbol</i>	<i>Cold form</i>	<i>Definition</i>	<i>Code</i>	<i>Units</i>
σ_{cr}		Critical normal stress	EC3 EC9	FL ⁻²
σ_{cr}		Critical normal stress of an element		FL ⁻²
$\bar{\sigma}_{cr}$		Normalized critical stress		–
$\sigma_{cr,beff}$		Critical stress for effective width		FL ⁻²
$\sigma_{cr,e}$		Elastic buckling stress		FL ⁻²
$\sigma_{cr,s}$		Elastic critical buckling stress for the stiffener	EC3 EC9	FL ⁻²
σ_{max}		Maximum normal stress along the unloaded edges		FL ⁻²
$\sigma_{max,Ed}$		Maximum compressive stress	EC3 EC9	FL ⁻²
s_n		Reduced critical stress		FL ⁻²
σ_{red}		Reduced stress		FL ⁻²
σ_x		Normal stress in the x direction		FL ⁻²
ω		Interaction coefficient taking into account the moment distribution due to transverse load	EC9	–
ω		Reduction coefficient used by CNR code in flexural buckling in compression		–
ω_1		Numerical coefficient		–
ω_1		Parameter	EC9	–
ω_2		Numerical coefficient		–
ω_2		Parameter	EC9	–
Ω		Factor of safety	AISI	–

Ω_b	Factor of safety for bending strength	AISI	–
Ω_c	Factor of safety for concentrically loaded compression member	AISI	–
Ω_t	Factor of safety for tension member	AISI	–
Ω_v	Factor of safety for shear strength	AISI	–
ζ_0	Exponent	EC9	–
ψ	Ratio of the stresses at the edges of the plate	EC9	–
ψ	Stress ratio	AISI	–

Preface

Writing a new book is always an exciting and challenging activity, especially in the field of metal structures, which is very rich in specific items connected to different technological applications. Among them, the increasing development of lightweight structures draws our attention to the cold-formed, thin-walled profiles made of both steel and aluminium alloys, which are the subject of this book.

Despite the many publications dealing with the above subjects, from different points of view, the main goal of this book is to fill the gap that exists by providing the designer of metal structures with *ad hoc* software, which represents a very useful tool in the application of the most up-to-date design codes.

A general overview of the main aspects of the design of cold-formed, thin-walled structures is necessary to understand the background to the design approach, on which the codified provisions are based.

Nowadays, it is generally recognized that design methodology in structural engineering in Europe is governed by the Eurocodes, which are still in the process of the so-called conversion phase from the initial version (ENV) submitted at the public enquiry to the final version (EN), which must be adopted in all countries of the European Community.

In the field of metallic structures, two Eurocodes are dealt with: Eurocode 3 for steel structures and Eurocode 9 for aluminium structures. Their status at the moment is different, because the two Eurocodes started at different times and developed in different ways.

Eurocode 3, as a whole, is reaching the end of the conversion phase, whereas Eurocode 9 only started its conversion phase in May 2001. In both Eurocodes, the problem of design of cold-formed, thin-walled structures is developed in Chapters 3 and 4, but using different methodologies.

For Eurocode 3 this subject is treated in Part 1.3, where Raffaele Landolfo is one of the six experts in the project team, which is effecting the conversion at this time.

For Eurocode 9, the provisions for trapezoidal sheeting have been treated in a separate document, which has been set up, in parallel with the development of Part 1.1 in the ENV phase, by an *ad hoc* group led by

Rolf Bahere, with Raffaele Landolfo playing both the role of expert and, at the same time, national technical contact (NTC) of Part 1.1.

Federico Mazzolani, who acts as chairman of the team that is working on the ENV version of Eurocode 9 (Part 1.1 General Rules; Part 1.2 Fire Design; Part 2 Structures Susceptible to Fatigue), has been recently re-elected to the same position for the next 3 years of the conversion phase.

According to the decision of the Committee CEN-TC 250, the previous document on trapezoidal sheeting will be transferred into an Annex to Eurocode 9 Part 1.1, which integrates the general rules for cold-formed thin-walled sections already included in Part 1.1. It is important also to observe that the methodologies used for steel and aluminium in the definition of the effective cross-section are different.

The situation concerning the design of metallic cold-formed thin-walled members is, therefore, not yet completely stabilized between the Eurocodes, but the way forward is very clear to the two abovementioned authors of this book, who were so closely involved in the preparation of the ENV versions of both Eurocode 3 and Eurocode 9 and are presently engaged in guaranteeing the continuity of calculation methods during this ongoing conversion phase.

By enlarging our view of international codification beyond Europe, we have to recognize the importance of the US code, the AISI Specification, which is based on a different philosophy and is, therefore, interesting to consider in comparison with the European codes.

After presentation of the main general aspects of metal cold-formed thin-walled members, including technology, materials and behaviour, the main applications and outstanding fields of interest for future applications are given in Chapter 1 with a view to defining the actual framework in which the proposed design tool can be utilized.

The basic assumptions, which all codifications refer to, are shown in Chapter 2 by presenting a comprehensive overview of plate buckling theories both for steel and for aluminium, the latter being less well known.

Chapters 3, 4 and 5 are devoted to outlining the main features of the design methods included in Eurocode 3, Eurocode 9 and the AISI Specification, respectively. They are organized in parallel, with a similar format, starting from an initial part which deals with the synthetic review of the specific background, followed by definition of mechanical and sectional properties. Then, the calculation methods are presented from the component (local buckling of plate elements), to the cross-section (resistance), up to the member (buckling resistance), by considering the effect of simple actions (tension, compression, bending and shear) and the combination of them.

Comparison between the three different methodologies of the codes under discussion is given in Chapter 6, by considering some typical cross-sections, with a view to demonstrating the main differences between each approach and their consequences from the design point of view. Finally, Chapter 7 is devoted to explanation of the ColdForm computer program, which represents the main issue of this book. By using a certain number of images, taken from the computer screen, utilization of this program is illustrated step by step from installation to exploitation of the various menus, giving a complete scenario of potential applications and underlining the great flexibility and user-friendly nature of this design tool. A CD-ROM containing the ColdForm program is attached to this book. Aurelio Ghersi, who has for many years researched in the field of cold-formed structures, is also a specialist in computer software, as has been shown in many of his previous activities.

We are convinced the ColdForm computer program will be used not only by designers in their daily activity, but also by academicians for research purposes and students seeking a better understanding of the behaviour of cold-formed thin-walled structures.

We would like to express our gratitude to all who participated in developing this work. In particular, we thank Edoardo Marino of the University of Catania and Luigi Fiorino of the University of Naples, who spent their undergraduate time in calibration of this software by preparing several *ad hoc* examples, which are only partially reported in this volume.

1

General aspects

1.1 BACKGROUND

The progress of structural engineering in the twentieth century and early in the twenty-first unquestionably tends toward the use of increasingly lighter elements, among which metallic thin-walled cold-formed members play an important role. Improved manufacturing technology, along with increased material strength as well as the availability of Codes of Practice for design represent some of the most important factors in the development of such structural typology.

Formerly, the use of cold-formed thin-walled metallic sections was mainly confined to products where weight saving was of prime importance (e.g. in the aircraft, railway and automotive industries).

Since the initial work of Winter (Winter, 1949), who pioneered this field, systematic research, carried out over the past five decades, has emphasized the substantial advantages provided by the cold-forming technique for optimizing products regarding their load-bearing function and space-covering ability, leading to the wider use of cold-formed sections in the construction industry as well.

On the other hand, improved techniques in manufacture and corrosion protection have led to increased competitiveness of the resulting products with parallel developments in practical applications (Davies, 1998, 2000). As a result of this, cold-formed metallic sections are becoming considerably more slender and complex than hot-rolled shapes and, therefore, more prone to local (Pekoz, 1987), distortional (Hancock, 1997) as well as coupled (Gioncu, 1994) instability phenomena. This evolution is inevitably accompanied as a consequence by demand for improved calculation methods and design provisions (Rondal, 2000), which sometimes have to take into account that the structural response of cold-formed members is influenced by additional problems (Rhodes, 1992), such as, for example, the presence of openings in flanges or webs (La Boube *et al.*, 1997).

At the same time, because of the comparative thinness of the material, special non-conventional connections have played an important role in the development of cold-formed construction. Bolts, screws, blind rivets or cartridge-fired pins are commonly used in joints between cold-formed members. As an alternative, new systems for joining light gauge members can be used, such as the clinching (Pedreschi *et al.*, 1997) and 'Rosette' (Makelainen and Kesti, 1999) techniques. Both of them are very quick, require no additional components and cause no damage to the coating.

The structural behaviour of cold-formed metallic members is one of the major research subjects that have been carried out at the Engineering Faculty of Naples (Mazzolani, 1994, 1995a). This comprehensive research is in-corporated in national and international developmental work, which covers many subjects. In particular, in the field of cold-formed steel sections, it includes: the bending behaviour of trapezoidal sheeting,

both standard (Landolfo and Mazzolani, 1994, 1995a) and long span (Landolfo and Mazzolani, 1990a; De Martino *et al.*, 1991); the flexural strength of cold-formed beams (De Martino *et al.*, 1992); the interaction between local and lateral instability (Gherzi *et al.*, 1994) as well as the possibility of using cold-formed members in seismic zones (Calderoni *et al.*, 1995, 1997, 1999). This research has analysed both experimental and theoretical aspects and the end results have been compared with provisions of the most recent codes in this field. Important research has been devoted to investigating the diaphragm action due to interaction between cold-formed cladding panels and framed structures, which is commonly called the ‘stressed skin design’ (Davies and Bryan, 1982). This research, sponsored by the European Community (Mazzolani *et al.*, 1996c), is aimed at the development of a suitable methodology of analysis able to both evaluate the contributing effect of cladding panels and see what such an effect has on the global structural analyses of steel-framed buildings. Although this research had fairly general aims, with regard to shear wall type, particular reference has been made to screwed sandwich panels. Both experimental and theoretical activities have been developed. Tests on both connection systems and single wall units have been preliminarily carried out under monotonic and cyclic loads (De Matteis and Landolfo, 1999a). This was followed by suitable interpretative models which have been set up both for fasteners (De Matteis and Landolfo, 1999b) and whole shear diaphragms (De Matteis and Landolfo, 2000a). Finally, the possibility of using cladding panels as a bracing system for steel structures in seismic areas, which make allowances for their actual hysteretic response, has been investigated with reference to both pin-jointed (De Matteis and Landolfo, 2000b) and moment-resistant steel frames (De Matteis *et al.*, 1998).

As far as aluminium cold-formed sections are concerned, the main research has recently been addressed to setting up suitable design curves which account for local instability phenomena in slender sections (Landolfo and Mazzolani, 1998; Mazzolani *et al.*, 1998; Landolfo *et al.*, 1999a, 1999b), to selecting the best design approach (Landolfo and Mazzolani, 1997) as well as to evaluating the influence of material non-linearity on the flexural response of thin-walled sections (Gherzi and Landolfo, 1996) and on the coupled instability phenomena (Landolfo, 2000).

1.2 TYPES AND SHAPES

Nowadays, cold-formed structural products can be classified into two main typologies:

- structural members;
- sheeting.

Typical sections belonging to the first typology of cold-formed products are shown in Figure 1.1. They are structural members mainly used, in the higher range of thickness, as beams for comparatively low loads on small spans (purlins and rails), as columns and vertical supports, and as bars in trusses. In general, the depth of cold-formed members ranges from 50 to 300 mm and the thickness of material ranges from 1.0 to 8.0 mm, although depth and thickness outside these ranges also are used.

The second category of cold-formed sections is shown in Figure 1.2. These sections are plane load-bearing members in the lower range of thickness, generally used when a

space-covering function under moderate distributed loading is needed (e.g. roof decks, floor decks, wall panels). The depth of panels generally ranges from 40 to 200 mm and the thickness of material ranges from 0.5 to 2.0 mm.

The development of profiles of metallic sheeting over the past years has been characterized by three generations of profiles, illustrated in Figure 1.3. The first generation includes plane trapezoidal profiles without stiffeners (Figure 1.3a), allowing spans between secondary members of no more than 3 m. In the second generation, the trapezoidal sheets are stiffened in longitudinal direction by appropriate folding (Figure 1.3b) and may span

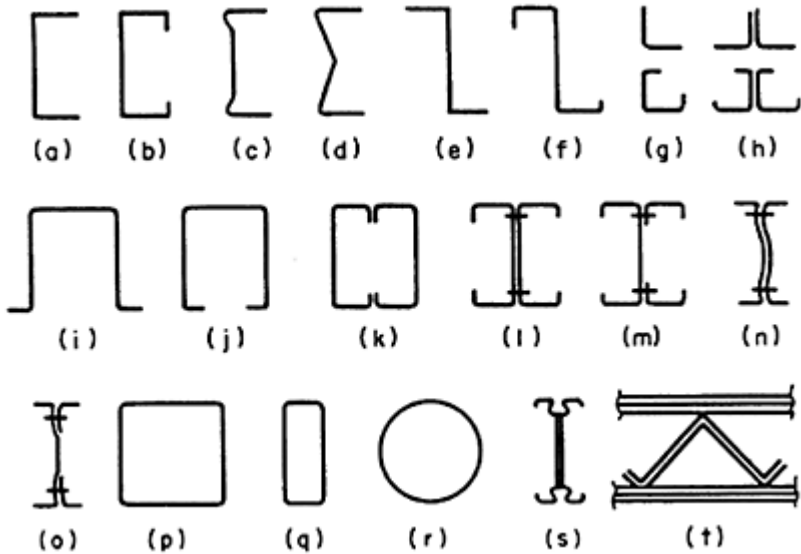


Figure 1.1 (Yu, 1992).

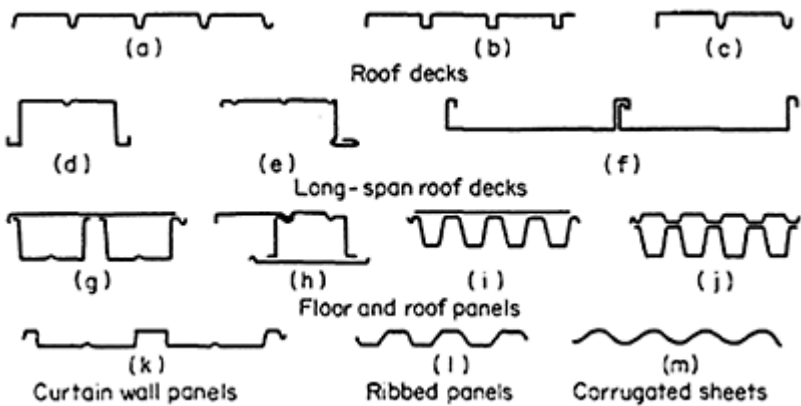


Figure 1.2 (Yu, 1992).

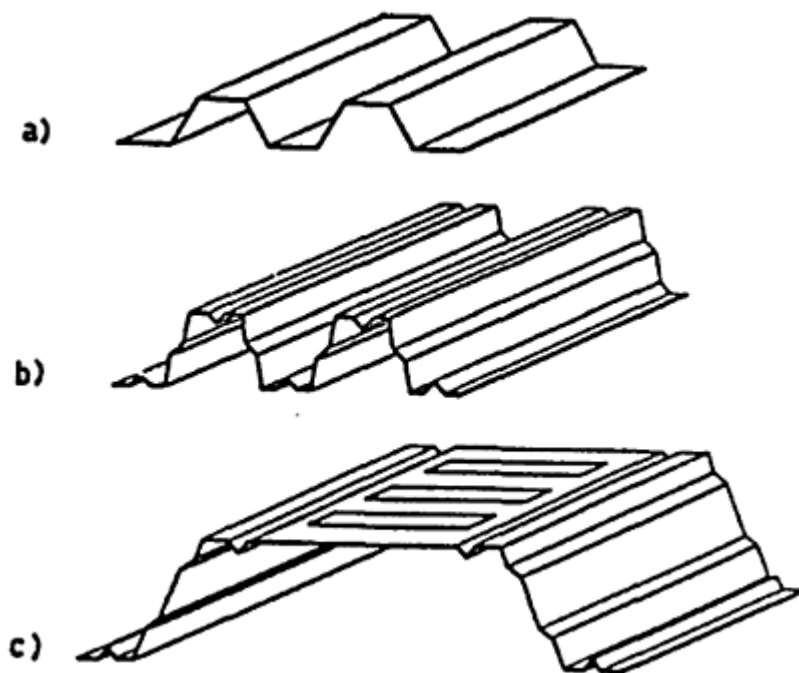


Figure 1.3 (Landolfo and Mazzolani, 1990a).

up to 6–7 m. The third-generation profiles are trapezoidal units with both longitudinal and transversal stiffeners (Figure 1.3c), which provide suitable solution for spans up to 12 m without purlins (Landolfo and Mazzolani, 1990a).

The combination of cold-formed members and sheeting can, of course, be successfully utilized in low-rise and light industrial buildings. Stressed-skin design philosophy can also be utilized in order to obtain interesting and convenient applications in the field of space structures.

1.3 BEHAVIOURAL FEATURES

As far as structural behaviour is concerned, when compared with conventional metallic members, thin-walled cold-formed elements are mainly characterized by: (1) the constant thickness of the formed section; (2) the relatively high width-to-thickness ratio of the elements that make up the cross-section; (3) the variety of cross-sectional shapes. In particular, (2) gives rise to local buckling phenomena, which compromise the load-bearing capacity; structural imperfections caused by the cold-forming process must also be considered. As a consequence, structural analysis and design of thin-walled cold-formed elements is generally complicated by the effects arising from these features,

which do not affect the structural response of simpler compact sections. The main factors that influence the structural behaviour of thin-walled sections are:

- local buckling of the compression parts;
- interaction between local and overall buckling modes;
- shear-lag and curling effects;
- effects of the cold-forming process.

Moreover, since cold-formed sections are generally thin walled and of open cross-section, torsional-flexural buckling may be the critical phenomenon influencing the design.

At the present time, there are several textbooks dealing with the above phenomena and their influence on the structural behaviour of cold-formed thin-walled members (Walker, 1975; Rhodes, 1990; Yu, 1992). In the following, they will only be briefly reviewed, together with the main characteristic of the cold-forming process and its effect. For a more comprehensive overview on cold-formed thin-walled structures, reference to the specialized literature should be made.

1.4 COLD-FORMING TECHNIQUES

Cold-formed sections can be generally obtained through two manufacturing methods: by rolling or by press or bending brake operations.

The process of cold-rolling is shown in Figure 1.4. It is widely used for the production of individual structural members and corrugated sheeting. The final required shape is obtained from a strip which is formed gradually, by feeding it continuously through successive pairs of rollers which act as male and female dies. Each pair of rollers progressively forms the strip until the finished cross-section is produced. The number of rollers that are used depends on the complexity of the final shape as well as thickness and strength of the strip used. The completed element is usually cut to required lengths by an automatic cut-off tool, without stopping the machine.

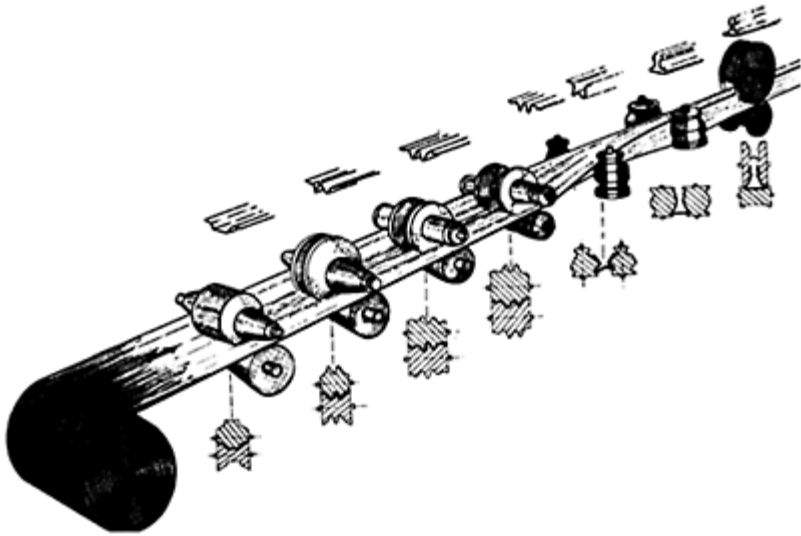


Figure 1.4 (Walker, 1975).

Cold-formed profiles manufactured by roll-forming are essentially uniform in cross-section and can be held within very close dimensional tolerances. The main advantages of cold-roll forming, when compared with other methods of fabrication, are: (1) the high production capacity; (2) the ability to maintain fine surface finishes during roll-forming operations. The latter benefit is particularly important where pre-galvanized steel or steel pre-coated with plastic are utilized.

When the section to be shaped is simple and the required quantity is quite limited, hydraulic folding or press-braking machines are commonly used (Figures 1.5 and 1.6). In these processes, short lengths of strip are fed into the brake and bent or pressed round shaped dies to form the final shape.

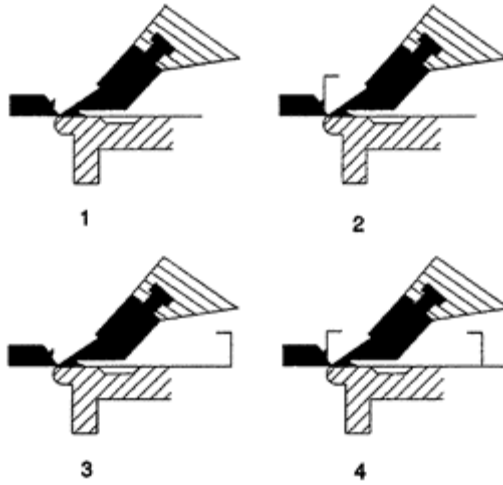


Figure 1.5 (ESDEP, 1994).

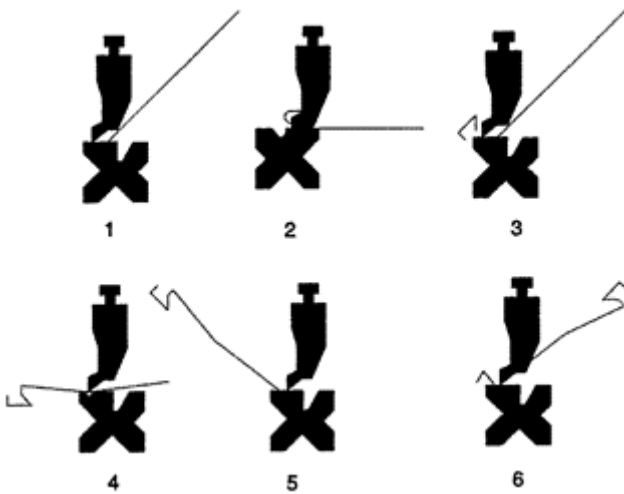


Figure 1.6 (ESDEP, 1994).

Usually, each bend is formed separately and the complexity of shape is limited to one in which the die can fit.

Finally, it should be noted that the cost of the product largely depends on the manufacturing process. The cold-rolling process is generally very highly automated. As a consequence, it will become cheaper the greater the quantity of a given section.

1.5 MATERIALS

Materials used in the production of cold-formed members have to be suitable for cold-forming and, if required, for galvanizing. In addition, their mechanical and chemical properties must fulfil specific requirements to enable the formed profile to be used for structural purposes.

As far as steel cold-formed sections are concerned, a wide variety of products are used, in the form of sheets, strips, plates or flat bars. Generally, cold-rolled continuously galvanized steels are preferred in order to minimize or eliminate corrosion problems, even if hot-rolled plates are used as well. Under normal conditions, zinc protection Z 275 (275 g/m^2) is sufficient; in more corrosive environments, improved protection using suitable coating systems may be necessary. Continuously applied zinc protective-coating systems are generally limited in core thickness to about 3.5 mm. For increased material thickness, hot-dip galvanizing and site- or shop-applied topcoats may be used.

With regards to mechanical properties, usually yield stresses are in the range of 200–550 MPa with a ratio of ultimate tensile strength to yield stress of at least 1.2 (Ballio and Mazzolani, 1983).

Moving on to aluminium alloys, sheet and plate products are available in most of the existing alloys. These products are commonly used in building and construction. Alloy types 3xxx, 5xxx and 6xxx can be formed into complex shapes and sections (Sharp, 1993). For these applications, the stress corresponding to a residual strain of 0.2% (conventionally called the elastic limit of aluminium alloys) generally ranges from 150 to 300 MPa. The ratio of ultimate tensile strength to elastic limit is at least 1.1 (Mazzolani, 1995b).

1.6 EFFECTS OF COLD-FORMING

Cold-rolling produces mechanical residual stresses which vary across the sheet thickness (Figure 1.7). In fact, the outer fibres tend to elongate, while the centre tends to remain undeformed, but some deformation between surface and centre must take place through the thickness. The internal fibres resist the elongation of the external fibres, which in turn try to stretch the internal ones. The result is a residual stress distribution with compression on the surface and tension within the thickness (Ballio and Mazzolani, 1983).

In hot-rolled plates, residual stresses are produced by cooling and their distribution is similar to that of cold-rolled sheets. In fact, the areas which cool off first (surface) undergo compressive residual stresses, whereas the last cooled areas (centre) are in tension.

Thin-walled sections, formed from both cold and hot-rolled sheets, have residual stresses distributed throughout the thickness of their individual parts. Within the thickness, the result of such a distribution is null and its effect on the overall behaviour of a thin-walled member can therefore be neglected in most cases. It should be considered

as just a local effect which can increase the danger of local buckling in the thin-walled parts.

In conclusion, from the point of view of residual stresses, thin-walled cold-formed sections are more accommodating compared with similar hot-rolled sections.

The second structural imperfection, the variation in mechanical characteristics over the cross-section, seems to be particularly important for these profiles, due to the strain-hardening effect, which the material undergoes during cold-forming. This procedure, in fact, produces an increase in the elastic limit of the material compared with its original value and its

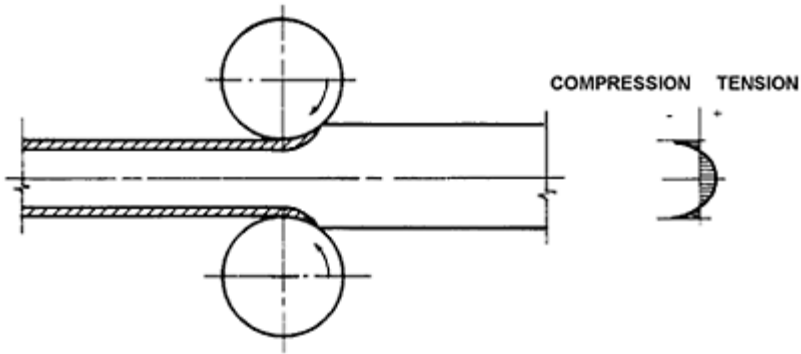


Figure 1.7 (Ballio and Mazzolani, 1983).

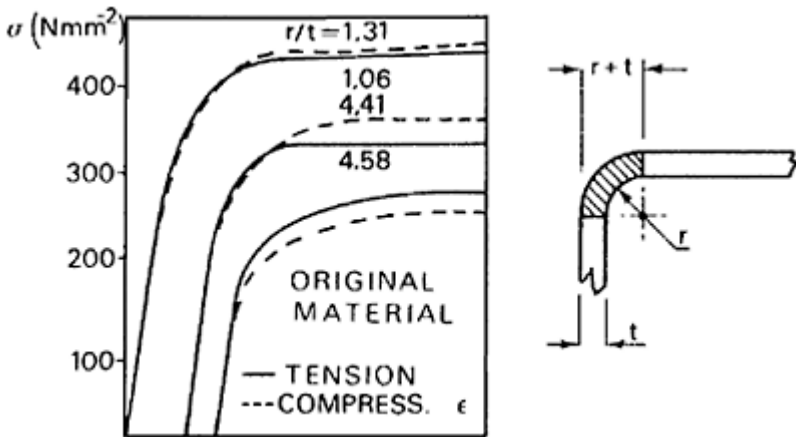


Figure 1.8 (Ballio and Mazzolani, 1983).

increment is proportional to the severity of folding, expressed as the ratio between fillet radius r and sheet thickness t (Figure 1.8).

The increase in strength due to strain hardening produces, as an immediate negative consequence, a lowering of toughness. Tests have shown a highly variable distribution of yield stress f_y (full lines) and of tensile strength (dashed lines) over the cross-section. It is characterized by peaks corresponding to the folds and minimum values at the centre of the individual parts of the profile. The material elastic limit increases up to 50% in the folded area in the case of profiles obtained by more than one folding operation (Figure 1.9).

Finally, the geometrical imperfection, due to the cold-forming which has to be considered, is the necking. Forming corners of small radius can have the effect of producing 'thinning' of the corners and this can have an effect on the section properties (Figure 1.10), but this effect is generally small since the corners usually are just a small proportion of the overall cross-sectional area (Rhodes, 1990).

When we need to take corner-thinning effects into account to determine section properties, this can be achieved, approximately, by assuming that the reduced thickness of the corners is given by the following expression:

$$t_r = \left(\frac{r + kt}{r + 0.5t} \right) t \quad (1.1)$$

where:

t_r =reduced thickness;

t =material thickness;

r =inside radius of the corner;

k =a numerical coefficient function of the ratio r/t :

$k=0.3$ for $r/t=1$;

$k=0.35$ for $r/t=1.5$.

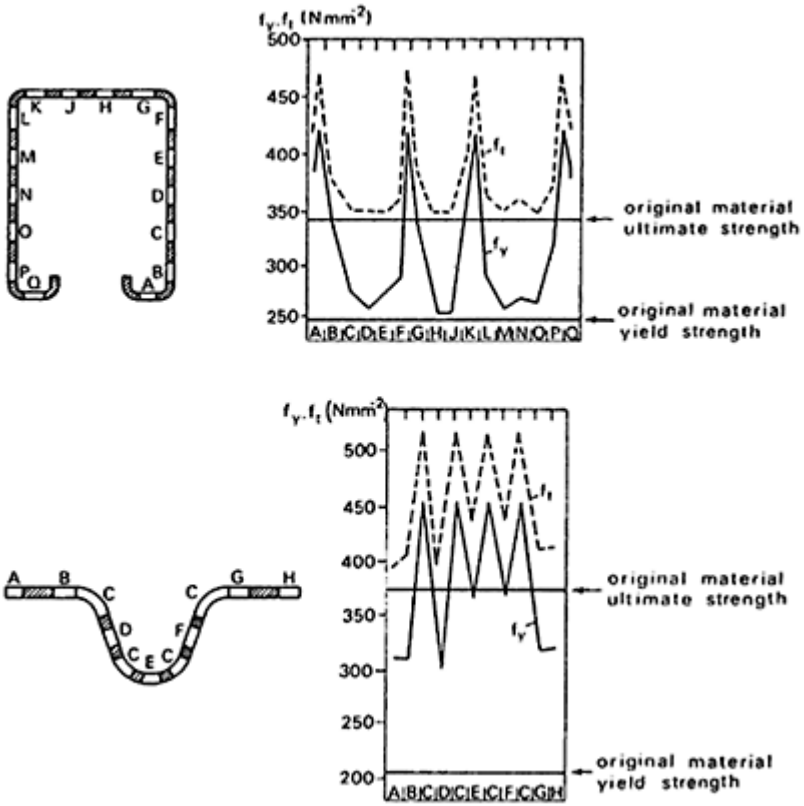


Figure 1.9 (Ballio and Mazzolani, 1983).

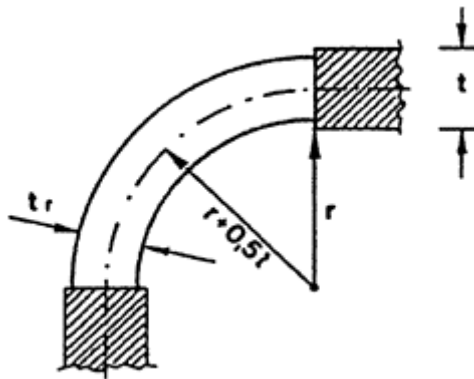
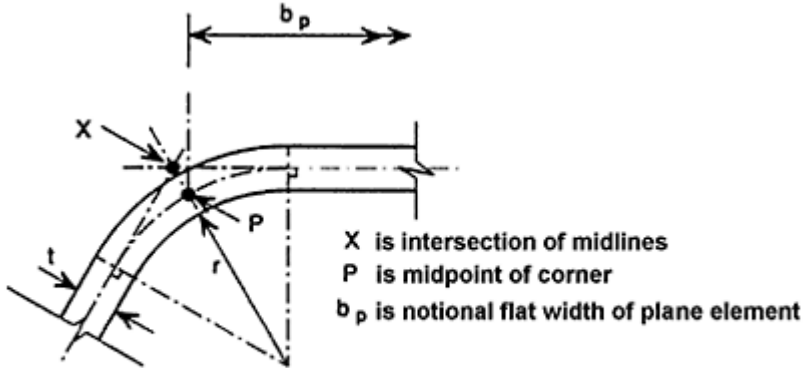


Figure 1.10 (Landolfo, 1992).

1.7 CROSS-SECTIONAL PROPERTIES

Cold-formed members generally have a nominally constant thickness and consist of a series of plane elements connected by rounded corners.

If the internal radius of the corners is small, its influence on cross-section properties may be neglected and the cross-section may be assumed to consist of plane elements with sharp corners. Both Eurocode 3 (CEN, ENV 1993–1–3)



EC3 : $r < 5 t$ and $r < 0.15 b_p$

EC9 : $r < 10 t$ and $r < 0.15 b_p$

Figure 1.11 (CEN, ENV 1993–1–3; CEN, ENV 1999–1–1).

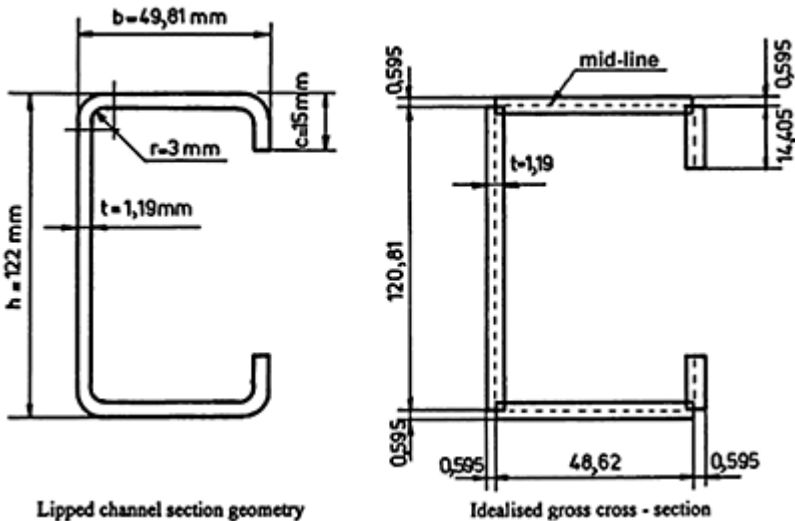


Figure 1.12 (Dubina and Vayas, 1995).

and Eurocode 9 (CEN, ENV 1999–1–1) allow this simplified approach, provided that proper limits of the radius are respected (Figure 1.11).

Furthermore, each plane element of the cross-section may be considered as a line element, concentrated along the midline of the actual element (Rhodes, 1990). The accuracy of this method for computing the properties of a given section depends on the thickness of metallic sheets and the shape of the section.

For the thickness of the metallic sheets generally used in cold-formed metallic constructions, the error in evaluation of the cross-sectional area and other properties is usually negligible (Yu, 1992).

As an example, for a lipped channel section member in which rounding of corners may be ignored, both the actual cross-section and the idealized one are shown in Figure 1.12.



Figure 1.13 (Davies, 2000).

1.8 APPLICATIONS AND FUTURE DEVELOPMENTS

As mentioned before, the use of the cold-formed thin-walled structural system is increasingly being used in the market both for civil and industrial buildings, and in the emerging field of retrofitting as well. As a consequence, it is difficult to provide a comprehensive overview of the most outstanding examples by looking at the various applications of such a structural system in the construction industry (roofing, flooring, cladding, framing, etc.).

Generally speaking, cold-formed members are employed as structural components, so that their main applications are in the field of purlins, sheeting, cladding, decking, etc.

More recently, there has been a growing development in the use of the cold-formed framing system for housing and other low-rise constructions.

With regards to conventional steel-frame light-weight systems, this development is being led by the USA, but interesting applications are also cropping up in Europe (Figure 1.13). The primary framing elements for this construction system are cold-formed steel wall studs and floor joists. Figures 1.14 (a, b) show a private house erected in Timisoara (Romania) (Dubina *et al.*, 1999) using such a structural system. The structure has been designed according to Romanian standards which take seismic activity into account as well. All members are made of cold-formed lipped channel steel sections, while the fastening technology is based on self-drilling screws.

The use of light steel framing as a method of house construction has increased significantly in the UK in recent years (Lawson and Ogden, 2001). Several houses have been constructed and the market is expanding, owing to intensive research activity and development, especially in the areas of

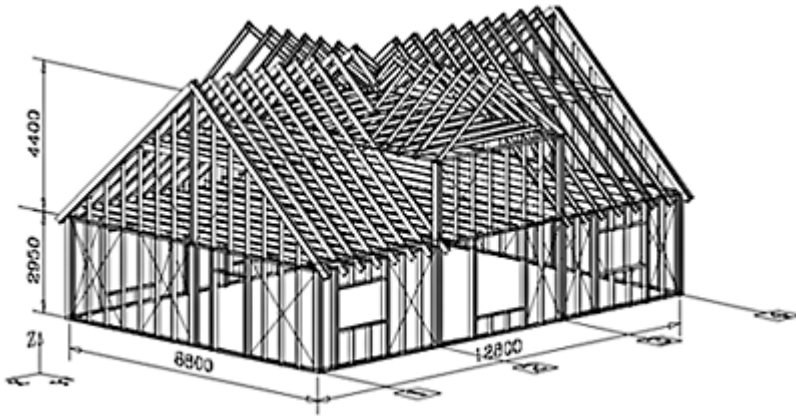


Figure 1.14a (Dubina *et al.*, 1999).



Figure 1.14b (Dubina *et al.*, 1999).

structural design, acoustic insulation, thermal performance and modular construction. In particular, the modular housing system (Figure 1.15) has proven to be an appropriate way of constructing cellular buildings such as hotels and student accommodation in universities.

Another significant development is the use of cassette wall construction (Davies, 2000). These have the advantage of providing a weather-proof wall as well as a structural frame by avoiding many of the stability problems affecting stud wall systems (Figure 1.16). This kind of structural configuration lends itself to the use of 'stressed skin' design methodology with regard

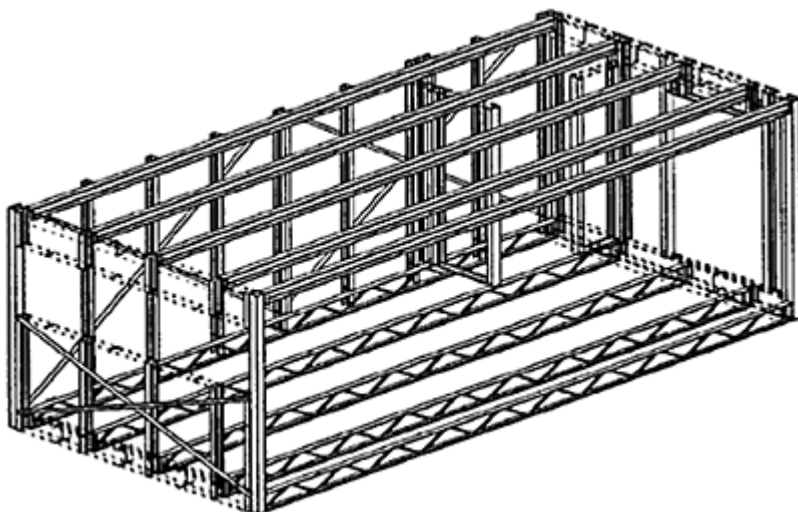


Figure 1.15 (Lawson and Ogden, 2001).

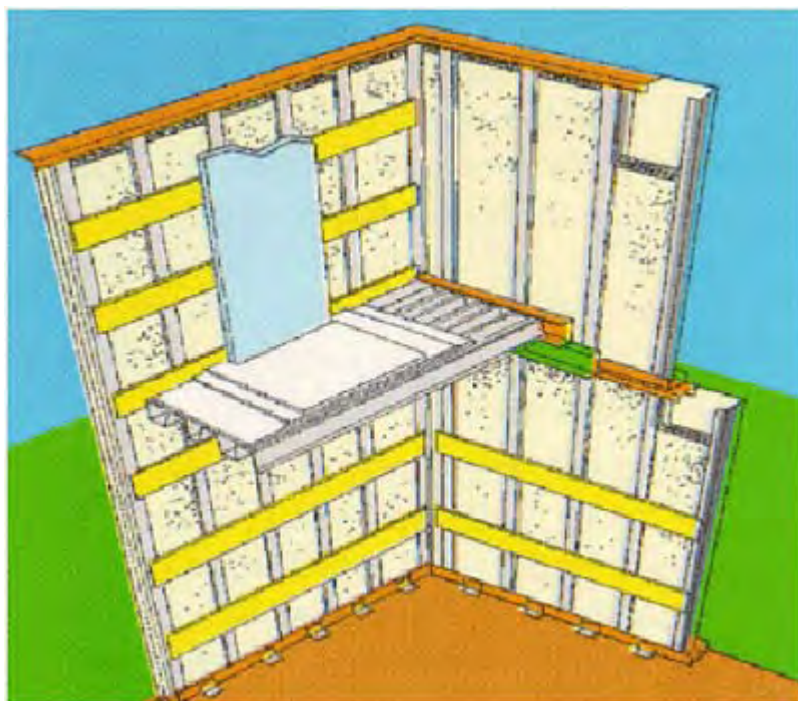


Figure 1.16 (Davies, 2000).

to horizontal loads, which allows the bracing system in the plane of the wall to be avoided. Typical applications of cassette wall construction are depicted in Figures 1.17 (a, b) in residential houses built in France at Reims (Davies, 2000).

In Italy, many applications can be seen of cold-formed sections in civil and industrial buildings, long-span roofing and retrofitting (De Martino *et al.*, 1992; Mazzolani, 1995a).

As for innovative products, worthy of note is a structural system based on a modular spatial element, called 'steel brick' (Figures 1.18 (a, b)), designed



Figure 1.17a (Davies, 2000).



Figure 1.17b (Davies, 2000).

by Pagano (Giannattasio et al., 1988). The ‘bricks’, which are made of cold-pressed galvanized steel sheeting, are assembled using rivets with interposed junction plates and can be used to build any shape and type of construction, including arches and shells.

As for long-span decking and roofing applications, the TRP 200 profile, produced in Sweden by Planja, has also been used in Italy. This structural element, which is made from hot-dipped galvanized steel sheet with a



Figure 1.18a.



Figure 1.18b (Giannattasio *et al.*, 1988).

thickness range from 0.75 to 1.50 mm, belongs to the so-called third generation of trapezoidal sheeting (Landolfo and Mazzolani, 1990a). Owing to its adaptability, it has been successfully used for roofing in industrial buildings (Figure 1.19a) or in floor structures of multi-storey buildings (Landolfo and Mazzolani, 1990b) by completing its cross-section with cast concrete (Figure 1.19b). Some applications of TRP 200 profiles have also been proposed for the renovation of old roofs and floor structures.

Finally, the BASIS (Building Activities Steel Integrated System) construction system undoubtedly represents the most comprehensive Italian proposal for buildings (Baldacci, 1984), which has also been designed to build seismic-resistant low-rise buildings. First presented in 1982, this system is based on the use of cold-formed steel beams, made of back-to-back channel sections, composite slabs with trapezoidal



Figure 1.19a (Landolfo and Mazzolani, 1990a).



Figure 1.19b (Landolfo and Mazzolani, 1990b).

sheeting and hot-rolled columns (Figure 1.20a). In order to withstand horizontal loads, a steel bracing structure or concrete core can alternatively be utilized

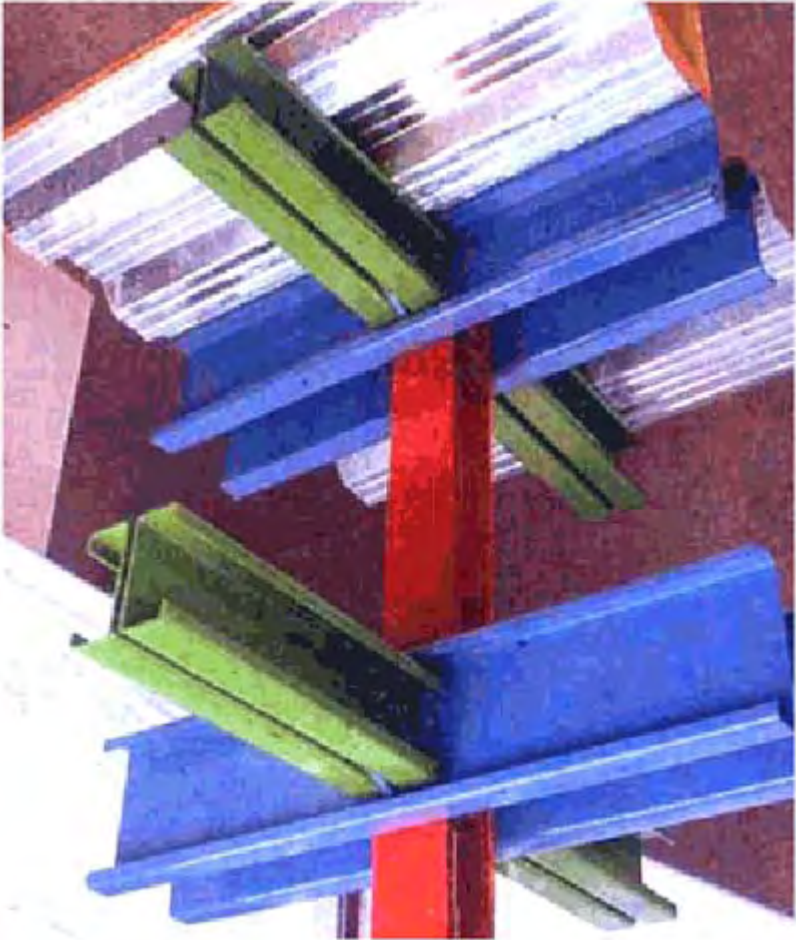


Figure 1.20a.



Figure 1.20b.

(Figure 1.20b). The BASIS system has been used in Italy and elsewhere for residential buildings. The Civil Center of Civitavecchia (Italy) is a very good example of the use of BASIS, where particular attention has been paid to avoid a box-like building and provide architectural features to the façade (Figure 1.21 (a, b)).



Figure 1.21a.

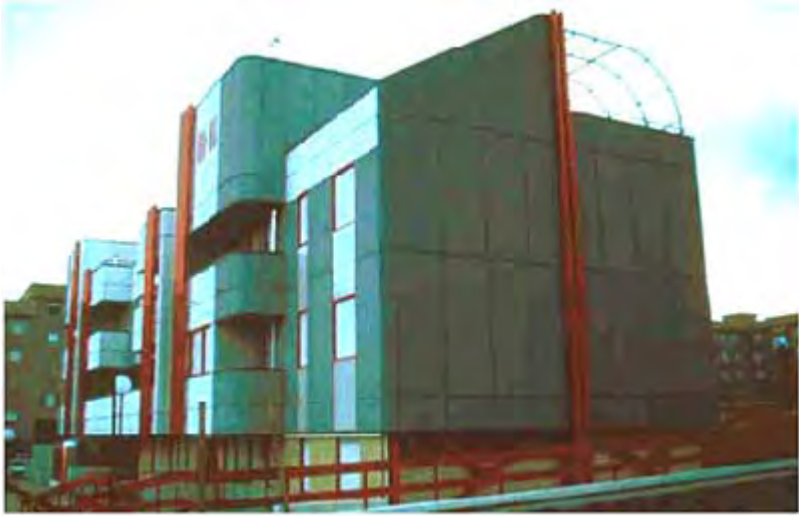


Figure 1.21b.

These developments in the practical use of cold-formed sections in building construction make demands on design procedures and require parallel developments in calculation models and design codes. Research workers have responded to this challenge in many ways. Viable design models have been developed for the treatment of local buckling, distortional buckling and the interaction between them (Davies, 2000). The latest trend is to move away from simplified design procedures based on ‘whole section’ analysis (Schafer and Peköz, 1998). In every case, the use of design software, such as that presented in this book, can help in the development of cold-formed thin-walled structures.

2

Codified design bases

2.1 BASIC ASSUMPTIONS

The behaviour of cross-sections and their ideal uses in structural analysis is related to the capability of reaching a given limit state which corresponds to a particular assumption about the state of stress acting on the section.

Referring to the global behaviour of cross-sections, regardless of the internal action considered (axial load, bending moment or shear), the following limit states can be defined:

- a *elastic buckling limit state*, related to the strength corresponding to the onset of local elastic instability phenomena in the compressed parts of the section;
- b *elastic limit state*, related to the strength corresponding to the attainment of the elastic limit of material in the most stressed parts of the section;
- c *plastic limit state*, related to the strength of the section, evaluated by assuming a perfectly plastic behaviour for material with a limit value equal to the elastic limit, without considering the effect of hardening;
- d *collapse limit state*, related to the actual ultimate strength of the section, evaluated by assuming a distribution of internal stresses accounting for the actual hardening behaviour of material. Since, under this hypothesis, the generalized force-displacement curve is generally increasing, the collapse strength must be referred to a given limit of the generalized displacement.

As is well known, the response of thin-gauge metal sections is strongly affected by local instability phenomena, which arise in the compressed parts, and the determinant limit state is, of course, the elastic buckling one.

Exact analysis of a thin-walled member requires us to treat it as a continuous folded plate, but the mathematical complexities of such an analysis are very cumbersome. Most analyses, therefore, consider the member as being made up of an assembly of individual plates, with proper boundary and loading conditions, such that the behaviour of the

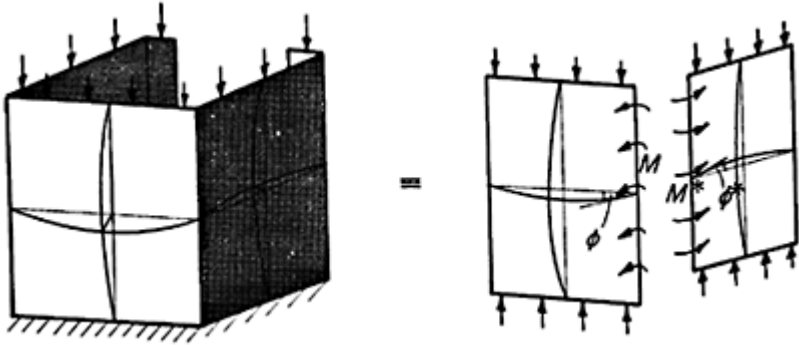


Figure 2.1 (Walker, 1975).

individual plates defines the behaviour of the whole section. The boundary conditions require compatibility of edge displacement and rotation between adjacent plates, as well as equilibrium of moments and shear forces. For simplicity, the design in most national standards is based on the common assumption that the plates support each other at boundaries, so that their mutual edges are kept straight, with no moments transmitted across these boundaries (Figure 2.1). Experience has proved that this analysis gives rise to no significant error in predicting either elastic deflections or collapse loads.

The big advantage of this hypothesis is that the design of quite complicated shapes becomes a fairly simple process. This, together with the wide range of shapes that can be cold-formed, offers considerable flexibility in the choice of member and its design (Walker, 1975).

Local buckling of a section is, therefore, studied by evaluating the buckling of each plane element according to the theory of compressed plates stability.

Analysis of the buckling behaviour of flat plates loaded by forces acting in their middle plane is rather complex because they are affected by two kinds of non-linearity: geometrical and mechanical.

By taking all this into consideration, it is commonly assumed that analysis of the stability of plate elements can be carried out at two different levels:

- according to linear theory, in which the behaviour of a perfectly elastic material in the field of small deformations is examined;
- according to non-linear theory, in which the behaviour of plates in the post-buckling range is analysed, taking into account both geometrical and mechanical non-linearities, together with the presence of geometrical and mechanical imperfections.

The methods based on linear theory lead to evaluation of the critical load (Euler load), but they are not valid for accurate estimate of the ultimate load, which can only be calculated using non-linear analysis (Landolfo, 1992).

2.2 STEEL PLATE BUCKLING OVERVIEW

Let us consider a rectangular flat element with length L , width b and uniform thickness t (Figure 2.2).

The stress distribution, before reaching elastic buckling, is uniform in the element, as shown in Figure 2.3a. After elastic buckling, a non-uniform stress distribution results and, therefore, a portion of load from the mid-strip transfers to the edges of the element, as shown in Figure 2.3b. The process continues until the maximum stress (along the plate edges) reaches the yield point of the material, and then the element begins to fail (Figure 2.3c).

The study of the elastic buckling behaviour of plates (linear theory), corresponding to stage (a) in Figure 2.3, leads to the following expression (Euler formula) of the critical stress σ_{cr} :

$$\sigma_{cr} = \frac{k\pi^2 E}{12(1 - \nu^2) \left(\frac{b}{t}\right)^2} = \frac{\pi^2 E}{\lambda_p^2} \tag{2.1}$$

where:

$$\lambda_p = \sqrt{\frac{12(1 - \nu^2)}{k}} \cdot \frac{b}{t}$$

λ_p is the plate slenderness;
 ν =Poisson's ratio;

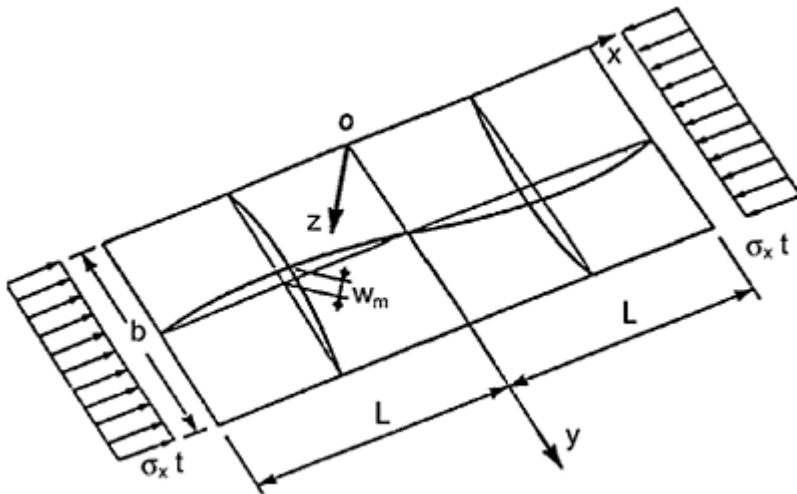


Figure 2.2 (Landolfo, 1992).

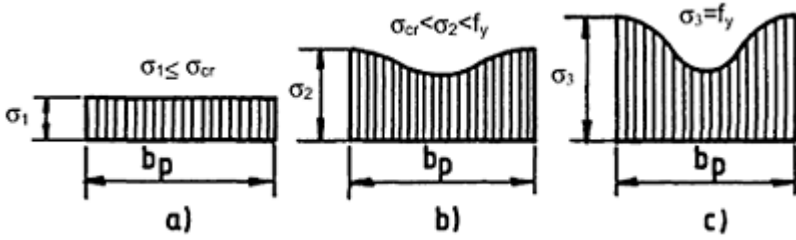


Figure 2.3 (Yu, 1992).

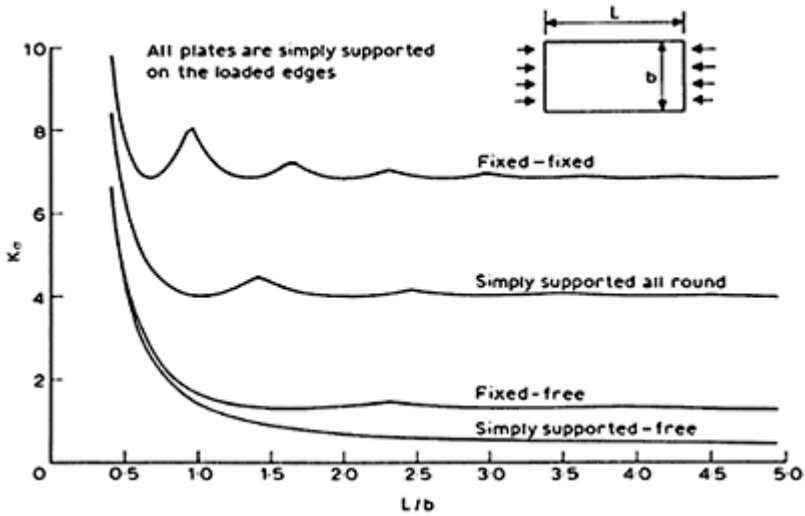


Figure 2.4 (Rhodes, 1990).

k_σ =the local buckling coefficient which depends on: distribution of axial stress; restraint conditions of the unloaded edges; geometrical dimensions (L/b).

For plates subjected to uniform stress distributions along the length, the variation of k_σ in relation to the length-over-width ratio L/b is shown in Figure 2.4 for various boundary conditions (Rhodes, 1990). Figure 2.5 (Ballio and Mazzolani, 1983) gives the minimum buckling coefficient k_σ for uniformly compressed elements in different restraint conditions along the unloaded edges.

Design codes generally suggest using buckling coefficients that correspond to simple support or free conditions. In the case of simply supported elements with unloaded edges subjected to linear stress distributions, corresponding to the combined axial force and bending moment, the buckling coefficients k_σ can be substantially different from those already mentioned. The minimum buckling coefficient, in this case, depends on the coefficient $\psi = \sigma_2 / \sigma_1$ as shown in Figure 2.6(a). Figure 2.6(b) illustrates the influence of the L/b ratio on the values of the buckling coefficient in the case of elements subjected to

eccentric load with unloaded edges which are simply supported and free, respectively (Landolfo, 1992).

According to von Karman's semi-empirical approach, the non-uniform distribution of stresses, which crop up in the post-buckling range, can be replaced by an equivalent uniform stress distribution $\sigma = \sigma_{max}$ acting on the 'effective width' of the plate (b_{eff}), with σ_{max} the actual stress along the unloaded edges (see Figure 2.7).

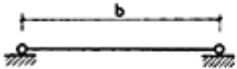
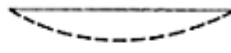
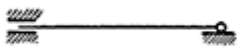
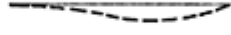
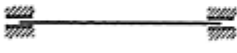
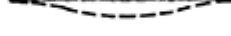

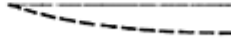


RESTRAINTS ALONG THE UNLOADED EDGES	DEFLECTED SHAPE	k_{σ}
		4.00
		5.42
		6.97
		0.425
		1.277

Figure 2.5 (Ballio and Mazzolani, 1983). Buckling coefficients for different restraint conditions.

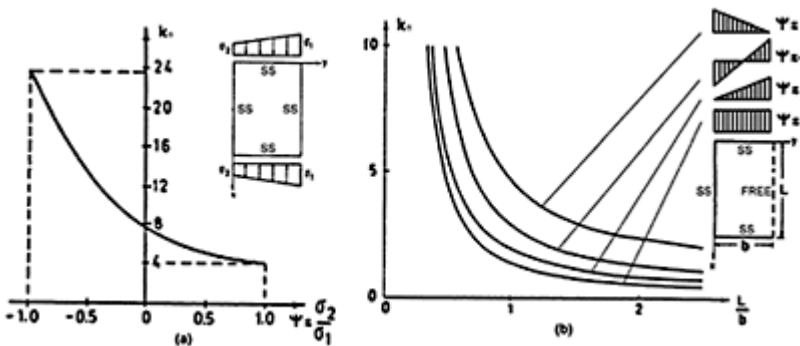


Figure 2.6 (Landolfo, 1992).

In particular, following von Karman's theory, b_{eff} is the width of a plate for which σ_{max} is equal to the elastic critical stress ($\sigma_{cr, b_{eff}}$), so that:

$$\sigma_{cr, b_{eff}} = \frac{k\pi^2 E}{12(1 - \nu^2) \left(\frac{b_{eff}}{t}\right)^2} = \sigma_{max} \quad (2.2)$$

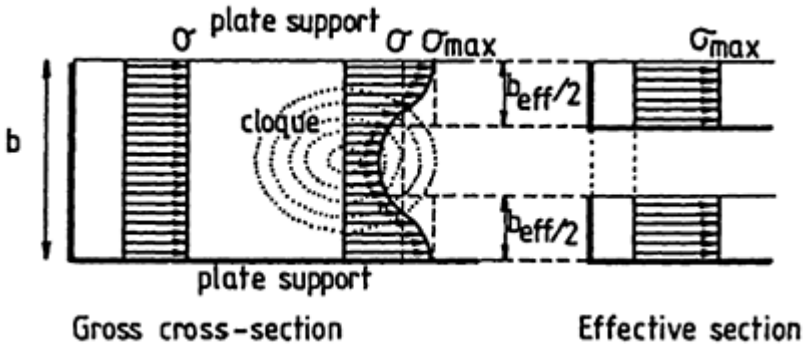


Figure 2.7 (Dubina and Vayas, 1995).

As a consequence, the normalized ultimate strength of a slender plate, without imperfection, may be easily obtained by considering equation (2.2) and substituting $\sigma_{max}=f_y$:

$$\bar{\sigma} = \frac{N_u}{N_y} = \frac{b_{eff}}{b} = \sqrt{\frac{\sigma_{cr}}{\sigma_{max}}} = \sqrt{\frac{\sigma_{cr}}{f_y}} = \frac{\lambda_1}{\lambda_p} = \frac{1}{\bar{\lambda}_p} \quad (2.3)$$

where $\lambda_1 = \pi\sqrt{E/f_y}$.

Winter (1949) modified equation (2.3) by taking into account geometrical and mechanical imperfections. On the basis of a large series of tests on cold-formed beams, the following formula for computing the effective width has been arrived at:

$$\frac{b_{eff}}{b} = \frac{1}{\lambda_p} \left(1 - \frac{0.22}{\bar{\lambda}}\right) \quad (2.4)$$

with:

$$\bar{\lambda}_p = \sqrt{\frac{f_y}{\sigma_{cr}}} = 1.052 \frac{b}{t} \sqrt{\frac{f_y}{k \cdot E}} \quad (2.5)$$

The equations of Winter (2.4), von Karman (2.3) and the critical curve of Euler (2.1) are plotted and compared in Figure 2.8 (Landolfo, 1992).

The expression (2.4) is now used in the Eurocode 3 (Part 1.3) (CEN, ENV 1993-1-3), the AISI Specification (AISI, 1996) and in other national codes for the design of cold-formed thin-walled steel members. A comprehensive appraisal of these European and American codes will be made in Chapters 3 and 5, respectively.

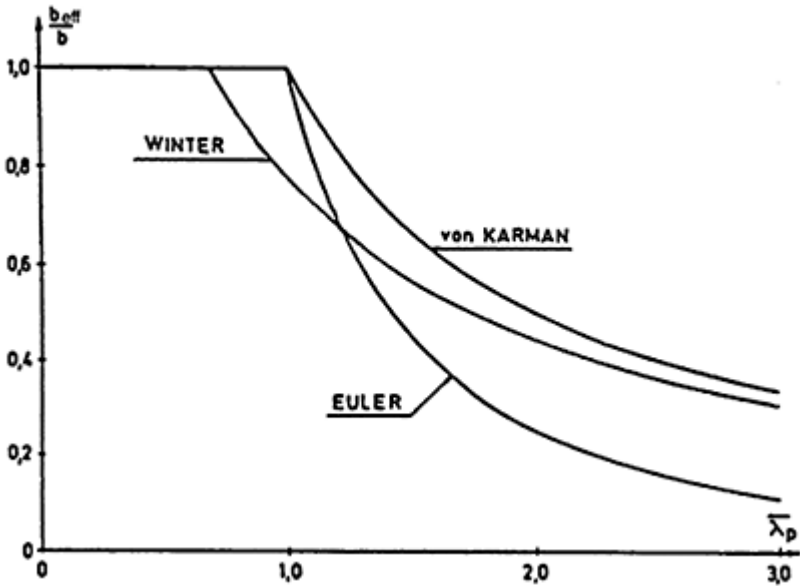


Figure 2.8 (Landolfo, 1992).

2.3 ALUMINIUM PLATE BUCKLING OVERVIEW

The onset and evolution of local instability phenomena are strictly connected to the mechanical behaviour of material, which may be of sharp-knee type (as in steel) or round-house type (as in aluminium alloys). The special hardening features of the latter can play a significant role in the post-critical behaviour of the plate elements which make up the section.

Several models have been proposed, in the technical literature, for modelling the stress-strain relationship of aluminium alloys (Mazzolani, 1995a, b): some of them employ discontinuous relationships, where different formulations are used for each portion of the diagram. Often, this approach is very complex because, although it

provides a very accurate approximation of the whole behaviour, it also creates difficulties for analytical and numerical studies.

Equation 2.6 describes a continuous model for round-house materials, proposed by Ramberg and Osgood (1943), which has enjoyed great success for many years:

$$\varepsilon = \frac{\sigma}{E} + \varepsilon_0 \left(\frac{\sigma}{f_{\varepsilon_0}} \right)^n \quad (2.6)$$

where:

E =the initial elastic modulus;

n =the hardening parameter of the material;

f_{ε_0} =the conventional elastic limit (usually assumed as the one related to the 0.2% offset proof stress= $f_{\varepsilon_0}=f_{0.2}$);

ε_0 =the corresponding residual deformation.

The exponent n of the Ramberg-Osgood law may be assumed as a material-characteristic parameter. As regards aluminium alloys, the hardening amount depends on several factors (namely, the chemical composition of the alloy, the fabrication process and the type of heat treatment). In particular, the latter is the most important, since it generally produces both an increase in strength and a decrease in hardening. As a matter of fact, n ranges from 8 to 15 for non-heat-treated alloys and from 20 to 40 for heat-treated alloys (Mazzolani, 1995a, b).

Similar to steel, the critical load for aluminium plates, which buckle in the elastic range, depends on the ratio of geometrical dimensions (b/t) and on the edge conditions, as well as on the properties of the basic material. Therefore, the elastic buckling stress ($\sigma_{cr,e}$) can be calculated by the well-known Euler formula (equation 2.1).

For a buckling load within the elastic-plastic range, the effect of the stress-strain relationship must be properly taken into account in determining the critical stress. More than 100 years ago, it became apparent that buckling in the inelastic range could be studied by the simpler tangent-modulus approach, first proposed by Engesser in late 1885 and then confirmed by Shanley in 1947 (Galambos, 1998). The tangent-modulus theory has been used for column members, but cannot easily be extended to different structural typologies. In particular, buckling analysis of plate elements in the plastic range is very complicated, and intuitive prediction of the physical behaviour is difficult. The main problem arises because of the irreversibility of plastic strain, which obliges us to formulate equations based on strain increments. However, when the load is nearly proportional, it is possible to use simple formulations, such as the deformation theory of plasticity.

Generally speaking, critical stress for inelastic buckling may be related to the elastic bifurcation stress by means of the following equation:

$$\sigma_{cr} = \eta \sigma_{cr,e} \quad (2.7)$$

where the non-dimensional factor η is a function of the shape of the stress-strain material curve, the stress state, the plate dimensions and the edge conditions.

Several theoretical approaches have been used in the technical literature to determine the plasticity factor η , expressed as a function of the initial elastic (E), tangent (E_t) and

secant (E_s) moduli. The most appropriate and frequently adopted formulations in the field of plate and shell stability are listed in Table 2.1 (Landolfo, 2000).

Table 2.1 Different formulations for the plasticity factor η

<i>Model</i>	<i>η factor</i>	<i>References</i> (see Ghersi and Landolfo, 1996)
1	E_t/E	Tangent modulus buckling curve
2	E_s/E	Stowell (1948), Bijlaard (1949), Vol'Mir (1965) and Gerard (1957)
3	$\sqrt{E_t/E}$	Bleich (1952), Vol'Mir(1965) and Pearson (1950)
4	$\sqrt{E_t/E_s}$	Radhakrishman (1956)
5	$\frac{\sqrt{E_t/E_s}}{E}$	Gerard (1962)
6	$\frac{E_s}{E} \sqrt{\frac{E_t}{E}}$	Weingarten et al. (1960)
7	$\frac{E_s}{E} \left(0.33 + 0.67 \sqrt{0.25 + 0.75 \frac{E_t}{E_s}} \right)$	Stowell (1948) and Bijlaard (1949)
8	$\frac{E_s}{E} \left(0.5 + 0.5 \sqrt{0.25 + 0.75 \frac{E_t}{E_s}} \right)$	Stowell (1948) and Gerard and Becker (1957)

Figure 2.9 (a, b) illustrates the non-dimensional buckling curves corresponding to η , evaluated using a Ramberg-Osgood-type law for material with $f_{0.2}=180$ MPa, $E=70,000$ MPa and two values of the strain-hardening ratio ($n=8$, valid for elastic-strain-hardening materials; $n=32$, valid for elastic-plastic materials) (Ghersi and Landolfo, 1996). In these curves, both critical stress and slenderness ratio have been normalized using $f_{0.2}$:

$$\bar{\sigma}_{cr} = \frac{\sigma_{cr}}{f_{0.2}}; \quad \bar{\lambda}_p = \frac{\lambda_p}{\sqrt{\pi^2 E / f_{0.2}}} \quad (2.8)$$

We can see that the differences between the different formulations of η are more evident in the case of strain-hardening materials (Figure 2.9a). For both $n=8$ and $n=32$, the curves are nearly always positioned between Curve 1 and Curve 2, with the exception of Curve

4, which provides particularly high values of $\bar{\sigma}_{cr}$ when $\bar{\lambda}_p$ is small.

Material non-linearity provides a similar effect on the ultimate strength of aluminium plate. This is apparent as soon as we observe that material non-linearity influences the plate critical stress. Moreover, this has also been

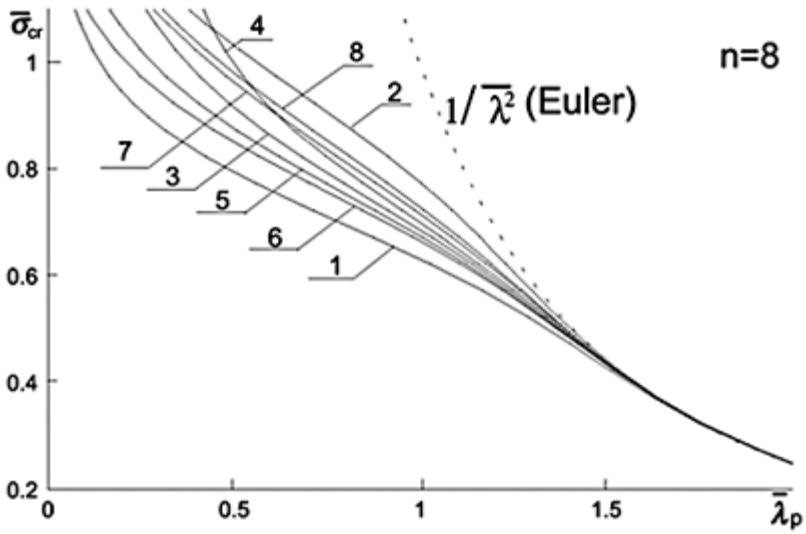


Figure 2.9a.

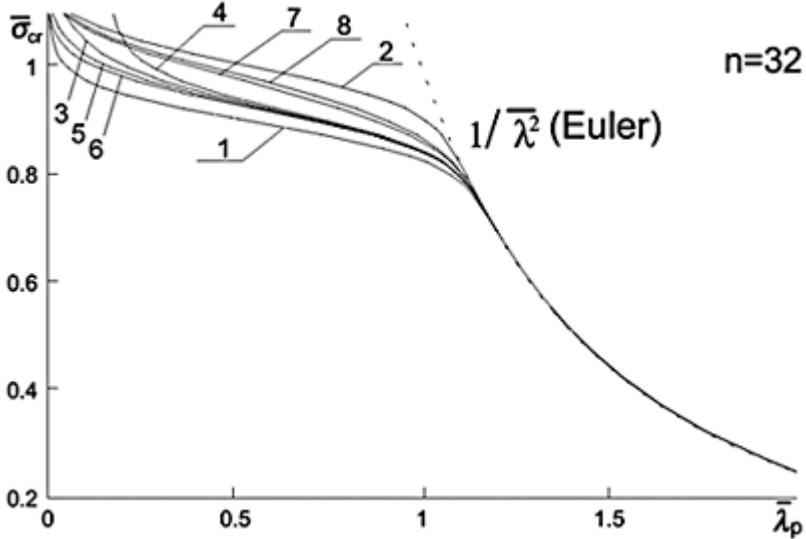


Figure 2.9b.

verified by experiments, which have led to strength curves that are different from carbon steel ones.

As for theoretical analysis, the effective-width approach can be extended to such materials, provided that plasticity factor η is properly accounted for in the evaluation of b_{eff} . For example, Figure 2.10 (a, b) (Gherzi and Landolfo, 1996) shows the effect of material non-linearity on the normalized ultimate strength ($\bar{\sigma} = \sigma_c / f_{0.2}$) of perfect plates for two different values of hardening and for each of the n factor formulations given in Table 2.1. In this example, the Ramberg-Osgood relationship has been used once again, with conventional elastic limit $f_{0.2} = 180$ MPa and $E = 70,000$ MPa. The effect of material non-linearity according to these theoretical models is clear

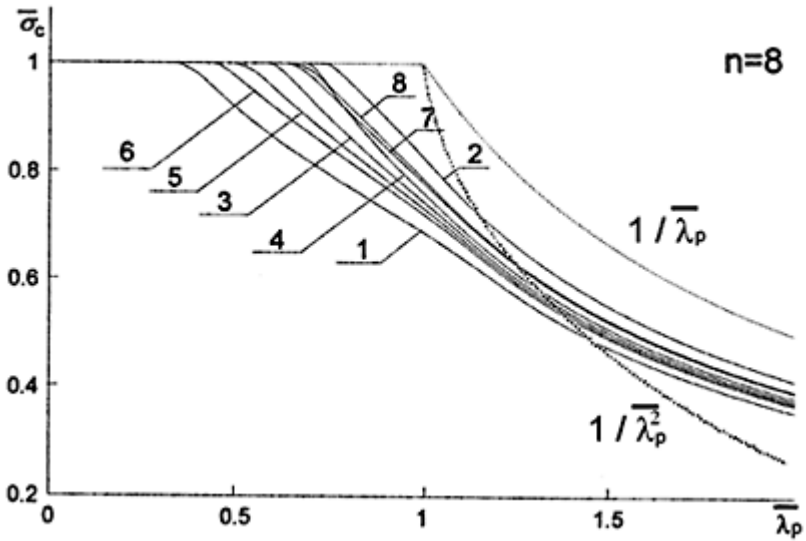


Figure 2.10a.

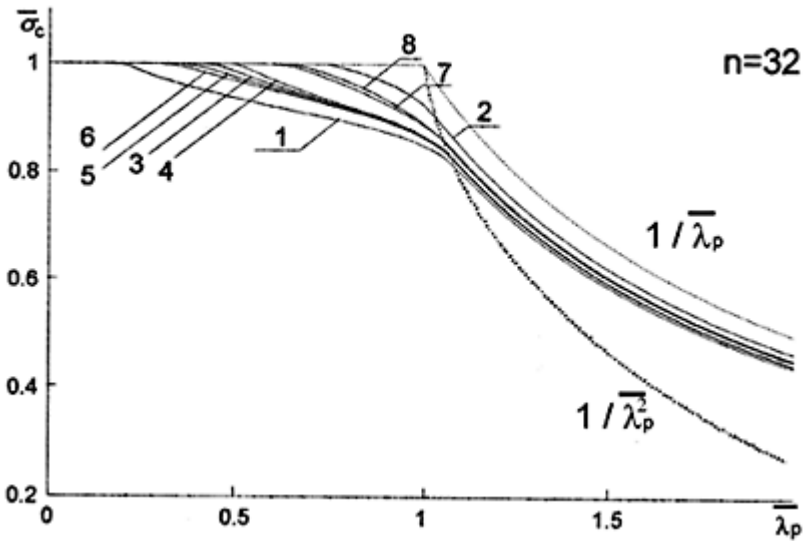


Figure 2.10b.

(see Table 2.1) and, so, we need to distinguish the post-critical behaviour of materials with different stress-strain relationships.

Obviously, we expect the influence of material non-linearity on single-plate element buckling to be reflected, to a similar extent, in the response of slender cross-sections, whose structural behaviour is affected by local buckling arising in compressed parts.

A comprehensive study on this was carried out by Gherzi and Landolfo (1996). By means of a scope-oriented simulation model, based on the effective-width approach, they investigated the effect of material hardening, buckling models and geometrical and mechanical imperfections on the flexural response of aluminium thin-walled sections. Figure 2.11 shows the moment-curvature relationships provided by the aforementioned simulation models for some aluminium box sections. These curves were obtained by describing material behaviour using the Ramberg-Osgood law with $f_{0.2}=180$ MPa. Different values of the exponent n (8, 16, 32), together with an elastic-perfectly plastic law ($n=\infty$), were used in order to check the influence of the strain hardening ratio. As far as local buckling phenomena are concerned, they were accounted for by assuming model 1 of η -factor (see Table 2.1).

Moment and curvature were normalized by assuming:

$$\bar{\chi} = \frac{\chi}{\chi_{0.2}}; \quad \bar{M} = \frac{M}{M_{0.2}}$$

where:

$M_{0.2}=f_{0.2}W$ is the conventional elastic moment;

$\chi_{0.2}=2f_{0.2}/Eh$ is the curvature corresponding to the strain $f_{0.2}/E$;

W =is the section modulus;

b =the height of the cross-section.

For the sake of comparison, curves corresponding to the behaviour of the same aluminium box sections, but ignoring local instability phenomena, are also plotted. Note that, in this case, the section strength is scarcely influenced by the value of exponent n . On the contrary, the slope of the

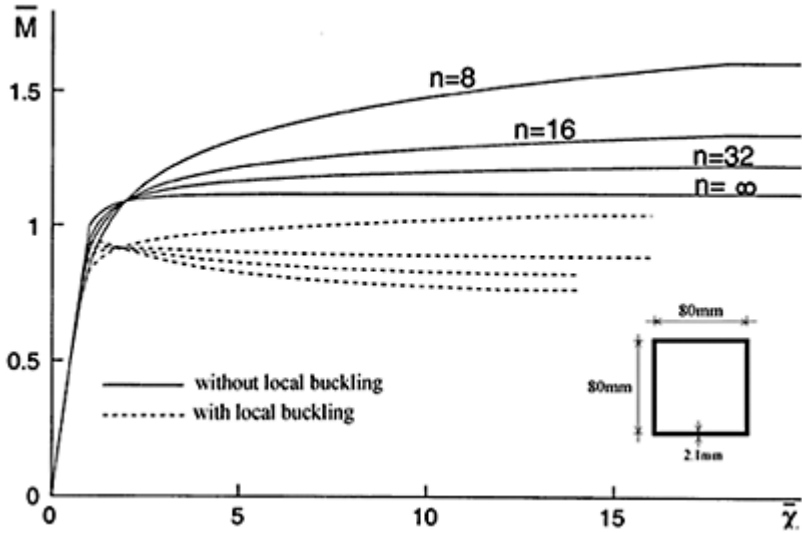


Figure 2.11.

post-buckling branch is strongly connected with hardening, which compensates for the lowering behaviour due to buckling.

The above considerations emphasize the importance of properly setting up the design curves for local buckling phenomena, by considering material properties as well.

On the other hand, this behavioural difference has been recognized worldwide and it has been taken on board by every relevant structural code. Figure 2.12 shows the

normalized design curves (with $\bar{\sigma} = \sigma_c / f_{0.2}$), proposed by Jombock and Clark (1968), for predicting the ultimate strength of aluminium plates. According to their model, aluminium alloys are classified into two categories (artificially and not artificially aged). The buckling stress and ultimate strength are coincident in the inelastic range,

where the $\bar{\sigma} - \bar{\lambda}_p$ relationship is represented by means of a linear law, while a non-linear relationship (with $\sigma_c > \sigma_{cr}$) is provided for evaluating the strength in the elastic range. These results were used in the USA, during the 1970s, as the basis for the Aluminium Association Code.

In Europe, at the beginning of the 1980s, a research program was developed at Cambridge University with the aim of setting up a calculation method for aluminium plate elements under compression. A basic behavioural distinction was made between

internal elements, supported at both longitudinal edges, and outstand elements, supported at one edge only with the other edge free.

The design of internal elements was based on the definition of four theoretical strength curves, all corresponding to a simply supported free-pull in edge condition (see the normalized representation of Figure 2.13 and

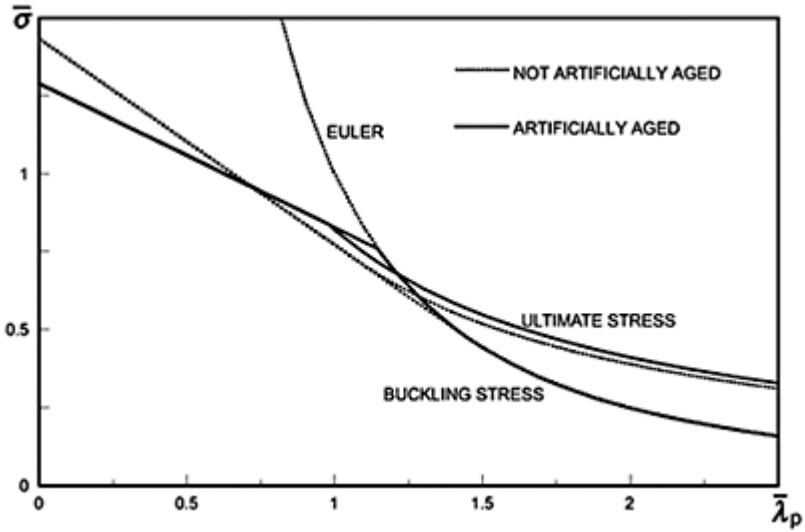


Figure 2.12.

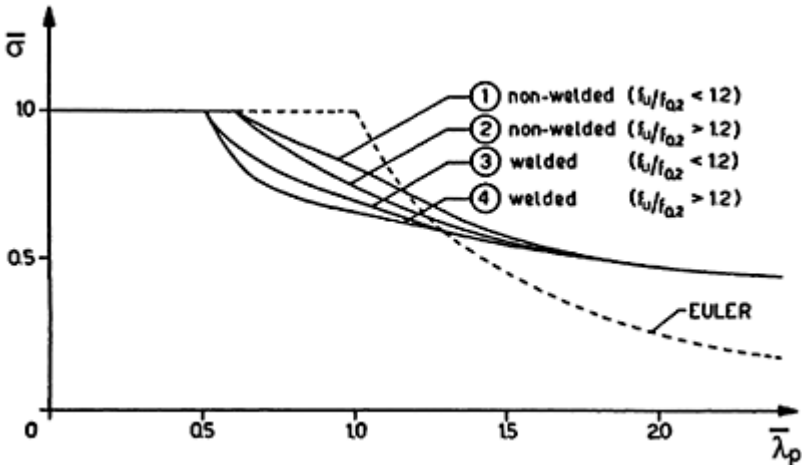


Figure 2.13 (Mazzolani, 1995).

the comparison with experimental data of Figure 2.14). They cover both welded (3 and 4) and non-welded (1 and 2) plates made of heat-treated ($n=15, f_u/f_{0.2} < 1.2$) and non-heat-treated ($n=8, f_u/f_{0.2} > 1.2$) alloys (Mazzolani, 1995). In the case of welded elements, both severely out-of-flatness and residual-stress distributions were considered. In the case of sections with outstand elements, many test results on short aluminium columns showed that all the experimental points were positioned above the theoretical curves for non-welded internal elements (1 and 2), because of the presence of the outstand. Furthermore,

in the case of beams with slender outstands ($\bar{\lambda}_p > 1.5$), which tend to fail more suddenly than webs due to the shedding of load from the free edges, the compressive stress in the outstand was limited to σ_{cr} , rather than σ_c .

On the basis of the research carried out in Cambridge, three design curves A, B, C, which cover both internal and outstand elements (welded and non-welded) belonging to all kinds of aluminium-alloy columns and beams, were proposed by Dwight and Moffin (1982) (Figure 2.15).

The highest curve (Curve A) corresponded to outstand elements in columns; Curve B represents the average of Curves 1 and 2 of Figure 2.13, while Curve C is virtually equivalent to Curve 4. They correspond to the following cases: Curve A for non-welded outstand elements; Curve B for non-welded internal elements and welded outstand elements; Curve C for welded internal elements. These curves, shown in Figure 2.15, may be represented by the empirical non-dimensional equation given by:

$$\bar{\sigma} = 1.1 \left(\frac{1}{\lambda_p} - \frac{p}{\lambda_p^2} + \frac{q}{\lambda_p^3} \right) \tag{2.9}$$

where p and q are numerical coefficients whose values are reported in Figure 2.15.

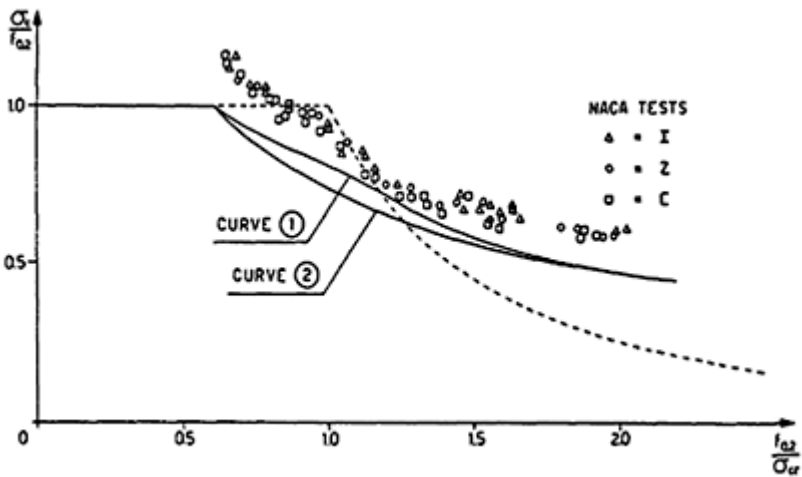


Figure 2.14 (Mazzolani, 1995).

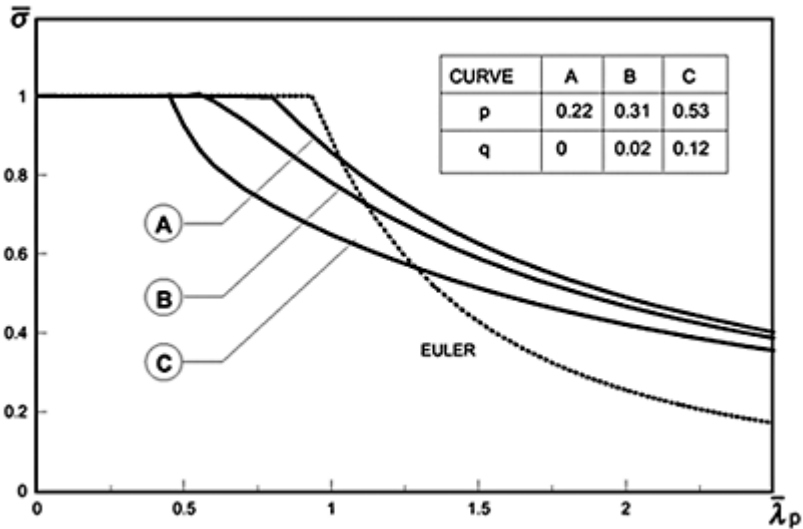


Figure 2.15.

Despite these results, the same authors, in a subsequent paper (Dwight and Moffin, 1984) about new results from a theoretical and experimental research program on the buckling strength of individual aluminium plate in compression, suggested use of a unified non-dimensional plate strength curve for all material types. However, such a conclusion has to be regarded as an attempt to simplify the approach, bearing in mind the considerable variation between plates made of different aluminium alloys, which has been observed experimentally.

The up-to-date version of the British Code of Practice for Structural Aluminium (BS 8118, 1991) was at the time of publication one of the most modern specifications in this field, because it was written in limit-state format and provided advanced calculation methods. First, a classification of cross-sections was assessed according to the slenderness of their parts, this was then divided into internal or outstand elements, either unreinforced or reinforced by means of stiffening ribs or lips.

The effect of local buckling in slender members was allowed for by replacing the true section by an effective one, obtained by using the local buckling coefficient k_L to factor down the thickness of any slender element that is wholly or partly in compression. The coefficient k_L is provided through standard curves as a function of the factor β/ϵ , where β is a slenderness parameter, depending on both the b/t ratio and the stress gradient of the element concerned, and $\epsilon = (250/f_{0.2})^{0.5}$. The design curves given by BS 8118 are shown in Figure 2.16 for welded or non-welded internal and outstand elements and for round tubes.

The convenor of the BS Committee Dr Bulsony emphasized that 'the reduced thickness concept has no physical meaning and used unwisely can lead to confusion and

subsequent error. However, for better or for worse this approach has been used in BS 8118.'

In order to compare the actually codified design curves (k_L versus β/ϵ) with those proposed by Cambridge University ($\bar{\sigma}$ versus $\bar{\lambda}_p$), it is necessary to define the factor k_L , which is equivalent to the non-dimensional strength of the plate $\bar{\sigma}$, together with the relationship between $\bar{\lambda}_p$ and β/ϵ . With

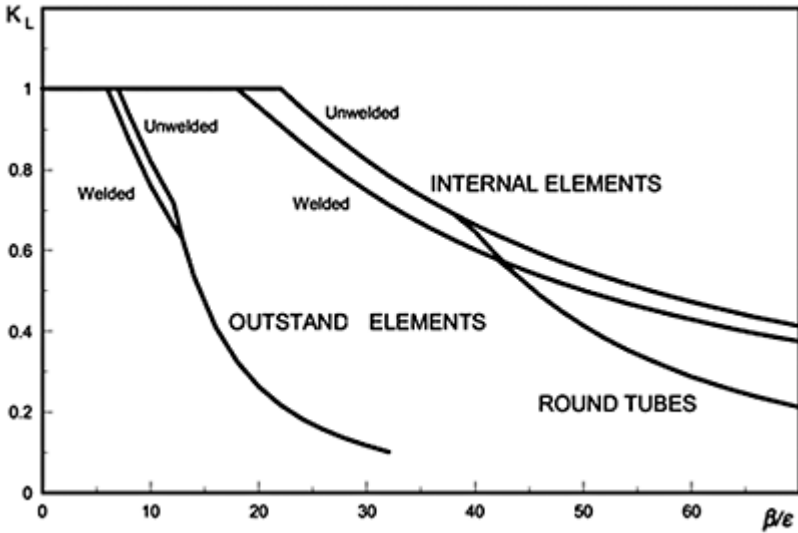


Figure 2.16.

regard to unreinforced flat elements under uniform stress, for which $\beta=b/t$, the following equations have been derived from equations (2.7) and (2.8), by assuming $\nu=0.3$ along with buckling coefficients $k_\sigma=4$ and $k_\sigma=0.425$ for internal and projecting elements, respectively:

$$\text{Internal elements } \bar{\lambda}_p = 0.25 \sqrt{250/E} \frac{B}{\epsilon} \tag{2.10}$$

$$\text{Outstand elements } \bar{\lambda}_p = 1.61 \sqrt{250/E} \frac{B}{\epsilon} \tag{2.11}$$

The aforementioned comparison between $E=70,000\text{MPa}$ and $f_{0.2}= 250 \text{ MPa}$ is shown in Figure 2.17.

In the case of internal elements, note that the codified curve for unwelded elements is very close to the corresponding Curve B. On the contrary, in the case of welded elements the scatter between the codified curves and Curve C is quite relevant in the range 0.5

$\bar{\lambda}_p < 1.25$.

For outstand elements, the differences appear to be significant in both welded and unwelded elements, the codified curve always being more conservative.

Furthermore, we can see that, for internal unwelded elements, the BS 8118 design curve can be expressed as a function of $\bar{\lambda}_p$, by the following equation:

$$k_L = \frac{1}{\bar{\lambda}_p} \left(1 - \frac{0.22}{\bar{\lambda}_p} \right) \tag{2.12}$$

Such a relationship is coincident with Winter's formulation (2.4), which is commonly used, in the American and European Codes for cold-formed steel sections, for evaluating the effective width ratio (see Section 2.2).

For a welded internal element, the design curve can be derived from the same equation (2.12) by assuming a reduction factor equal to 1/1.1. As far as outstand elements are concerned, other than the range in slenderness where the critical curve is directly assumed, the design curve for unwelded elements fits Winter's formulation with good approximation, while greater scatter can be seen in the case of welded elements.

According to these results, we can conclude that, for unwelded elements, the relationship, given the thickness reduction in slender elements according to BS 8118, is substantially the same as those used in the most advanced codes for cold-formed steel profiles for determining the effective width of the element. Such an assessment can be extended to welded elements, provided that an appropriate reduction factor is introduced in Winter's formulation.

Comparisons between the predicted capacities of aluminium members, evaluated on the basis of the above methods together with several experimental results, have confirmed these assumptions.

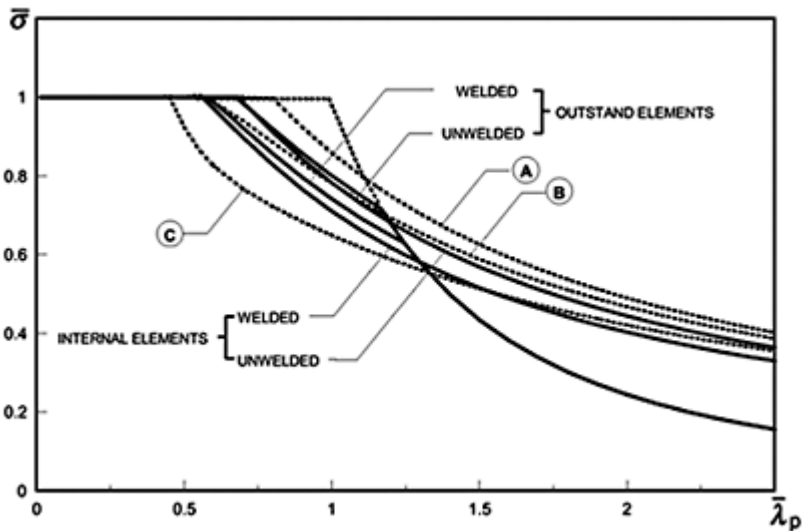


Figure 2.17.

The above considerations emphasize the importance of properly setting up design curves for local buckling phenomena, by also considering material properties. This was done in Landolfo and Mazzolani (1998), where the imperfection factor was determined in relation to the material properties and manufacturing process, as well as in agreement with existing experimental results. In particular, three design curves were identified that completely characterize the buckling behaviour of aluminium plates; they correspond to the following cases:

- A unwelded plates in heat-treated alloy ($n > 10$);
- B welded plates in heat-treated alloy ($n > 10$) and unwelded plates in non-heat-treated alloy ($n \leq 10$);
- C welded plates in non-heat-treated alloy ($n \leq 10$).

These curves, shown in Figure 2.18, can be expressed in non-dimensional form by the following equation:

$$\bar{\sigma} = (\omega_1 \bar{\lambda}_p)(1 - \omega_2 / \bar{\lambda}_p) \tag{2.13}$$

where ω_1 and ω_2 are numerical coefficients, whose values are reported in the Table 2.2 together with the limit value of normalized slenderness ($\bar{\lambda}_0$) which corresponds to $\bar{\sigma} = 1$.

For Curve A, such relationships are coincident with Winter’s formulation, which is assumed in the American and European Codes on cold-formed steel

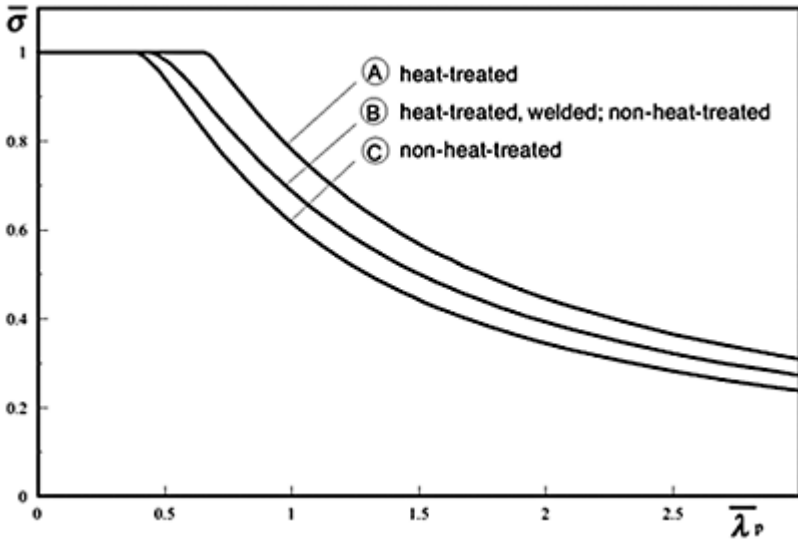


Figure 2.18

Table 2.2 Numerical coefficients for the buckling curves

<i>Curve</i>	ω_1	ω_2	$\bar{\lambda}_0$
A	1.00	0.22	0.673
B	0.88	0.22	0.440
C	0.76	0.19	0.380

sections for determining the effective width ratio. For the others, a similar structure is kept, by assuming appropriate equivalent reduction factors in Winter's formulation. This approach was used to check slender sections in the 1998 version of Eurocode 9 (CEN, ENV 1999-1-1). These provisions will be illustrated in Chapter 4.

3

Eurocode 3

3.1 BACKGROUND

The European code for the design of steel structures, Eurocode 3, provides in Part 1.1 (CEN, ENV 1993-1-1) general rules for structures and specific rules for buildings. In addition, Part 1.3 (CEN, ENV 1993-1-3) provides supplementary rules for cold-formed thin-gauge members and sheeting.

A cross-section can be classified according to its capability to reach the limit states defined in Chapter 2 (elastic buckling limit state, elastic limit state, plastic limit state, collapse limit state). Such a classification refers both to the strength and to the capability of getting into the plastic range and is strongly related to the influence of local buckling. The European code defines four classes, as follows:

- 1 *ductile cross-sections*, which can develop collapse resistance without the problem of local buckling and with full exploitation of the hardening properties of the material, until reaching the ultimate value of deformation (collapse limit state);
- 2 *compact cross-sections*, which are capable of developing ultimate plastic resistance without fully exploiting the hardening properties of material, which is prevented by the onset of plastic instability phenomena (plastic limit state);
- 3 *semi-compact cross-sections*, which can develop the elastic limit resistance only without getting into inelastic range, owing to instability phenomena which prevent the development of important plastic deformations, giving rise to a substantially brittle behaviour (elastic limit state);
- 4 *slender cross-sections*, whose strength is governed by the occurrence of local buckling phenomena, which produce a reduction in effective resistance, giving rise to a remarkably brittle behaviour (elastic buckling limit state).

Cross-sections belong to one of the above classes depending on the proportions of each of their compression elements (plane elements that are either totally or partially in compression, due to axial force or bending moment, under the load combination considered). In general, different compression elements in a cross-section (such as webs or flanges) can belong to different classes. In the absence of a more precise criterion, cross-sections shall be classified in the least favourable class of its compression elements.

Part 1.1 of Eurocode 3 defines limit values of the slenderness b/t of an element, based on the stress distribution (uniform or variable) and the mutual restraint between adjoining elements (internal or projecting elements). Specific rules are provided to evaluate the effective width of compression elements of Class 4 cross-sections.

Part 1.3 considers that, in most cases, the cross-sections of cold-formed thin-gauge members belong to Class 4, because of the thin gauge of the sheeting they are made of. Furthermore, it considers that the sheeting is often folded so as to obtain edge or

intermediate stiffeners, necessary to reduce the effect of local buckling. The rules for calculating the effective width of compression elements are thus integrated by provisions for plane elements with edge or intermediate stiffeners. Specific formulations are also provided for trapezoidal sheeting in order to evaluate the reduced effective area of intermediate stiffeners in flanges and webs.

3.2 MATERIAL PROPERTIES

Part 1.3 of Eurocode 3 provides a list of the minimum values of ultimate tensile strength f_u and basic yield strength f_{yb} for structural steels conforming to the European and International Standards (Table 3.1).

A specific problem of cold-formed elements is that yield strength can locally increase because of cold working. Eurocode 3, therefore, defines the average yield strength f_{ya} , which may be determined from the results of full-size tests or by the expression

$$f_{ya} = f_{yb} + \frac{knt^2}{A_g} (f_u - f_{yb}) \quad \text{but} \quad f_{ya} \leq \frac{f_u + f_{yb}}{2} \quad (3.1)$$

where:

t =the material thickness before cold-forming (mm);

A_g =the gross cross-section area (mm²);

k =a numerical coefficient that depends on the type of forming as follows ($k=7$ for cold-rolling and $k=5$ for other methods of forming);

n =the number of 90° bends in the cross-section with an internal radius $r \leq 5t$ (fractions of 90° bends should be counted as fractions of n).

Table 3.1 Nominal values of basic yield strength f_{yb} and ultimate tensile strength f_u (CEN, ENV 1993–1–3)

<i>Type of steel</i>	<i>Standard</i>	<i>Grade</i>	f_{yb} (N/mm ²)	f_u (N/mm ²)
Hot-rolled steel	EN 10025	S 235	235	360
sheet of structural quality		S 275	275	430
		S 355	355	510
Hot-rolled steel	EN 10113:	S 275 N	275	370
sheet of high-yield strength of structural quality	Part 2	S 355 N	355	470
		S 420 N	420	520
		S 460 N	460	550
	EN 10113:	S 275 M	275	360
	Part 3	S 355 M	355	450

		S 420 M	420	500
		S 460 M	460	530
Cold-reduced steel	ISO 4997	CR 220	220	300
sheet of structural		CR 250	250	330
quality		CR 320	320	400
Continuous hot-dip	EN 10147	FeE 220 G	220	300
zinc-coated carbon		FeE 250 G	250	330
steel sheet of		FeE 280 G	280	360
structural quality		FeE 320 G	320	390
		FeE 350 G	350	420
High-yield strength	prEN 10149:	S 315 MC	315	390
steels for cold	Part 2	S 355 MC	355	430
forming		S 420 MC	420	480
		S 460 MC	460	520
		S 500 MC	500	550
		S 550 MC	550	600
	prEN 10149:	S 260 NC	260	370
	Part 3	S 315 NC	315	430
		S 355 NC	355	470
		S 420 NC	420	530

According to Eurocode 3 provisions, the resistance of the cross-section shall be calculated using the average yield strength when the section is fully effective and the basic yield strength when local buckling reduces the resistance of any compression element of the section. The increase in yield strength due to cold forming shall not be utilized for members that are subjected to heat treatment after forming.

3.3 SECTION PROPERTIES

A peculiarity of cold-formed sections is the presence of rounded corners. Eurocode 3 requests us to refer to the notational flat width b_p of each plane

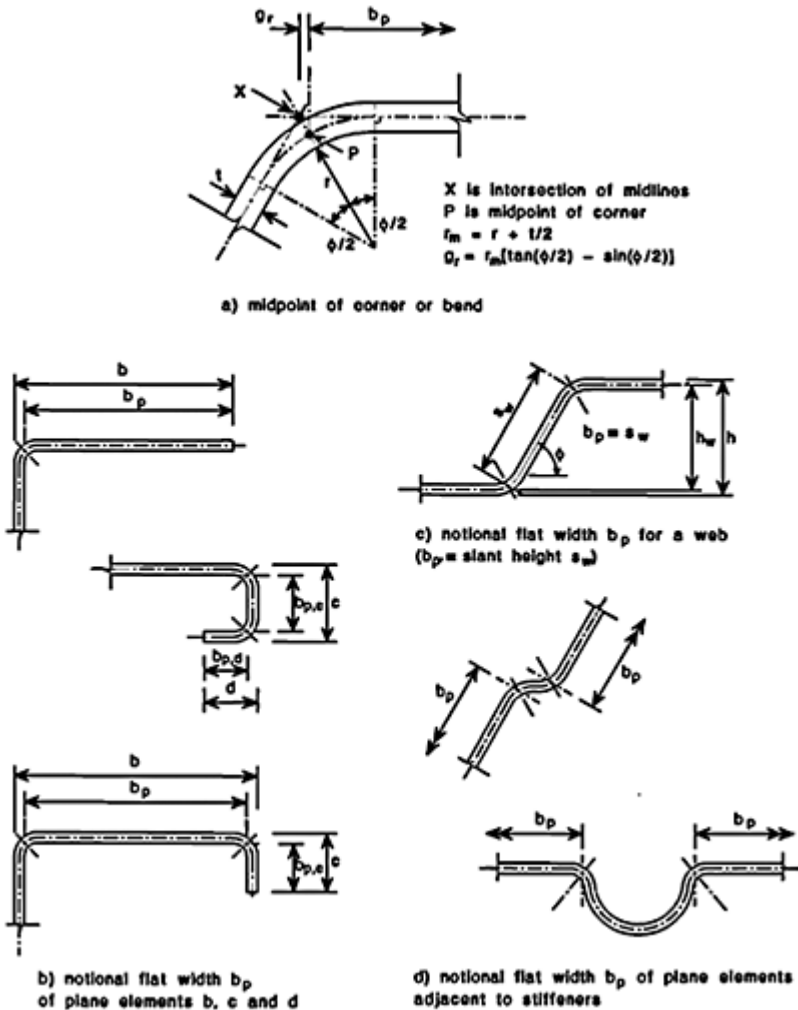


Figure 3.1 (CEN, ENV 1993-1-3, 1996).

element, measured from the midpoints of adjacent corner elements (Figure 3.1).

According to code provisions, the influence of rounded corners with internal radius $r \leq 5t$ and $r \leq 0.15b_p$ on section properties can be ignored, and the cross-section can be assumed to consist of plane elements with sharp corners. However, the computer program presented in Chapter 7 always considers the actual geometry of the cross-section as having rounded corners.

The provisions of Part 1.3 of Eurocode 3 should only be applied to cross-sections within the range of width-to-thickness ratios for which sufficient

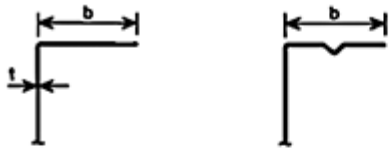
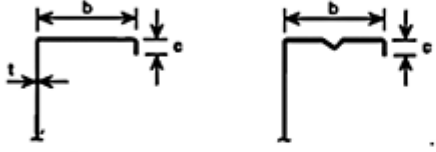
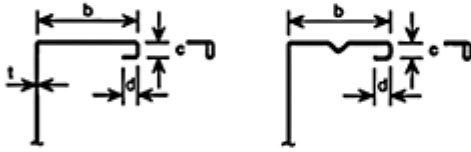
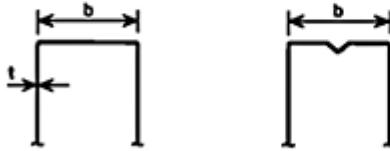
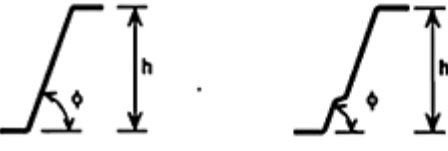
Element of cross-section		Maximum value
		$b/t \leq 50$
		$b/t \leq 60$
		$b/t \leq 90$
		$b/t \leq 500$
		$45^\circ \leq \phi \leq 90^\circ$ $h/t \leq 500 \sin \phi$

Figure 3.2 (CEN, ENV 1993–1–3, 1966).

experience and verification by testing is available, as shown in Figure 3.2. The computer program presented in Chapter 7 checks these limits, so as to warn the user, but it may be forced to calculate the member resistance also when the limits are exceeded.

3.4 LOCAL BUCKLING

3.4.1 General

As discussed in Section 2.2, the effect of local buckling on each compression element of the cross-section shall be taken into account by replacing the non-uniform distribution of

stress, arising in the post-buckling range, with a uniform distribution of the maximum stress acting on a reduced portion of the element, having the same thickness but a reduced width (effective width). The effective width of each compression element, or each portion of element between adjacent corner elements or stiffeners, shall be calculated based on formulas obtained by the theory of steel-plate buckling. Edge and intermediate stiffeners shall be analysed assuming that they behave as compression members with continuous elastic restraint, having spring stiffness dependent on the flexural stiffness of the adjacent elements.

3.4.2 Plane elements without stiffeners

The effective width b_{eff} of a compression element is evaluated as:

$$b_{eff} = \rho b_p \quad (3.2)$$

that is, by means of a reduction factor ρ based on the largest compressive stress $\sigma_{com,Ed}$ acting in the element when the resistance of the cross-section is reached.

When $\sigma_{com,Ed} = f_{yb} / \gamma_{M1}$, the reduction factor ρ should be obtained from the following expressions:

$$\rho = 1.0 \quad \text{if } \bar{\lambda}_p \leq 0.673$$

$$\rho = \frac{1.0 - 0.22/\bar{\lambda}_p}{\bar{\lambda}_p} \quad \text{if } \bar{\lambda}_p > 0.673 \quad (3.3)$$

as a function of the plate slenderness $\bar{\lambda}_p$ given by:

$$\bar{\lambda}_p = \sqrt{\frac{f_{yb}}{\sigma_{cr}}} = \frac{b_p}{t} \sqrt{\frac{12(1-\nu^2)f_{yb}}{\pi^2 E k_\sigma}} \cong 1.052 \frac{b_p}{t} \sqrt{\frac{f_{yb}}{E k_\sigma}} \cong \frac{b_p/t}{28.4 \varepsilon \sqrt{k_\sigma}} \quad (3.4)$$

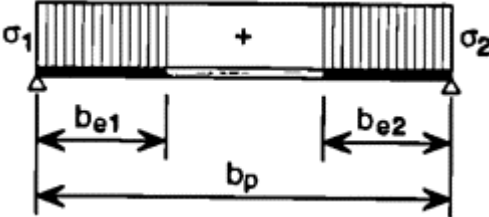
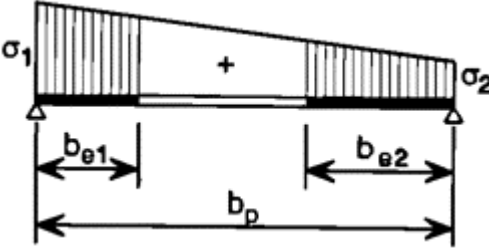
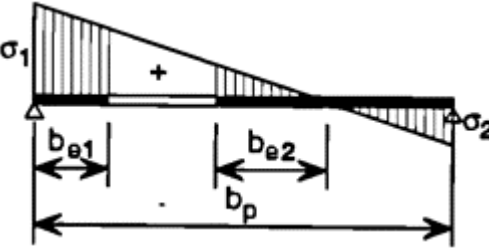
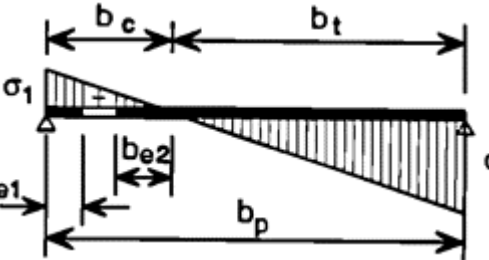
where:

k_σ = the buckling factor, which depends on the stress distribution and the boundary conditions (see Tables 3.2 and 3.3);

ε = the ratio $\sqrt{235/f_{yb}}$ with f_{yb} in N/mm².

In the case of doubly supported compression elements subject to non-uniform stress distribution, the effective width b_{eff} shall be divided in two different portions, b_{e1} and b_{e2} , according to the criteria described in the abovementioned tables.

Table 3.2 Reduction factor for doubly supported compression elements (CEN, ENV 1993-1-3, 1996)

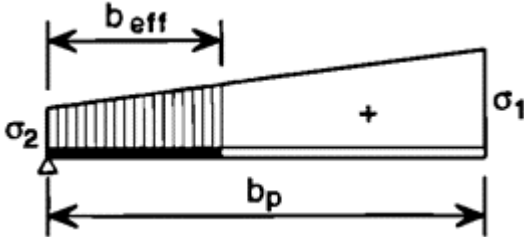
Stress distribution [compression positive]		Effective width b_{eff}				
		$\psi = +1$ $b_{eff} = \rho b_p$ $b_{e1} = 0.5 b_{eff}$ $b_{e2} = 0.5 b_{eff}$				
		$+1 > \psi \geq 0$ $b_{eff} = \rho b_p$ $b_{e1} = \frac{2 b_{eff}}{5 - \psi}$ $b_{e2} = b_{eff} - b_{e1}$				
		$0 > \psi \geq -1$ $b_{eff} = \rho b_p$ $b_{e1} = 0.4 b_{eff}$ $b_{e2} = 0.6 b_{eff}$				
		$\psi < -1$ $b_{eff} = \rho b_p$ $b_{e1} = 0.4 b_{eff}$ $b_{e2} = 0.6 b_{eff}$				
$\psi = \sigma_2 / \sigma_1$	+1	+1 > ψ > 0	0	0 > ψ > -1	-1	-1 > ψ > -3
Buckling factor k_σ	4.0	$\frac{8.2}{1.05 + \psi}$	7.81	$7.81 - 6.29\psi + 9.78\psi^2$	23.9	$5.98(1 - \psi)^2$
Alternatively, for $+1 \geq \psi \geq -1$:						

$$k_{\sigma} = \frac{16}{\sqrt{(1 + \psi)^2 + 0.112(1 - \psi)^2} + (1 + \psi)}$$

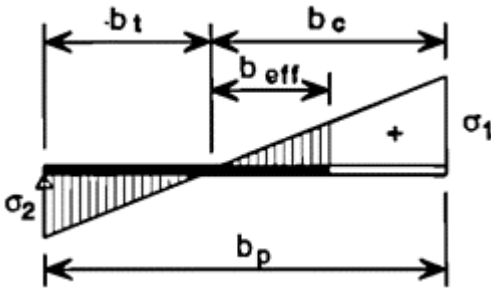
Table 3.3 Reduction factor for projecting compression elements (CEN, ENV 1993-1-3, 1996)

Stress distribution [compression positive]

Effective width b_{eff}



$$+1 > \psi > 0 \quad b_{eff} = \rho b_p$$



$$\psi < 0 \quad b_{eff} = \rho b_c$$

$$\psi = \sigma_2 / \sigma_1$$

+1

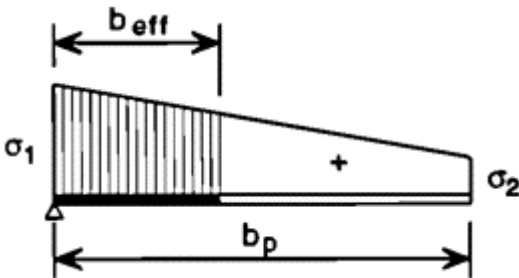
0 -1 +1 > psi > -1

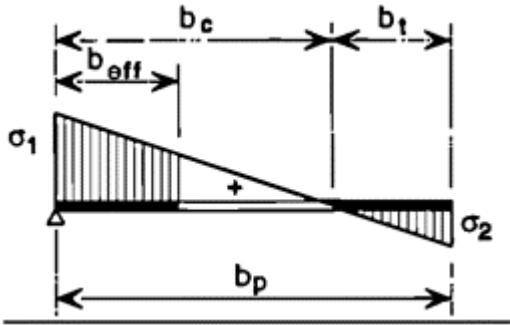
Buckling factor k_{σ}

0.43

0.57 0.85 $0.57 - 0.21\psi + 0.007\psi^2$

$$+1 > \psi > 0 \quad b_{eff} = \rho b_p$$





$$\psi < 0 \quad b_{\text{eff}} = \rho b_c$$

$\psi = \sigma_2 / \sigma_1$	+1	+1 > ψ > 0	0	0 > ψ > -1	-1
Buckling factor k_σ	0.43	$\frac{0.578}{\psi + 0.34}$	1.70	$1.70 - 5\psi + 17.1\psi^2$	23.8

If $\sigma_{\text{com.Ed}} < f_{yb} / \gamma_{M1}$, the reduction factor ρ should be determined as a function of reduced plate slenderness $\bar{\lambda}_{p,\text{red}}$:

$$\bar{\lambda}_{p,\text{red}} = \bar{\lambda}_p \sqrt{\frac{\sigma_{\text{com.Ed}}}{f_{yb} / \gamma_{M1}}} \quad (3.5)$$

from the expressions:

$$\rho = 1.0 \quad \text{if } \bar{\lambda}_{p,\text{red}} \leq 0.673$$

$$\rho = \frac{1.0 - 0.22 / \bar{\lambda}_{p,\text{red}}}{\bar{\lambda}_{p,\text{red}}} + 0.18 \frac{\bar{\lambda}_p - \bar{\lambda}_{p,\text{red}}}{\bar{\lambda}_p - 0.6} \quad \text{but } \rho \leq 1.0 \quad \text{if } \bar{\lambda}_{p,\text{red}} > 0.673 \quad (3.6)$$

3.4.3 Plane elements with edge or intermediate stiffeners

The design of compression elements with edge or intermediate stiffeners requires a double-step procedure.

First, the effective widths of the elements shall be evaluated considering each element restrained by the adjacent elements or stiffeners. Specific values of the buckling coefficient k_σ are provided in Part 1.3 for outstand elements with a single— or double-edge fold (Figure 3.3a, b):

$$k_\sigma = 0.5 \quad \text{if } b_{p,c} / b_p \leq 0.35$$

$$k_\sigma = 0.5 + 0.83 \sqrt[3]{(b_{p,c} / b_p - 0.35)^2} \quad \text{if } 0.35 < b_{p,c} / b_p \leq 0.6 \quad (3.7)$$

Second, each stiffener shall be considered as a compression member with continuous partial restraint, subject to the risk of buckling. The cross-section of this member is constituted by the rounded corner and by the

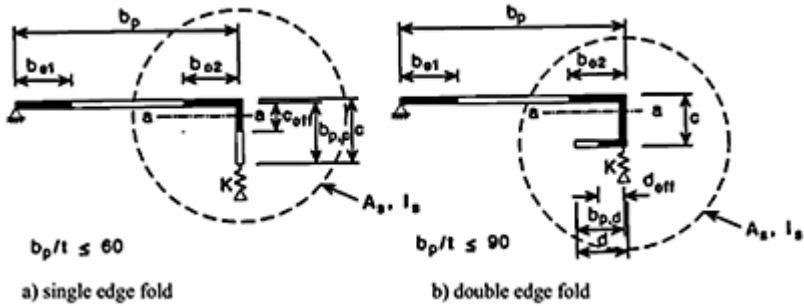


Figure 3.3 CEN, ENV 1993-1-3, 1996).

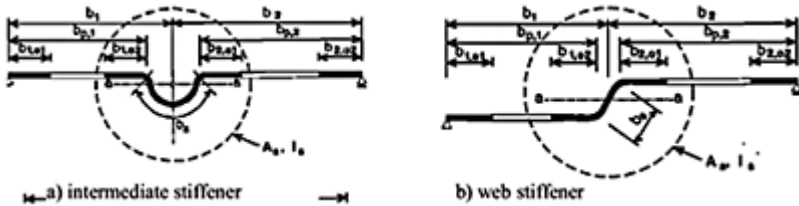


Figure 3.4 CEN, ENV 1993-1-3, 1996).

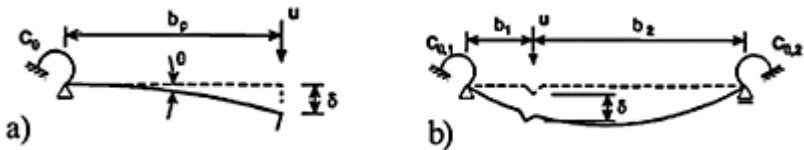


Figure 3.5 (CEN, ENV 1993-1-3, 1996).

adjacent effective portions of the elements connected to the stiffeners, as shown in Figure 3.3 (a, b) for edge stiffeners and in Figure 3.4 (a, b) for intermediate stiffeners.

The spring stiffness $K=u/\delta$ should be determined by applying a unit load per unit length u , as illustrated in Figure 3.5 (a) for edge stiffeners and in Figure 3.5 (b) for intermediate stiffeners.

In the case of edge stiffeners, the computer program assumes that the rotational spring stiffness C_θ depends on the geometry of the adjacent element:

$$C_\theta = \frac{\alpha E t^3}{12(1 - \nu^2) b_{p,ad}} \quad (3.8)$$

where $b_{p,ad}$ is the notational flat width of the adjacent element.

The coefficient a is equal to 3.0 in the case of bending moment or when the cross-section is made of more than three elements. It is equal to 2.0 in the case of uniform compression in cross-sections made of three elements, in order to take into account the effect of the stiffener at the other edge of the cross-section (Figure 3.6). The spring stiffness K is, thus, given by the expression:

$$K = \frac{0.25Et^3}{(1 - \nu^2)b_p^2(b_p + b_{p,ad}3/\alpha)} \tag{3.9}$$

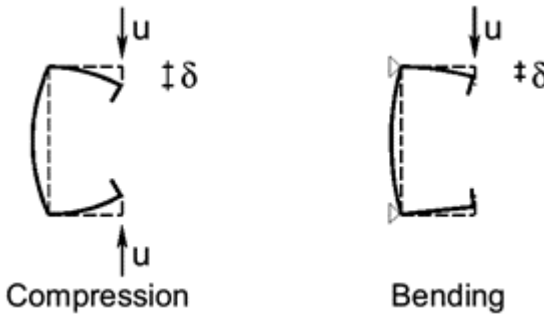


Figure 3.6.

In the case of intermediate stiffeners, the program follows the code suggestion to consider $C_{\theta,1}$ and $C_{\theta,2}$ equal to zero, thus assuming:

$$K = \frac{0.25(b_1 + b_2)Et^3}{(1 - \nu^2)b_1^2b_2^2} \tag{3.10}$$

The elastic critical buckling stress $\sigma_{cr,s}$ for the stiffener is:

$$\tau_{cr,s} = \frac{2\sqrt{KEI_s}}{A_s} \tag{3.11}$$

where:

K =the spring stiffness per unit length;

A_s =the effective cross-sectional area of the stiffener;

I_s =the effective second moment of area of the stiffener (i.e. that of its effective area about the centroidal axis $a-a$ of its effective section) (Figures 3.3 and 3.4).

The reduction coefficient χ for Ae flexural buckling of the stiffener is obtained from the general expressions of the design buckling resistance for axial compression (Part 1.1, 5.5.1, and Part 1.3, 6.2.1, of Eurocode 3), using buckling curve a_0 (imperfection factor $\alpha=0.13$) for the relative slenderness:

$$\bar{\lambda} = \sqrt{f_{yb}/\sigma_{cr,s}} \quad (3.12)$$

The reduced effective area of the stiffener is thus taken as:

$$A_{s,red} = \chi A_s \left[\frac{f_{yb}/\gamma_{M1}}{\sigma_{com,Ed}} \right] \quad (3.13)$$

in which $\sigma_{com,Ed}$ is the calculated stress at the centreline of the stiffener. In order to determine effective section properties, the reduced effective area is represented by using a reduced thickness $t_{red} = t A_{s,red}/A_s$ for all the elements included in the stiffener.

In the case of cross-sections subject to bending moment, this will require an iterative procedure, which will be repeated until the reduced effective area of the stiffener is sufficiently close to the value obtained from the previous iteration.

3.5 RESISTANCE OF CROSS-SECTIONS

3.5.1 Resistance under axial tension

The design tension resistance of a cross-section $N_{t,Rd}$ shall be determined by assuming that it is subjected to a uniform tensile stress equal to f_{yd}/γ_{M0} (average yield strength):

$$N_{t,Rd} = \frac{A_g f_{yd}}{\gamma_{M0}} \quad (3.14)$$

where A_g is the gross area of the cross-section. Obviously, it is also necessary to check the net-section resistance when connections with mechanical fasteners such as blind rivets, self-tapping screws, cartridge-fired pins, bolts are used (this check is not included in the computer program).

3.5.2 Resistance under axial compression

The design compression resistance of a cross-section $N_{c,Rd}$ shall be determined by considering the effective area A_{eff} of the cross-section subject to a uniform compressive stress $\sigma_{com,Ed}$ equal to f_{yb}/γ_{M1} :

$$N_{c,Rd} = \frac{A_{eff} f_{yb}}{\gamma_{M1}} \quad (3.15)$$

where A_{eff} is itself obtained by assuming a uniform distribution of stress equal to $\sigma_{com,Ed}$.

If the centroid of the effective cross-section does not coincide with the centroid of the gross cross-section, the shift e_N of the centroidal axes shall be taken into account, considering the effect of combined compression and bending (Figure 3.7).

If A_{eff} is equal to A_g the design compression resistance shall be determined by considering the gross area subjected to a uniform compressive stress equal to f_{yd}/γ_{M0} :

$$N_{t,Rd} = \frac{A_g f_{yd}}{\gamma_{M0}} \tag{3.16}$$

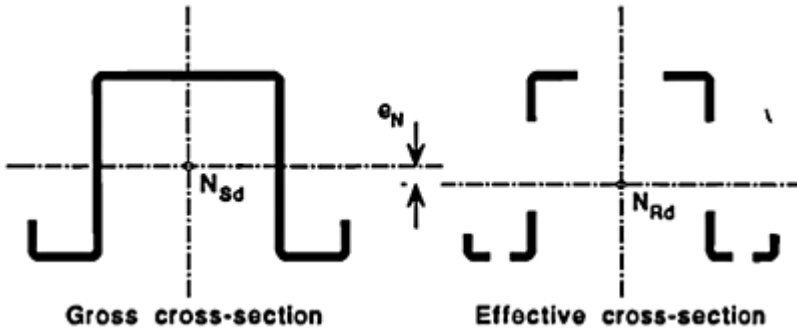


Figure 3.7 CEN, ENV 1993-1-3, 1996).

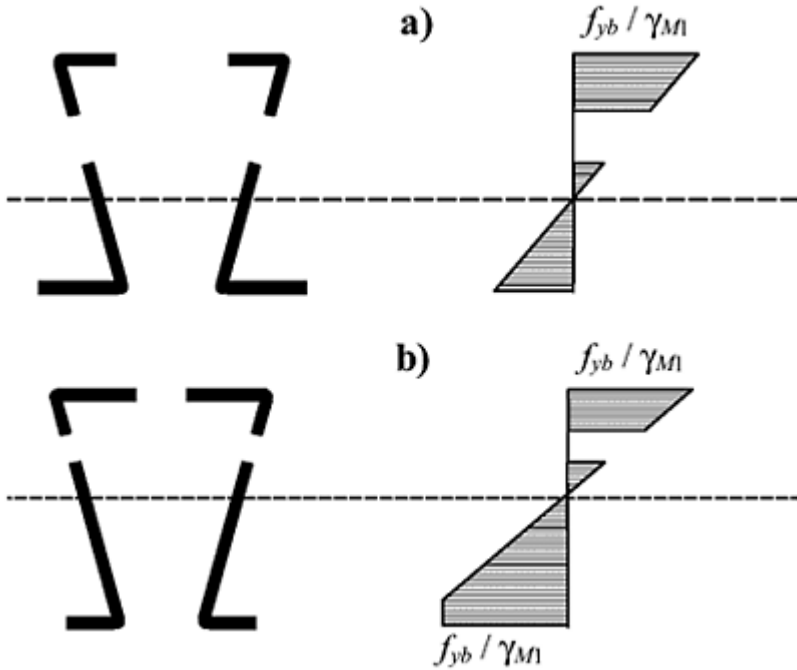


Figure 3.8.

3.5.3 Resistance under bending moment

The design moment resistance of a cross-section for bending about a principal axis $M_{c,Rd}$ shall be determined by considering the effective area of the cross-section subjected to a linear stress distribution, with a maximum compressive stress equal to f_{yb}/γ_{M1} (Figure 3.8(a)):

$$M_{c,Rd} = \frac{W_{eff} f_{yb}}{\gamma_{M1}} \quad (3.17)$$

If the bending moment is applied only about one principal axis of the cross-section and yielding occurs first at the tension edge, plastic reserves in the tension zone may be utilized without any strain limit until the maximum compressive stress $\sigma_{max,Ed}$ reaches f_{yb}/γ_{M1} . In this case, the design moment resistance is given by:

$$M_{c,Rd} = \frac{W_{pp,eff} f_{yb}}{\gamma_{M1}} \quad (3.18)$$

and the effective partially plastic section modulus $W_{pp,eff}$ should be based on a stress distribution that is bilinear in the tension zone but linear in the compression zone (Figure 3.8(b)). Part 1.3 of Eurocode 3 also allows utilization, in some cases, of plastic reserves in the compression zone.

When part of the cross-section is in the plastic range, the strain distribution is still linear; the coordinate z (or y) of the point G_{ep} having zero strain is:

$$z(G_{ep}) = z(G_{el}) + \frac{\varepsilon_y A_{pl,c} - A_{pl,t}}{\chi A_{el}} \quad (3.19)$$

and the design bending moment about y (or z) axis is:

$$M_{cy,Rd} = \left\{ \frac{I_{el}}{z(G_{ep})} + A_{pl,c} [z(G_{pl,c}) - z(G_{el})] - A_{pl,t} [z(G_{pl,t}) - z(G_{el})] \right\} \frac{f_y}{\gamma_{M1}} \quad (3.20)$$

where:

$G_{pl,t}$ = the centroid of the plastic tension zone;

$G_{pl,c}$ = the centroid of the plastic compression zone;

G_{el} = the centroid of the elastic zone;

$A_{pl,t}$ = the area of the plastic tension zone;

A_{el} = the area of the elastic zone;

I_{el} = the second moment of area of the elastic zone;

χ = the slope of the strain diagram;

ε_y = the strain corresponding to the yield limit $\varepsilon_y = (f_y/\gamma_{M1})/E$.

The present version of the computer program, described in Chapter 7, automatically takes into account the plastic reserves in the tension zone for cross-sections having at least one symmetry axis, but it does not consider plastic reserves in the compression zone.

Differently from the case of axial compression, the strain or stress distribution in the case of bending cannot be defined a priori. The computer program, therefore, performs an iterative procedure. Each step assigns a tentative position of the neutral axis and a stress distribution that reaches f_{yb}/γ_{M1} at the compression edge, then evaluates from this the effective section and finally calculates the axial force resulting from the stresses acting on the effective section. The procedure is repeated until the resulting axial force is negligible.

If the effective section modulus W_{eff} is equal to the gross elastic section modulus W_{el} , the design moment resistance shall be determined by considering the cross-section subject to a linear stress distribution, with a maximum compressive stress $\sigma_{max,Ed}$ equal to f_{yd}/γ_{M0} :

$$M_{c,Rd} = \frac{W_{el} f_{yd}}{\gamma_{M0}} \quad (3.21)$$

Eurocode 3 also gives us the opportunity of taking into account the effects of shear lag in flanges of flexural members if the length between the points of zero moment is less than $20b_0$, where b_0 is the width of flange contributing to shear lag. This check is not included in the computer program.

3.5.4 Resistance under shear

The design shear resistance of the web $V_{w,Rd}$ shall be taken as smaller than the plastic shear resistance $V_{pl,Rd}$ and shear buckling resistance $V_{b,Rd}$. When:

$$\bar{\lambda}_w \leq 0.83 \frac{f_{yb}/\gamma_{M1}}{f_y/\gamma_{M0}} \quad (3.22)$$

(where $\bar{\lambda}_w$ is the relative web slenderness) the first is smaller than the second; that is:

$$V_{w,Rd} = V_{pl,Rd} = \frac{h_w / \sin \phi t f_y / \sqrt{3}}{\gamma_{M0}} \quad (3.23)$$

where:

h_w = the web height between the midlines of the flanges (see Figure 3.1 (c));

ϕ = the slope of the web relative to the flanges.

Otherwise, shear resistance is given by:

$$V_{w,Rd} = V_{b,Rd} = \frac{h_w / \sin \phi t f_{bv}}{\gamma_{M1}} \quad (3.24)$$

where f_{bv} is the shear buckling strength, which depends on the value of $\bar{\lambda}_w$.

In the case of webs without longitudinal stiffeners, the relative web slenderness is given by the expression:

$$\bar{\lambda}_w = 0.346 \frac{s_w}{t} \sqrt{\frac{f_{yb}}{E}} \quad (3.25)$$

while a more complex expression, which includes the second moment of area of the longitudinal stiffener, shall be used in the case of stiffened webs; when no stiffening at the support is arranged to prevent distortion of the web, the shear buckling strength is given by:

$$f_{bv} = 0.48 \frac{f_{yb}}{\bar{\lambda}_w} \quad \text{if } \bar{\lambda}_w < 1.40 \quad (3.26)$$

$$f_{bv} = 0.67 \frac{f_{yb}}{\bar{\lambda}_w^2} \quad \text{if } \bar{\lambda}_w \geq 1.40$$

3.5.5 Combined axial force and bending

Cross-sections subject to combined axial force N_{sd} and bending moments $M_{y,sd}$ and $M_{z,sd}$ shall satisfy the criterion:

$$\frac{N_{sd}}{A f_y / \gamma_M} + \frac{M_{y,sd}}{W_y f_y / \gamma_M} + \frac{M_{z,sd}}{W_z f_y / \gamma_M} \leq 1 \quad (3.27)$$

where:

A = the area of the cross-section (gross area in the case of tensile force, effective area in the case of compressive force);

W_y , W_z = the section moduli for maximum stress, if they are only subject to the moment about the y - y and z - z axes, respectively (elastic or effective moduli, according to the appropriate case);

f_y = the maximum strength (f_{ya} if the section is fully effective; f_{yb} otherwise);

γ_M = the appropriate partial factor (γ_{M0} if the section is fully effective; γ_{M1} otherwise).

Additional moments due to shifts of the centroidal axes shall be taken into account.

3.5.6 Combined shear force and bending moment

Cross-sections subjected to the combined action of a bending moment M_{sd} and a shear force V_{sd} shall satisfy:

$$\left[\frac{M_{Sd}}{M_{c,Rd}} \right]^2 + \left[\frac{V_{Sd}}{V_{w,Rd}} \right]^2 \leq 1 \quad (3.28)$$

3.6 BUCKLING RESISTANCE

3.6.1 Flexural buckling

The effects of local buckling are taken into account by using effective section properties. The design buckling resistance for axial compression $N_{b,Rd}$ shall, therefore, be obtained from:

$$N_{b,Rd} = \frac{\chi A_{eff} f_{yb}}{\gamma_{M1}} \quad (3.29)$$

where:

A_{eff} = the effective area of the cross-section, obtained by assuming a uniform compressive stress $\sigma_{com,Ed}$ equal to f_{yb}/γ_{M1} ;

χ = the appropriate value of the reduction factor for buckling resistance, obtained as a function of both the relative slenderness for the relevant buckling mode $\bar{\lambda}$ and the imperfection factor α (see Table 3.4 and Figure 3.9):

$$N_{b,Rd} = \frac{\chi A_{eff} f_{yb}}{\gamma_{M1}} \quad (3.30)$$

$$\phi = 0.5[1 + \alpha(\bar{\lambda} - 0.2) + \bar{\lambda}^2] \quad (3.31)$$

$\bar{\lambda}$ = the relative slenderness for flexural buckling about a given axis, determined as:

$$\bar{\lambda} = \frac{\lambda}{\lambda_1} \sqrt{\frac{A_{eff}}{A_g}} \quad (3.32)$$

Table 3.4 Imperfection factor α

Buckling curve	$a0$	a	b	c
α	0.13	0.21	0.34	0.49

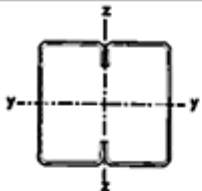
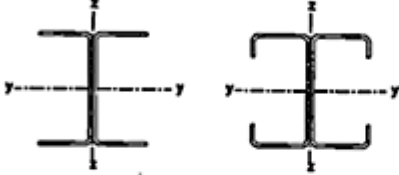
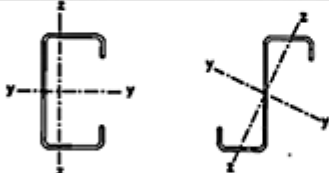
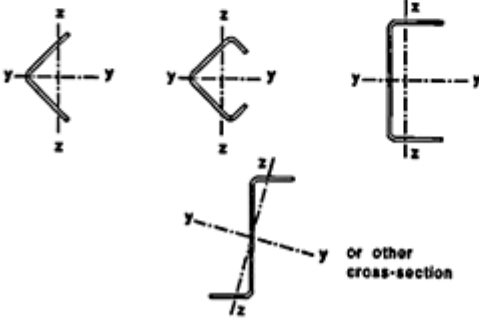
Type of cross-section	Buckling about axis	Buckling curve	
	if f_{yb} is used	any	b
	if f_{ys} is used *	any	c
	$y-y$	a	
	$z-z$	b	
	any	b	
 or other cross-section	any	c	
* The average yield strength f_{yb} should not be used unless $A_{eff} = A_g$			

Figure 3.9 (CEN, ENV 1993-1-3, 1996).

with $\lambda = L/i$ and $\lambda_1 = \pi \sqrt{E/f_y}$ where L is the buckling length for flexural buckling about the relevant axis; and z is the radius of gyration about the corresponding axis, based on the properties of the gross section;

γM_1 = partial safety factor for buckling.

As an alternative, the design buckling resistance may be obtained from second-order analysis of the member, based on the properties of the effective cross-section.

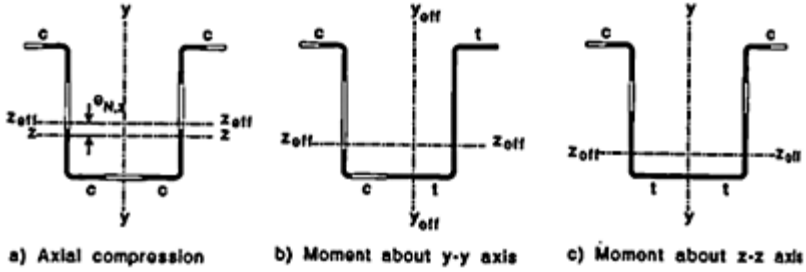


Figure 3.10 (CEN, ENV 1993-1-3, 1996).

3.6.2 Bending and axial compression

All members subject to combined bending and axial compression shall satisfy the criterion:

$$\frac{N_{Sd}}{\chi_{\min} A_{\text{eff}} f_{yb} / \gamma_{M1}} + \frac{\kappa_y (M_{y,Sd} + \Delta M_{y,Sd})}{W_{\text{eff},y} f_{yb} / \gamma_{M1}} + \frac{\kappa_z (M_{z,Sd} + \Delta M_{z,Sd})}{W_{\text{eff},z} f_{yb} / \gamma_{M1}} \leq 1 \quad (3.33)$$

where:

A_{eff} = the effective area of the cross-section, obtained by assuming a uniform compressive stress $\sigma_{\text{com,Ed}}$ equal to f_{yb} / γ_{M1} (Figure 3.10 (a));

$W_{\text{eff},y}$, $W_{\text{eff},z}$ = the effective section moduli for maximum compressive stress in a cross-section that is subjected only to bending moment about the y - y and z - z axes, respectively (Figure 3.10 (b, c));

$\Delta M_{y,Sd}$, $\Delta M_{z,Sd}$ = the additional moments due to possible shifts of the centroidal axes in the y and z directions, respectively (Figure 3.10(a));

χ_{\min} = the lesser of the reduction factors for buckling about the y - y and z - z axes;

K_y, K_z = factors that also depend on the equivalent uniform moment factor (i.e. on the bending moment distribution along the member).

4

Eurocode 9

4.1 BACKGROUND

The unavoidable complexity of a code for aluminium structures is essentially down to the nature of the material itself (much more 'critical' and less known than steel), which involves the solution of difficult problems and demands careful analysis. In this case, the need for the code to be educational as well as informative, and not just normative, has been particularly determinant in the elaboration of Eurocode 9 (CEN, ENV 1999-1-1, 1998).

The present edition of Eurocode 9 is based on the most recent developments in the field of aluminium-alloy structures, and includes the previous research by ECCS which led to the first edition of the *European Recommendations for Aluminium Alloy Structures* (ECCS, 1978) and in revision of outstanding codes, like BS 8118 (BS 8118, 1991).

The innovative element of Eurocode 9 (Part 1.1 'General Rules') relates to introduction, for the first time in a structural aluminium code, of analysis of inelastic behaviour from the cross-section up to the structure as a whole. The classification of cross-sections has been done on the basis of experimental results, which come from an *ad hoc* research project supported by the main representatives of the European Aluminium Industry, which provided the material for specimens (Mazzolani and Piluso, 1995).

By assessing behavioural classes based on the b/t slenderness ratio, using an approach qualitatively similar to that for steel, but with different extension of behavioural ranges, we have obtained data which are based on experimental evidence (Mazzolani *et al.*, 1996b) and confirmed by numerical simulation (Mazzolani *et al.*, 1997).

Cold-formed thin-walled members usually belong to Class 4 (slender sections) and the local buckling effect is taken into account by means of a new calculation method, based on the effective thickness concept. Three new buckling curves for slender sections have been set up which consider both heat-treated and work-hardened alloys, together with welded and non-welded shapes (Landolfo and Mazzolani, 1995b).

The problem of the evaluation of internal actions was faced by considering several stress-strain relationships, from the simplest to the most sophisticated, giving rise to different degrees of approximation. Global analysis of structural systems in the inelastic range (plastic, strain hardening) was based on a simple method, which is similar to the well-known method of plastic hinge, but considers the typical parameters of aluminium alloys such as absence of yielding plateau, continuous strain-hardening behaviour, limited ductility of some alloys (Mandara and Mazzolani, 1995).

The importance of ductility in the local and global behaviour of aluminium structures was emphasized, due to the sometime poor values of ultimate elongation, and a new *ad hoc* method for evaluation of rotation capacity for members in bending was set up (Mazzolani and Piluso, 1995).

For the behaviour of connections, a new classification system was proposed according to strength, stiffness and ductility (Mazzolani *et al.*, 1996a).

Part 1.1 provides all the calculation methods (Class 4), which cover thin-walled aluminium sections. More specific provisions for cold-formed sections have been worked out in a separate document, provisionally named Part 1.3 ‘Supplementary rules for thin-walled sheeting’ (CEN, prENV 1999–1–3, 1999), which no longer has official status, but represents a background document for introducing this subject into the revised Eurocode 9 during the incoming conversion phase.

4.2 GENERAL RULES

4.2.1 Definitions

Part 1.1 of Eurocode 9 defines the same four classes of cross-sections used in the European steel code (see Chapter 3). The following basic types of thin-walled elements are identified in the classification process:

- a flat outstand element;
- b flat internal element;
- c curved internal element.

These elements can be unreinforced, or reinforced by longitudinal stiffening ribs or edge lips or bulbs (Figure 4.1).

4.2.2 Slenderness of unreinforced flat elements

The basic parameter to decide which class a given cross-section belongs to is the b/t ratio between the width and the thickness of each element. A research project has been expressly developed on aluminium sections (square and rectangular hollow sections, channels), in order to identify the

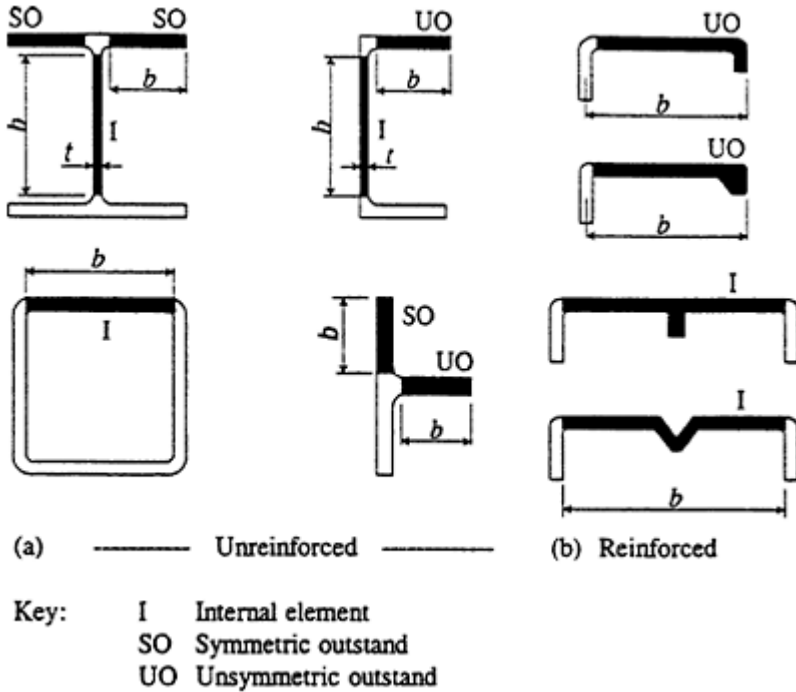


Figure 4.1 (CEN, ENV 1999-1-1, 1998).

influence of the width-to-thickness ratios on the local buckling phenomenon. On the basis of results of stub-column tests on heat-treated unwelded hollow sections, the following limit values for the b/t ratio have been assessed (Mazzolani *et al.*, 1996b):

- Class 1 $b/t \leq 11$;
- Class 2 $11 < b/t \leq 16$;
- Class 3 $16 < b/t \leq 21$;
- Class 4 $b/t > 21$.

Eurocode 9 relates the classification of elements in a cross-section to the value of the slenderness parameter β , which is defined according to the type of elements as a function of the b/t ratio.

In the case of plane unstiffened elements, β is related to the stress gradient (Figure 4.2):

$$\beta = gb/t \quad \text{or} \quad \beta = gd/t \quad (4.1)$$

where:

b = the width of an element;

d = the depth of a web element in a beam;

t = the element thickness;

g = the stress gradient coefficient, given by the expressions

$$g = 0.70 + 0.30\psi, \quad -1 < \psi < 1$$

$$g = 0.80 / (1 + \psi) \quad \psi \leq -1 \text{ or } 1$$

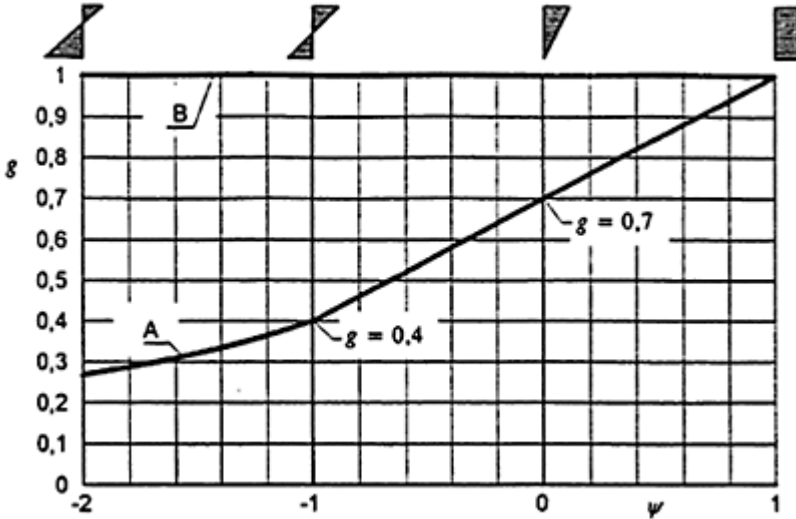


Figure 4.2 (CEN, ENV 1999-1-1, 1998).

where ψ is the ratio of the stresses at the edges of the plate under consideration related to the maximum compressive stress.

4.2.3 Slenderness of reinforced flat elements

In the case of plane-stiffened elements, more complex formulations are provided in order to take into account three possible buckling modes:

- 1 the stiffened element buckles as a unit, so that the stiffener buckles with the same curvature as the element (Figure 4.3 (a));
- 2 the subelements and the stiffener buckle as individual elements with the junction between them remaining straight (Figure 4.3 (b));
- 3 this is a combination of Modes 1 and 2, in which subelement buckles are superimposed on the whole element (Figure 4.3 (c)).

4.2.4 Element classification

Table 4.1 reports the element classification; the value of the limit parameters β_1 , β_2 and β_3 are given in Table 4.2, where $\varepsilon = \sqrt{250/f_{0.2}}$ and $f_{0.2}$ is the 0.2% proof strength in MPa.

4.3 MATERIAL PROPERTIES

The minimum limiting values of 0.2% proof strength $f_{0.2}$ and the ultimate tensile strength f_u for aluminium alloys for a range of tempers and

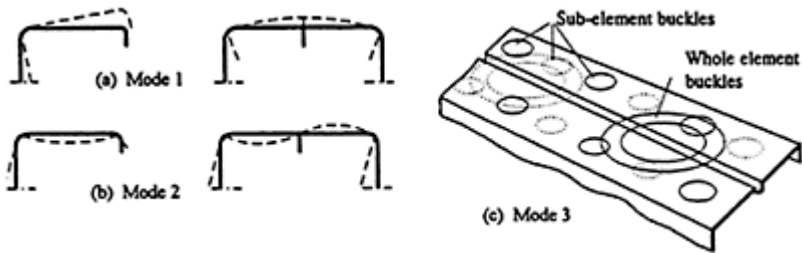


Figure 4.3 (CEN, ENV 1999–1–1, 1998).

Table 4.1 Element classification

Elements in beams		Elements in struts	
$\beta \leq \beta_1$	Class 1	$\beta \leq \beta_2$	Class 1 or 2
$\beta_1 < \beta \leq \beta_2$	Class 2		
$\beta_2 < \beta \leq \beta_3$	Class 3	$\beta_2 < \beta \leq \beta_3$	Class 3
$\beta_3 < \beta$	Class 4	$\beta_3 < \beta$	Class 4

Table 4.2 Values of β_1 , β_2 and β_3

Elements	Heat-treated unwelded			Heat-treated welded or non-heat-treated unwelded			Non-heat-treated unwelded		
	β_1	β_2	β_3	β_1	β_2	β_3	β_1	β_2	β_3
Outstand	3 ε	4.5 ε	6 ε	2.5 ε	4 ε	5 ε	2 ε	3 ε	4 ε
Internal	11 ε	16 ε	22 ε	9 ε	13 ε	18 ε	7 ε	11 ε	15 ε

thicknesses are given in Table 4.3 for sheet, strip and plate products. These values may be adopted as characteristic values in calculations for structures subjected to service temperatures below 100°C.

4.4 SECTION PROPERTIES

As already pointed out for Eurocode 3, Eurocode 9 likewise takes rounded corners into account by referring to the notational flat width b_p of each plane element, measured from the midpoints of adjacent corner elements.

The influence of rounded corners with internal radius $r \leq 5t$ and $r \leq 0.15b_p$ on section properties can also be ignored in this case, and the cross-section can be assumed to consist of plane elements with sharp corners. However, the computer program presented in this book always considers the actual geometry of the cross-section with rounded corners.

The provisions of Eurocode 9 should be applied only to cross-sections within the range of width-to-thickness ratios $b/t \leq 300$ for compressed

Table 4.3 (CEN, ENV 1999–1–1, 1998)

Alloy	Temper	t Thickness (mm)		$f_{0.2}$ 0.2% proof strength (MPa)	f_u Ultimate strength (MPa)	A_{50} Minimum elongation (%)
		Over	Up to			
EN AW-3103	H14	0.2	25	120	140	2
	H16	0.2	4	145	160	1
EN AW-5052	H12	0.2	4	160	210	4
	H14	0.2	2	180	230	3
EN AW-5454	O/H111	0.2	8	85	215	12
	H24/H34	0.2	25	200	270	4
EN AW-5754	O/H111	0.2	100	80	190	12
	H24/H34	0.2	25	160	240	6
EN AW-5083	O/H111	0.2	50	125	275	11
		50	80	115	270	14
	H24/H34	0.2	25	250	340	4
EN AW-6061	T4	0.4	12.5	110	205	12

	T6	0.4	12	240	290	6
EN AW-6082	T4	0.4	12	110	205	12
	T6	0.4	6	260	310	6
		6	12.5	255	300	9
	T651	12	100	240	295	8
EN AW-7020	T6	0.4	12.5	280	350	7
	T651	12.5	40			9

flanges and $b/t \leq E/f_{0.2}$ for webs. The computer program (Chapter 7) checks these limits as a warning to the user, but it can also be forced to calculate member resistance when the limits are exceeded.

4.5 LOCAL BUCKLING

4.5.1 General

The effect of local buckling on each compression element of the cross-section shall be conventionally accounted for by replacing the non-uniform distribution of stress, arising in the post-buckling range, with a uniform distribution of the maximum stress acting on a reduced portion of the element, having the same width but a reduced thickness (effective thickness).

As discussed in Section 2.3, the most suitable expression for evaluating the local buckling coefficient ρ , which factors down the thickness (or, equivalently, the strength) of an aluminium compressed plate, is:

$$\rho = 1.0 \quad \text{if } \bar{\lambda}_p \leq \bar{\lambda}_{lim} \quad (4.2)$$

$$\rho = \frac{\omega_1}{\bar{\lambda}_p} \left(1 - \frac{\omega_2}{\bar{\lambda}_p} \right) \quad \text{if } \bar{\lambda}_p > \bar{\lambda}_{lim}$$

Table 4.4 Parameters ω_1 , ω_2 and $\bar{\lambda}_{lim}$

Curve	Type of alloy	ω_1	ω_2	$\bar{\lambda}_{lim}$
A	Heat treated	1.00	0.22	0.673
B	Non-heat treated	0.88	0.22	0.440

The reduction thus depends on the parameters ω_1 , ω_2 and $\bar{\lambda}_{lim}$, reported in Table 4.4, and on the plate slenderness $\bar{\lambda}_p$, given by:

$$\bar{\lambda}_p = \sqrt{\frac{f_{0.2}}{\sigma_{cr}}} = \frac{b_p}{t} \sqrt{\frac{12(1-\nu^2)f_{0.2}}{\pi^2 E k_\sigma}} \cong 1.052 \frac{b_p}{t} \sqrt{\frac{f_{0.2}}{E k_\sigma}} \quad (4.3)$$

which takes into account stress distribution and boundary conditions by means of the buckling factor k_σ .

Part 1.1 of Eurocode 9 uses this approach for Class 4 compression elements. For the sake of simplicity, it modifies the formulations by explicitly introducing the $\beta=b/t$ ratio and rounding the subsequent coefficients so as to obtain integers. It, furthermore, prescribes using the same formulations for stiffened elements as well and to apply the factor ρ to the area of the stiffener as well as to the basic plate thickness.

A more specific and detailed approach is reported in Part 1.3 of Eurocode 9 (CEN, prENV 1999-1-3, 1999). This is presently a provisional document not yet included in the Eurocode, but it will represent a basis of discussion for the incoming conversion phase. Its provisions are mainly devoted to thin-walled aluminium sheeting, although they can easily be extended to aluminium cold-formed members. The formulations allow evaluation of the effective thickness of each compression element, or each portion of the element between adjacent corner elements or stiffeners. The effectiveness of the restraint provided by the stiffeners is analysed, assuming that they behave as compression members with continuous elastic restraint, having spring stiffness dependent on the flexural stiffness of the adjacent elements. The approach is, therefore, analogous to the one followed by Eurocode 3 and described in Section 3.4, with some modifications to take into account the peculiarities of aluminium-plate buckling.

In the analysis of aluminium cold-formed members and sheeting, the computer program presented in this book generally follows the approach used in Part 1.3 of Eurocode 9. However, some formulations are directly taken from Part 1.1, when it seems to comply in a better way with the peculiarities of aluminium. In a few cases, for which no specific provision is found in Eurocode 9, the computer program uses the expressions given in Part 1.3 of Eurocode 3, properly modified to comply with the effective thickness approach.

4.5.2 Plane elements without stiffeners

The effective thickness t_{eff} of a compression element is evaluated as:

$$t_{eff} = \rho t \quad (4.4)$$

by means of the reduction factor ρ based on the largest compressive stress $\sigma_{com,Ed}$ acting in the element when the resistance of the cross-section is reached. If only a part of the element is in compression (as in webs of beams under bending moment), the reduction shall be applied only to the compression part of the element.

When $\sigma_{com,Ed} = f_{yb}/\gamma M_1$ Part 1.3 of Eurocode 9 suggests the reduction factor ρ should be evaluated by means of the following expressions:

$$\rho = 1.0 \quad \text{if } \bar{\lambda}_p \leq \bar{\lambda}_{lim} \quad (4.5)$$

$$\rho = \frac{\alpha - 0.22/\bar{\lambda}_p}{\bar{\lambda}_p} \quad \text{if } \bar{\lambda}_p > \bar{\lambda}_{lim}$$

which slightly differ from those presented in Section 2.3 and many used in Part 1.1 of Eurocode 9. In this case, equations (4.2) are deemed more appropriate to the behaviour of aluminium plates and, thus, are used in the computer program, with parameters ω_1 , ω_2 and $\bar{\lambda}_{lim}$ as reported in Table 4.4.

In evaluating the plate slenderness $\bar{\lambda}_p$, the buckling factor $k\sigma$ for doubly supported elements is taken from Table 4.5 (given in Part 1.3 of Eurocode 9). In the absence of further data, the values for outstand compression elements are taken from the corresponding provisions described in Chapter 3 (Table 3.3).

Following the approach used in Part 1.3 of Eurocode 9, if $\sigma_{com,Ed} < f_{0.2}/\gamma M_1$ the reduction factor ρ shall be determined by expressions (4.2), but replacing the plate slenderness $\bar{\lambda}_p$ with the reduced plate slenderness $\bar{\lambda}_{p,red}$, given by:

$$\bar{\lambda}_{p,red} = \bar{\lambda}_p \sqrt{\frac{\sigma_{com,Ed}}{f_{0.2}/\gamma M_1}} \quad (4.6)$$

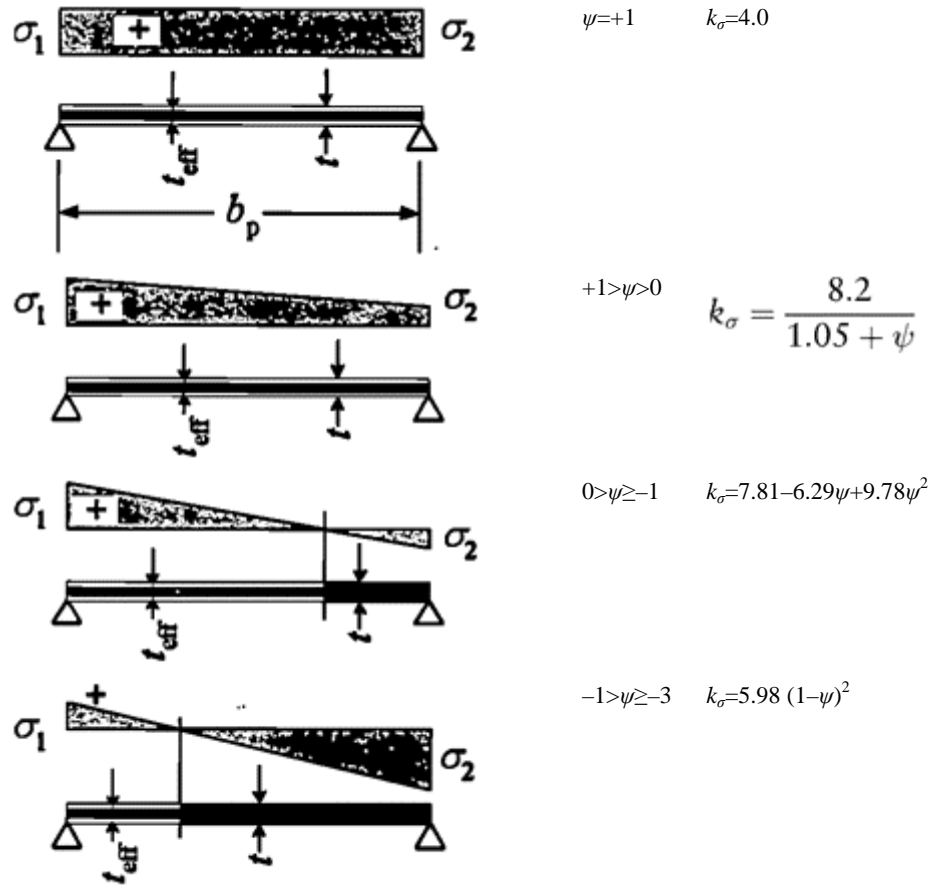
4.5.3 Plane elements with intermediate stiffeners

According to Part 1.3 of Eurocode 9, the design of compression elements with intermediate stiffeners requires a double-step procedure, analogous to that described in Chapter 3.

First, the effective thickness of the elements shall be evaluated by considering each element that is restrained by adjacent elements or stiffeners.

Table 4.5 Buckling factor for doubly supported compression elements (CEN, prENV 1999–1–3, 1999)

<i>Stress distribution [compression positive]</i>	$\psi = \sigma_2/\sigma_1$	<i>Buckling factor k_σ</i>
---	----------------------------	--



Second, each stiffener shall be considered as a compression member with continuous partial restraint, subject to the risk of buckling, so reducing its area by coefficient x . The cross-section of this member is constituted by the rounded corner and by the adjacent effective portions of the elements connected to the stiffeners, as shown in Figure 4.4 (a, b).

The two steps shall be repeated until the reduced effective area of the stiffener is sufficiently close to the value obtained from the previous iteration.

When analysing the buckling stress of the stiffener, the spring stiffness per unit length $K = u/\delta$ should be determined by applying a unit load per unit length u , as illustrated in Figure 4.5. The computer program follows the code suggestion to consider $C_{\theta,1}$ and $C_{\theta,2}$ equal to zero, and assumes in the case of intermediate stiffeners:

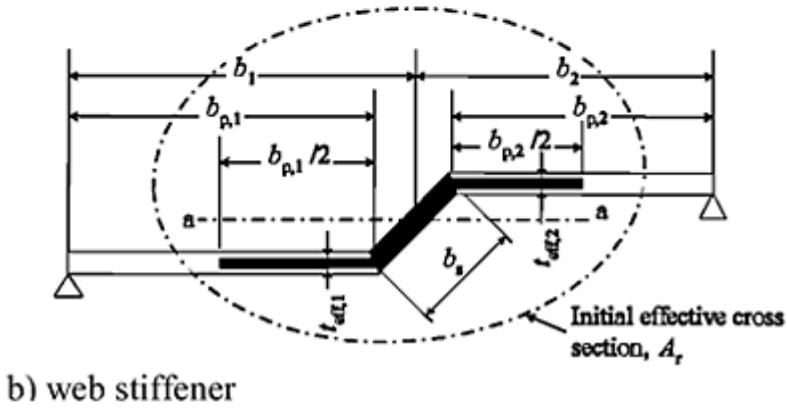
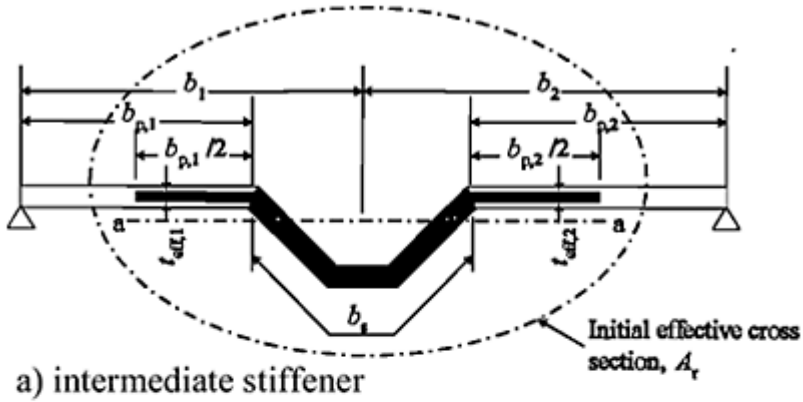


Figure 4.4 (CEN, prENV 1999-1-3, 1999).

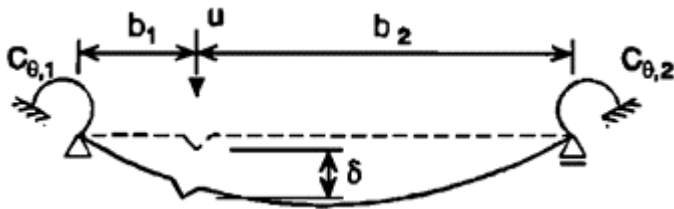


Figure 4.5 (CEN, prENV 1999-1-3, 1999).

$$K = \frac{0.25 (b_1 + b_2) E t^3}{(1 - \nu^2) b_1^2 b_2^2} \quad (4.7)$$

The elastic critical buckling stress $\sigma_{cr,s}$ for the stiffener is:

$$\sigma_{cr,s} = \frac{2\sqrt{KEI_s}}{A_s} \quad (4.8)$$

where:

K =the spring stiffness per unit length:

A_s =the effective cross-sectional area of the stiffener ($A_s=t_{eff,1}b_{p,1}\sqrt{2}+tb_s+t_{eff,2}b_{p,2}/2$);

I_s =the effective second moment of area of the stiffener.

The reduction coefficient χ for Ae flexural buckling of the stiffener is obtained as a function of the relative slenderness:

$$\bar{\lambda}_s = \sqrt{f_{0.2}/\sigma_{cr,s}} \quad (4.9)$$

by the following expressions:

$$\chi = 1 \quad \text{when } \bar{\lambda}_s \leq 0.25 \quad (4.10)$$

$$\chi = 1.555 - 0.62\bar{\lambda}_s \quad \text{when } 0.25 < \bar{\lambda}_s < 1.04$$

$$\chi = 0.53/\bar{\lambda}_s \quad \text{when } 1.04 \leq \bar{\lambda}_s$$

4.6 RESISTANCE OF CROSS-SECTIONS

4.6.1 Resistance under axial tension

The design tension resistance of a cross-section $N_{t,Rd}$ shall be determined by assuming that it is subjected to a uniform tensile stress equal to $f_{0.2}/\gamma M_1$:

$$N_{t,Rd} = \frac{A_g f_{0.2}}{\gamma M_1} \quad (4.11)$$

where A_g is the gross area of the cross-section. Obviously, it is also necessary to check the net-section resistance when connections with mechanical fasteners are used (this check is not included in the computer program).

4.6.2 Resistance under axial compression

The design compression resistance of a cross-section $N_{c,Rd}$ shall be determined by considering the effective area A_{eff} of the cross-section subject to a uniform compressive stress $\sigma_{com.Ed}$ equal to $f_{0.2}/\gamma M_1$:

$$N_{c,Rd} = \frac{A_{eff} f_{0.2}}{\gamma_{M1}} \quad (4.12)$$

where A_{eff} is obtained by assuming a uniform distribution of stress equal to $\sigma_{com,Ed}$.

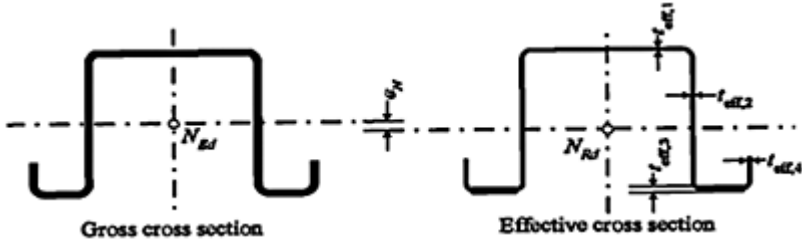


Figure 4.6 (CEN, prENV 1999–1–3, 1999).

If the centroid of the effective cross-section does not coincide with the centroid of the gross cross-section, the shift e_N of the centroidal axes shall be taken into account, considering the effect of combined compression and bending (Figure 4.6).

4.6.3 Resistance under bending moment

The design moment resistance of a cross-section for bending about a principal axis $M_{c,Rd}$ shall be determined by considering the effective area of the cross-section subject to a linear stress distribution, with a maximum compressive stress equal to $f_{0.2}/\gamma_{M1}$ [Figure 4.7(a)]:

$$M_{c,Rd} = \frac{W_{eff} f_{0.2}}{\gamma_{M1}} \quad (4.13)$$

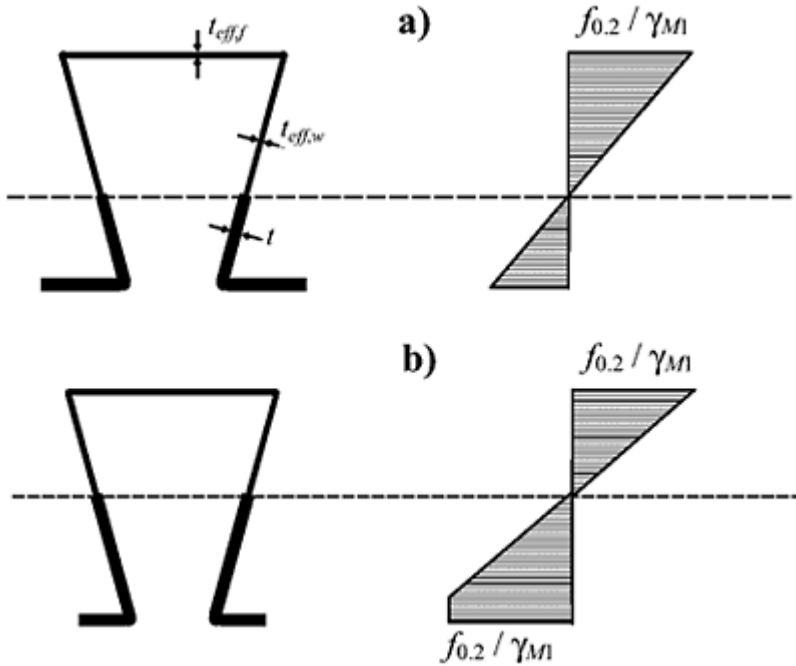


Figure 4.7.

According to Part 1.3 of Eurocode 9, if the bending moment is applied only about one principal axis of the cross-section and the limit stress $f_{0.2}/\gamma_{M1}$ occurs first at the tension edge, plastic reserves in the tension zone may be utilized without any strain limit until the maximum compressive stress $\sigma_{max,Ed}$ reaches $f_{0.2}/\gamma_{M1}$. In this case, the design moment resistance is given by:

$$M_{c,Rd} = \frac{W_{pp,eff} f_{0.2}}{\gamma_{M1}} \quad (4.14)$$

The effective partially plastic section modulus $W_{pp,eff}$ should be based on a stress distribution that is bilinear in the tension zone but linear in the compression zone (Figure 4.7 (b)). The formulations used in this case have been already described in detail in Chapter 3 (Section 3.5.3).

4.6.4 Resistance under shear

The design shear resistance of the web $V_{w,Rd}$ shall be taken as the lesser of the plastic shear resistance $V_{pl,Rd}$ and the shear buckling resistance $V_{b,Rd}$. When the former is smaller than the latter:

$$V_{w,Rd} = V_{pl,Rd} = \frac{h_w / \sin \phi t f_{0.2} / \sqrt{3}}{\gamma_{M0}} \quad (4.15)$$

where:

h_w = the web height between the midlines of the flanges;

ϕ = the slope of the web relative to the flanges.

Otherwise, the shear resistance is given by:

$$V_{w,Rd} = V_{b,Rd} = \frac{h_w / \sin \phi t f_{bv}}{\gamma_{M1}} \quad (4.16)$$

where f_{bv} is the shear buckling strength, which depends on the value of the relative web slenderness $\bar{\lambda}_w$.

In the case of webs without longitudinal stiffeners, the relative web slenderness is given by the expression:

$$\bar{\lambda}_w = 0.346 \frac{s_w}{t} \sqrt{\frac{f_{0.2}}{E}} \quad (4.17)$$

where s_w is the slant height of the web. In the case of stiffened webs, more complex expressions, which include the second moment of area of the longitudinal stiffener, are provided in Part 1.1 and in Part 1.3 of Eurocode 9.

Table 4.6 Shear buckling strength for webs with transverse stiffeners at supports (CEN, ENV 1999–1–1, 1999)

<i>Rigid end post</i>	<i>Non-rigid end post</i>	$\bar{\lambda}_w$
$\eta f_{0.2}$	$\eta f_{0.2}$	$\bar{\lambda}_w < 0.48/\eta$
$f_{bv} = \frac{0.48}{\bar{\lambda}_w} f_{02}$	$f_{bv} = \frac{0.48}{\bar{\lambda}_w} f_{02}$	$0.48/\eta < \bar{\lambda}_w < 0.949$
$f_{bv} = \frac{1.32}{1.66 + \bar{\lambda}_w} f_{02}$	$f_{bv} = \frac{0.48}{\bar{\lambda}_w} f_{02}$	$\bar{\lambda}_w \geq 0.949$

For webs with transverse stiffeners at supports, Part 1.1 of Eurocode 9 provides the expressions of the shear buckling strength reported in Table 4.6, where $\eta = 0.4 + 0.2f_u/f_{0.2}$ but not more than 0.7.

When no stiffening at the support is arranged to prevent distortion of the web, the shear buckling strength is, according to Part 1.3 of Eurocode 9:

$$f_{bv} = \frac{0.48}{\bar{\lambda}_w} f_{02} \quad \text{if } \bar{\lambda}_w < 1.40 \quad (4.18)$$

$$f_{bv} = \frac{0.67}{\bar{\lambda}_w^2} f_{02} \quad \text{if } \bar{\lambda}_w \geq 1.40$$

The computer program presented in Chapter 7 uses these expressions, which are safer than the previous ones.

4.6.5 Combined axial force and bending

Cross-sections subject to combined axial force N_{sd} and bending moments $M_{y,sd}$ and $M_{z,sd}$ shall satisfy the criterion:

$$\left(\frac{N_{sd}}{Af_{0.2}/\gamma_{M1}} \right)^{\eta_0} + \left(\frac{M_{y,sd}}{W_y f_{0.2}/\gamma_{M1}} \right)^{\gamma_0} + \left(\frac{M_{z,sd}}{W_z f_{0.2}/\gamma_{M1}} \right)^{\xi_0} \leq 1 \quad (4.19)$$

where:

A =the area of the cross-section (gross area in the case of tensile force, effective area in the case of compressive force);

W_y, W_z =the section moduli for maximum stress, if subjected only to moment about the y - y and z - z axes, respectively (elastic or effective moduli, according to the appropriate case). and the exponents η_0 , γ_0 and ξ_0 are:

$$\eta_0 = 1 \text{ or, alternatively, } \eta_0 = \alpha_z^2 \alpha_y^2 \text{ but } 1 \leq \eta_0 \leq 2$$

$$\gamma_0 = 1 \text{ or, alternatively, } \gamma_0 = \alpha_z^2 \text{ but } 1 \leq \gamma_0 \leq 1.56$$

$$\xi_0 = 1 \text{ or, alternatively, } \xi_0 = \alpha_y^2 \text{ but } \xi_0 \geq 1$$

where α_z and α_y are shape factors (which take into account local buckling).

The abovementioned interaction equation is provided by Part 1.1 of Eurocode 9 for I-beams subject to bending and axial tension and for every thin-walled cross-section subject to bending and axial compression. A slightly different expression is proposed for hollow cross-sections subject to bending and axial tension. Part 1.3 of Eurocode 9 suggests using equation (4.19) with exponents $\eta_0 = \gamma_0 = \xi_0 = 1$ in all cases; this approach is also followed by the computer program presented in Chapter 7.

The additional moments due to shifts of the centroidal axes should always be taken into account.

4.6.6 Combined shear force and bending moment

The theoretical resistance moment of a cross-section is reduced by the presence of shear, particularly when the design value of the shear force exceeds 50% of the design shear resistance. In such a case, Part 1.1 of Eurocode 9 prescribes basing the contribution of the

webs to the cross-section's moment capacity on a reduced value of the material strength f_{0w} , given by:

$$f_{0w} = f_{02} \sqrt{1 - \left(\frac{V_{Sd}}{V_{w,Rd}} \right)^2} \quad (4.20)$$

Alternatively, Part 1.3 of Eurocode 9 suggests checking cross-sections subject to the combined action of a bending moment M_{sd} and a shear force V_{sd} by the conditions:

$$\left[\frac{M_{Sd}}{M_{c,Rd}} \right]^2 \leq 1 \quad (4.21)$$

$$\left[\frac{V_{Sd}}{V_{w,Rd}} \right]^2 \leq 1$$

$$\left[\frac{M_{Sd}}{M_{c,Rd}} \right]^2 + \left[\frac{V_{Sd}}{V_{w,Rd}} \right]^2 \leq 1.05$$

This last approach has been adopted in the computer program.

4.7 BUCKLING RESISTANCE

4.7.1 Flexural buckling

The effects of local buckling are taken into account by using effective section properties. The design buckling resistance for axial compression $N_{b,Rd}$ shall, therefore, be obtained from:

$$N_{b,Rd} = \frac{\chi A_{eff} f_{02}}{\gamma_{M1}} \quad (4.22)$$

where:

A_{eff} = the effective area of the cross-section, obtained by assuming a uniform compressive stress $\sigma_{com,Ed}$ equal to $f_{0,2}/\gamma_{M1}$;

χ = the appropriate value of the reduction factor for buckling resistance, obtained as a function of the relative slenderness for the relevant buckling mode $\bar{\lambda}$ and the imperfection factors α and $\bar{\lambda}_0$

$$\chi = \frac{1}{\phi + \sqrt{\phi^2 + \bar{\lambda}^2}} \quad \text{but } \chi \leq 1 \tag{4.23}$$

$$\phi = 0.5[1 + \alpha(\bar{\lambda} - \bar{\lambda}_0) + \bar{\lambda}^2] \tag{4.24}$$

$\bar{\lambda}$ the relative slenderness for flexural buckling about a given axis, determined as:

$$\bar{\lambda} = \frac{\lambda}{\lambda_1} \sqrt{\frac{A_{eff}}{A_g}} \tag{4.25}$$

with $\lambda=L/i$ and $\lambda_1 = \pi\sqrt{E/f_{0.2}}$ where L is the buckling length for flexural buckling about the relevant axis and i is the radius of gyration about the corresponding axis, based on the properties of the gross section.

The values of the imperfection factors α and $\bar{\lambda}_0$ provided by Eurocode 9 are reported in Table 4.7. Finally, note that, in the case of asymmetric cross-sections, Part 1.1 of Eurocode 9 factors down the values given by equation (4.22) by means of coefficient k_1 .

4.7.2 Bending and axial compression

Part 1.1 of Eurocode 9 gives general provisions for checking bending and axial compression, which include reduction factors for buckling. Nevertheless, it expressly denies the possibility of using these expressions

Table 4.7 Values of the imperfection factors α and $\bar{\lambda}_0$ (CEN, ENV 1999-1-1, 1998; CEN, prENV 1999-1-3, 1999)

	<i>Code</i>	α	$\bar{\lambda}_0$
Heat-treated alloys	EC9, Part 1.1	0.20	0.10
Non-heat-treated alloys	EC9, Part 1.1	0.32	0.00
Sheeting	EC9, Part 1.3	0.13	0.20

in the case of thin-walled cross-sections; for these, however, it suggests using the interaction equation (4.19), which does not include coefficients able to account for member instability, anyway.

A more specific approach is carried out in Eurocode 3, which prescribes that all members subject to combined bending and axial compression shall satisfy the criterion:

$$\frac{N_{Sd}}{\chi_{min} A_{eff} f_{0.2}/\gamma_{M1}} + \frac{\kappa_y (M_{y,Sd} + \Delta M_{y,Sd})}{W_{eff,y} f_{0.2}/\gamma_{M1}} + \frac{\kappa_z (M_{z,Sd} + \Delta M_{z,Sd})}{W_{eff,z} f_{0.2}/\gamma_{M1}} \leq 1 \quad (4.26)$$

where:

A_{eff} =the effective area of the cross-section, obtained by assuming a uniform compressive stress $\tilde{A}_{com,Ed}$ equal to $f_{0.2}/\gamma_{M1}$;

$W_{eff,y}$, $W_{eff,z}$ =the effective section moduli for the maximum compressive stress in a cross-section that is subjected only to bending moment about the y - y and z - z axes, respectively;

$\Delta M_{y,sd}$, $\Delta M_{z,sd}$ =the additional moments due to possible shifts of the centroidal axes in the y and z directions, respectively;

ω =an interaction coefficient that takes into account the moment distribution due to transverse load, which for simplification may be assumed equal to 1;

χ_{min} =the lesser of the reduction factors for buckling about the y - y and z - z axes;

K_y , K_z =factors that also depend on the equivalent uniform moment factor (i.e. on the bending moment distribution along the member).

5

AISI Specification

5.1 BACKGROUND

During the 1930s, the acceptance and development of cold-formed steel construction in the USA faced some difficulties due to the lack of an appropriate design specification. Various building codes did not make any provision for cold-formed steel construction at that time. It became apparent that the development of a new design specification for cold-formed steel construction was highly desirable.

Realizing the need for a special design specification and the absence of factual background and research information, the AISI Committee on Building Research and Technology (then named Committee on Building Codes) sponsored a research project at Cornell University, under the direction of George Winter from 1939, and to a lesser extent at some other institutions.

As far as design criteria are concerned, the first edition of the ‘Specification for the Design of Light Gage Steel Structural Members’, prepared by the AISI Technical Subcommittee, was issued by the American Iron and Steel Institute in 1946. This specification was based on the findings of the research conducted at Cornell University up to that time and the accumulated practical experience obtained in this field (Yu, 1992).

The current specification is entitled ‘Specification for the Design of Cold-Formed Steel Structural Members’ and is included in the *Cold-formed Steel Design Manual* (AISI, 1996). The objective of the manual is to provide a more useful reference for both the specialist and occasional user of cold-formed steel products. Since the *AISC Manual of Steel Construction* is one of the best known references for steel designers, a similar format has been used in the AISI manual for cold-formed steel products. This manual provides much of the same type of information, and in a similar layout, as that for hot-rolled shapes. This similar style of presentation is also intended to help the designer in applying conventional steel design approaches (Kaehler and Seaburg, 1996).

The design manual is composed by the following parts:

- I ‘Dimension and Properties’ contains information regarding the availability and properties of steels referenced in the ‘Specification’, tables of section properties, formulas and examples of calculations of section properties.
- II ‘Beam Design’ contains tables and charts to aid in beam design, giving examples for solution of beam design problems.
- III ‘Column Design’ contains tables to aid in column design, giving examples for solution of column design problems.
- IV ‘Connection’ contains tables to aid in connection design, giving examples for solution of connection problems.

- V 'Specification' is the 1996 edition of the AISI 'Specification for the Design of Cold-Formed Steel Structural Members'.
- VI 'Commentary' provides a commentary on the 1996 edition of the AISI 'Specification for the Design of Cold-Formed Steel Structural Members'.
- VII 'Supplementary Information' contains design procedures of specification nature which are not included in the 'Specification' itself, either because they are infrequently used or are regarded as too complex for routine design, together with other information intended to assist users of cold-formed steel.
- VIII 'Test Procedures' contains test methods for cold-formed steel, illustrated by an example, along with literature about other pertinent test methods.

Since 1946, the method of designing cold-formed steel structural members, as prescribed in previous editions of the AISI Specification, was based on the Allowable Stress Design method. In 1991, AISI published the first edition of the 'Load and Resistance Factor Design Specification for Cold-Formed Steel Structural Members'. Both AISI Allowable Stress Design and Load and Resistance Factor Design methods were combined as a single document in the current Specification (Yu *et al.*, 1996).

Allowable stress design (ASD) is a method of designing structural components such that the allowable design value (stress, force or moment), permitted by various sections of the Specification, is not exceeded when the structure is subjected to all appropriate combinations of nominal loads as given in Specification Section A5.1.2.

Load and resistance factor design (LRFD) is a method of designing structural components such that the applicable limit state is not exceeded when the structure is subjected to all appropriate load combinations as given in Specification Section A6.1.2.

5.2 MATERIAL PROPERTIES

The AISI Specification provides a list of the minimum basic yield strength F_y , of the minimum ultimate tensile strength F_u , the elongation over 2 inches and the ratio of minimum ultimate tensile strength to minimum basic yield strength for cold-formed steel structures conforming to the ASTM Standard (Table 5.1). This code provides specific expressions for evaluation of the increase in basic yield strength due to strain hardening:

$$F_{ya} = CF_{yc} + (1 - C)F_{yf} \quad (5.1)$$

in which:

$$F_{yc} = \frac{B_c F_y}{(R/t)^m}$$

$$B_c = 3.69 \frac{F_u}{F_y} - 0.819 \left(\frac{F_u}{F_y} \right)^2 - 1.79$$

$$m = 0.192 \frac{F_u}{F_y} - 0.068$$

where:

- F_{ya} =the full-section tensile yield strength;
- F_{yc} =the average tensile yield strength of corners;
- F_{yf} =the average tensile yield strength of flat;
- F_y =the virgin yield strength;
- F_u =the virgin ultimate strength;
- C =the ratio of corner area to total cross-sectional area;
- R =the inside-bend radius;
- t =the sheet thickness.

5.3 SECTION PROPERTIES

As we know from Chapter 2, every thin-gauge member may be considered as a set of straight and rounded walls. While modelling the actual section as a set of plates, the AISI recommendation refers to the flat width w , which excludes corners (Figure 5.1).

The AISI recommendation provides the maximum allowable flat-width-to-thickness ratios w/t , ignoring intermediate stiffeners and taking the actual thickness t of the element shown in Figure 5.2. The computer program presented in Chapter 7 checks these limits, as a warning to the user, but it can also be forced to calculate member resistance when the limits are exceeded.

Computation of the properties of cold-formed sections can be simplified if we consider the material of the section concentrated along the centreline of the steel sheet and area elements replaced by straight or curved ‘line elements’. However, the computer program presented in Chapter 7 always considers the actual geometry of the cross-section.

Table 5.1 (AISI, 1996)

ASTM designation	Product	Grade	F_y (min)		F_u (min/max)		Percent elongation over 2 inches (min)	F_u/F_y (min)
			ksi	MPa	ksi	MPa		
A36/A36M-94	Plates and	–	36	248	58/80	400/552	23	1.61

bars								
A242-A242M-93a	Plates and bars $t \leq \frac{3}{4}$ in.	—	50	345	70	483	21	1.40
A283/A283M-93a	Plate	A	24	166	45/60	311/414	30	1.88
		B	27	186	50/65	345/449	28	1.85
		C	30	207	55/75	380/518	25	1.83
		D	33	228	60/80	414/552	23	1.82
A500-93	Round tubing	A	33	228	45	311	25	1.36
		B	42	290	58	400	23	1.38
		C	46	317	62	428	21	1.35
		D	36	248	58	400	23	1.61
	Shaped tubing	A	39	269	45	311	25	1.15
		B	46	317	58	400	23	1.26
		C	50	345	62	428	21	1.24
		D	36	248	58	400	23	1.61
A529/A529M-94	Plate and bars	42	42	290	60/85	414/587	22	1.43
		50	50	345	70/100	483/690	21	1.40
A570/A570M-95	Sheet and strip	30	30	207	49	338	21	1.63
		33	33	228	52	359	18	1.58
		36	36	248	53	366	17	1.47
		40	40	276	55	380	15	1.38
		45	45	311	60	414	13	1.33
		50	50	345	65	449	11	1.30
A572/A572M-94c	Plates and bars	42	42	290	60	414	24	1.43
		50	50	345	65	449	21	1.30
		60	60	414	75	518	18	1.25
		65	65	449	80	552	17	1.23
A606-91a	Sheet and strip	Hot rolled— as rolled cut lengths	50	345	70	483	22	1.40
		Hot rolled— as rolled coils	45	311	65	449	22	1.44
		Hot rolled— annealed	45	311	65	449	22	1.44

		or							
		normalized	45	311	65	449	22	1.44	
		cold rolled							
		Class 1	45	45	311	60	414	H: 23 C: 22	1.33
ASTM designation	Product	Grade	F _y (min)		F _u (min/max)		Percent elongation over 2 inches (min)	F _u /F _y (min)	
			ksi	MPa	ksi	MPa			
		50	50	345	65	449	H: 20 C: 20	1.30	
		55	55	380	70	483	H: 18 C: 18	1.27	
		60	60	414	75	518	H: 16 C: 16	1.25	
		65	65	449	80	552	H: 14 C: 15	1.23	
		70	70	483	85	587	H: 12 C: 14	1.21	
A607-92a	Sheet and strip	Class 2							
		45	45	311	55	380	H: 23 C: 22	1.22	
		50	50	345	60	414	H: 20 C: 20	1.20	
		55	55	380	65	449	H: 18 C: 18	1.18	
		60	60	414	70	483	H: 16 C: 16	1.17	
		65	65	449	75	518	H: 14 C: 15	1.15	
		70	70	483	80	552	H: 12 C: 14	1.14	
							H: hot rolled		
							C: cold rolled		
A611-94	Sheet	A	25	173	49	338	26	1.68	
		B	30	207	52	359	24	1.50	
		C Types 1,2	33	228	53	366	22	1.45	
		D Types 40	1,2	276	55	380	20	1.30	
A653/A653M-95	Sheet	SQ							
		33	33	228	45	311	20	1.36	
		37	37	255	52	359	18	1.41	
		40	40	276	55	380	16	1.38	
		50 Class 1	50	345	65	449	12	1.30	

		50 Class 3	50	345	70	483		12	1.40
		HSLA							
		Type 1							
		50	50	345	60	414		20	1.20
		60	60	414	70	483		16	1.17
		70	70	483	80	552		12	1.14
		80	80	552	90	621		10	1.13
		HSLA							
		Type 2							
		50	50	345	60	414		22	1.20
		60	60	414	70	483		18	1.17
		70	70	483	80	552		14	1.14
		80	80	552	90	621		12	1.13
A715-92a	Sheet and strip	50	50	345	60	414		22	1.20
		60	60	414	70	483		18	1.17
		70	70	483	80	552		16	1.14
		80	80	552	90	621		14	1.13
A792/A792M- 95	Sheet	33	33	228	45	311		20	1.36
		37	37	255	52	359		18	1.41
		40	40	276	55	380		16	1.38
		50A	50	345	65	449		12	1.30

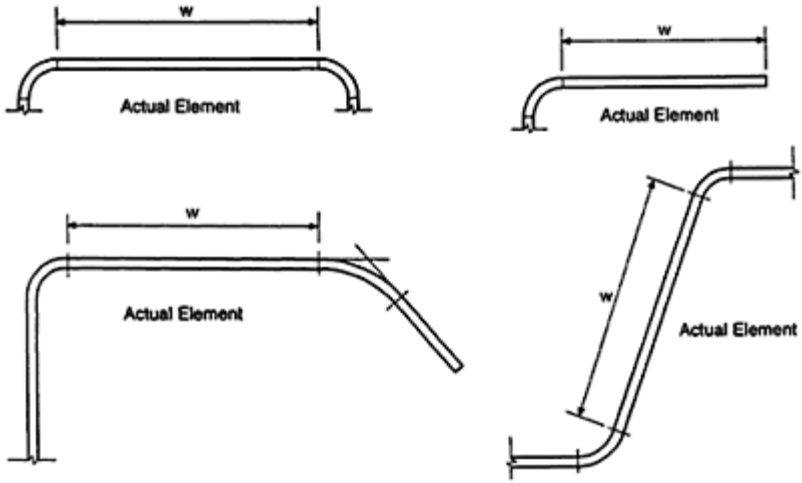


Figure 5.1 (AISI, 1996).





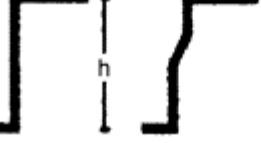
elements	limits
	<p>30 (60)</p>
	<p>60</p>
	<p>90</p>
	<p>250 (500)</p>
	<p>200</p>

Figure 5.2.

5.4 LOCAL BUCKLING

5.4.1 General

The local buckling of a section is studied by evaluating the buckling of each straight element on the basis of the theory of compressed-plate stability. The restraint mutually provided by adjacent elements is considered to be a simple support, but the AISI Specification prescribes geometrical conditions to be fulfilled by the stiffening element in order to rely on the effectiveness of restraint; if these are not satisfied, a reduced restraint must be considered.

5.4.2 Uniformly compressed stiffened and unstiffened elements

The effective width b of a compression element (Figures 5.3, 5.4) shall be determined by the following equation:

$$b = \rho w \tag{5.2}$$

where:

w =the flat width;

ρ =the reduction factor:

$$\rho = 1.0 \quad \text{if } \lambda \leq 0.673$$

$$\rho = \frac{1.0 - 0.22/\lambda}{\lambda} \quad \text{if } \lambda > 0.673$$

λ =a slenderness factor determined as follows:

$$\lambda = \frac{1.052}{\sqrt{k}} \left(\frac{w}{t} \right) \sqrt{\frac{f}{E}}$$

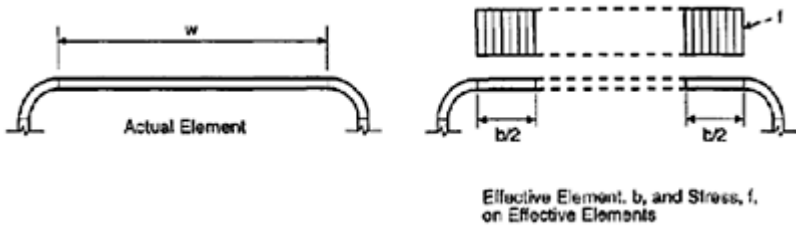


Figure 5.3 (AISI, 1996).

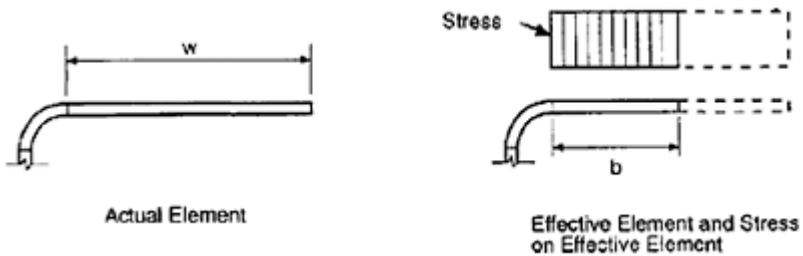


Figure 5.4 (AISI, 1996).

where k is the buckling factor, which depends on boundary conditions— $k=4$ for stiffened elements and $k=0.43$ for unstiffened element—and f is the stress in the element.

The AISI Specification gives a different equation which should only be used in checking the serviceability state of uniformly compressed elements supported by webs on both edges:

$$b_e = \rho w \quad (5.3)$$

where:

$$\rho = 1.0 \quad \text{if } \lambda \leq 0.673$$

$$\rho = \frac{1.358 - 0.461/\lambda}{\lambda} \quad \text{if } 0.673 < \lambda < \lambda_c$$

$$\rho = \frac{0.41 + 0.59\sqrt{F_y/f_d} - 0.22/\lambda}{\lambda} \quad \text{if } \lambda \geq \lambda_c$$

and:

$$\lambda_c = 0.256 + 0.328 \left(\frac{w}{t} \right) \sqrt{\frac{F_y}{E}}$$

5.4.3 Webs and stiffened elements with stress gradient

The effective widths b_1 and b_2 (Figure 5.5) shall be determined as follows:

$$b_1 = \frac{b}{3 - \psi} \quad (5.4)$$

$$b_2 = b/2 \quad \text{if } \psi \leq 0.236 \text{ with } b_1 + b_2 \leq b$$

$$b_2 = b - b_1 \quad \text{if } \psi > 0.236$$

where:

$$\psi = f_2/f_1$$

b = the effective width determined in accordance with Section 5.4.2 (uniformly compressed stiffened elements) with f_1 substituted by f and with k determined from $k = 4 + 2(1 - \psi)^3 + 2(1 - \psi)$.

5.4.4 Unstiffened elements and edge stiffened with stress gradient

In this case, the code suggests evaluating the effective widths in accordance with Section 5.4.2 (uniformly compressed unstiffened elements) using a uniform distribution with the maximum value of stress f .

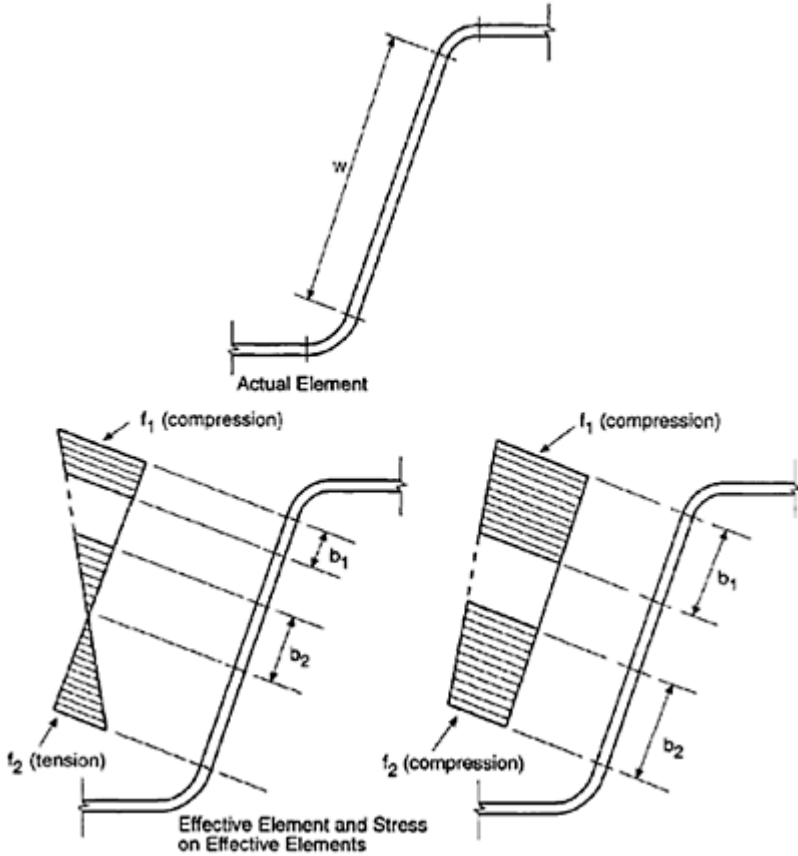


Figure 5.5 (AISI, 1996).

5.4.5 Uniformly compressed elements with one intermediate stiffener

The effective width b (Figure 5.6) shall be determined using cases:

- I for $b_o/t \leq S - b = \omega$;
- II for $S < b_o/t \leq 3S - b$ is calculated according to Section 5.4.2 (uniformly compressed stiffened elements) with $k = 3(I_s/I_o)^{1/2} + 1 \leq 4$;
- III for $b_o/t \geq 3S - b$ is calculated according to Section 5.4.2 (uniformly compressed stiffened elements) with $k = 3(I_s/I_o)^{1/3} + 1 \leq 4$;

where:

$$S = 1.28 \sqrt{E/f};$$

I_s is the moment of inertia of the full section of the stiffener about its own centroidal axis parallel to the element to be stiffened, and

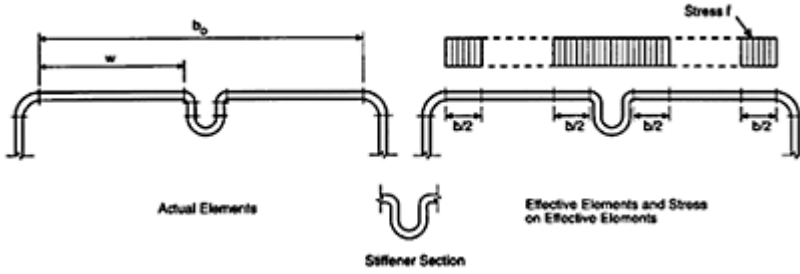


Figure 5.6 (AISI, 1996).

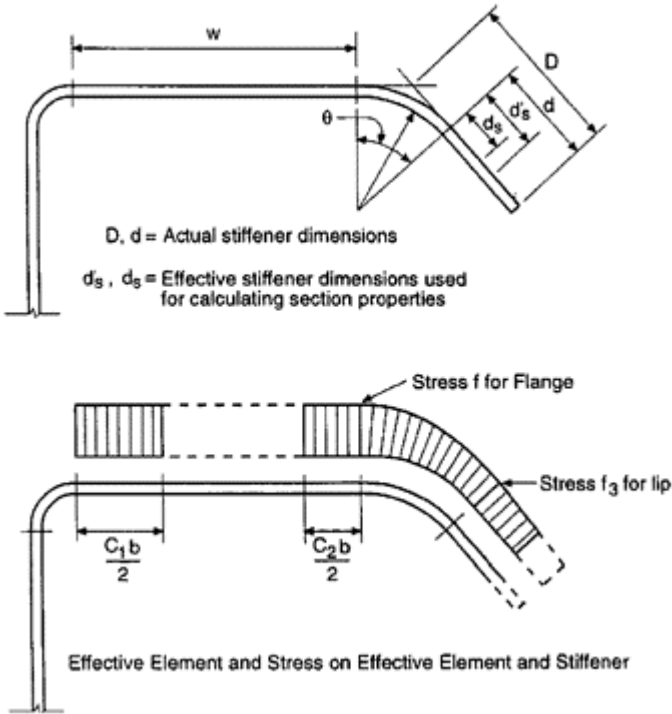


Figure 5.7 (AISI, 1996).

I_a is the adequate moment of inertia of the stiffener, so that each component element will behave as a stiffened element.

5.4.6 Uniformly compressed elements with an edge stiffener

The effective width b and the effective stiffener dimension d_s (Figure 5.7) shall be determined using cases:

I for $\omega/t \leq S/3 - b = \omega$ and $d_s = d'_s$;

II for $S/3 < \omega/t \leq S - b$ is calculated according to Section 5.4.2 (uniformly compressed stiffened elements) with $k = C_1^{1/2} (k_a - k_u) + k_u$, $k_u = 0.43$ and (for $40^\circ \leq \theta \leq 140^\circ$ and $D/w \leq 0.8$) $k_a = 5.25 - 5(D/\omega) \leq 4.0$ and $d_s = C_2 d'_s$;

III for $\omega/t \geq S - b$ is calculated according to Section 5.4.2 (uniformly compressed stiffened elements) with $k = C_2^{1/3} (k_a - k_u) + k_u$, $k_u = 0.43$ and (for $40^\circ \leq \theta \leq 140^\circ$ and $D/w \leq 0.8$) $k_a = 5.25 - 5(D/\omega) \leq 4.0$ and $d_s = C_2 d'_s$;

where $S = 1.28 \sqrt{E/f}$, d_s is the reduced effective width of the stiffener as specified in this section, d'_s is the effective width of the stiffener calculated according to Section 5.4.2 (uniformly compressed unstiffened elements), $C_2 = I_s/I_a \leq 1$, I_s is the moment of inertia of the full section of the stiffener about its own centroidal axis parallel to the element to be stiffened, and I_a is the adequate moment of inertia of the stiffener, so that each component element will behave as a stiffened element.

5.5 RESISTANCE OF CROSS-SECTIONS

5.5.1 General

Differently from Eurocodes 3 and 9, the AISI Specification does not separately examine the resistance of cross-sections and buckling resistance of members. However, this distinction is maintained here to give better correspondence with the previous chapters. A further difference between the European and American codes is that the latter allows two different approaches—ASD and LRFD. According to the AISI Specification, the structural check shall be performed by verifying that the required strength R is smaller than the design strength provided by the structural component (factored resistance ϕR_n or allowable strength R_n/Ω depending on the method adopted—LRFD or ASD, respectively). The nominal strength R_n shall be evaluated as described in the following sections, which also give appropriate values of the safety factors ϕ and Ω .

5.5.2 Resistance under axial tension

The nominal tensile strength T_n shall be determined as follows:

$$T_n = A_n F_y \tag{5.5}$$

where:

A_n —the net area of the cross-section (the computer program always considers the gross area of the cross-section—in the case of bolted connections, further manual checks should be performed by the user);

F_y —the design yield stress, which takes into account the increase in basic yield strength due to strain-hardening as shown in Section 5.2.

The safety factors which depend on the method of design are:

$$\begin{aligned} \Omega_t &= 1.67 && \text{for ASD method;} \\ \phi_t &= 0.95 && \text{for LRFD method.} \end{aligned}$$

5.5.3 Resistance under axial compression

A member is only subject to axial compression, without bending moment, if the resultant of all loads acting on it is an axial load passing through the centroid of the effective cross-section (i.e. if this coincides with the centroid of the gross cross-section). In this case, if the member is not subject to the risk of axial buckling, the nominal axial strength P_n shall be calculated as follows:

$$P_n = A_e F_y \tag{5.6}$$

where:

A_e =the effective area at the stress F_y ;

F_y =the design yield stress.

This equation is obtained from the more general one provided by AISI, which also takes member buckling into account and is discussed in Section 5.6.1 of this book, assuming yield stress F_y to be the reference stress.

The safety factors which depend on the method of design are:

$$\begin{aligned} \Omega_t &= 1.80 && \text{for ASD method;} \\ \phi_t &= 0.85 && \text{for LRFD method.} \end{aligned}$$

If the centroid of the effective cross-section does not coincide with the centroid of the gross cross-section, the cross-section shall be checked for axial compression and bending moment, in accordance with Section 5.5.7. For angle sections, a minimum value $PL/1,000$ for the additional bending moment shall always be considered.

5.5.4 Resistance under bending moment

The nominal flexural strength M_n shall be determined as follows:

$$M_n = S_e F_y \tag{5.7}$$

where:

S_e =the elastic section modulus of the effective section, calculated for extreme compression or tension fibre at F_y ;

F_y =the design yield stress—for the section to be fully effective it should take into account the increase of the basic yield strength due to strain-hardening as shown in Section 5.2.

The safety factors which depend on the method of design are:

for sections with stiffened or partially stiffened compression flange:

$$\begin{aligned}\Omega_b &= 1.67 && \text{for ASD method,} \\ \phi_b &= 0.95 && \text{for LRFD method;}\end{aligned}$$

for sections with unstiffened compression flange:

$$\begin{aligned}\Omega_b &= 1.67 && \text{ASD method;} \\ \phi_b &= 0.90 && \text{for LRFD method.}\end{aligned}$$

5.5.5 Resistance under shear

The nominal shear strength V_n shall be determined as follows:

$$\text{Case (a) for } \frac{b}{t} \leq 0.96 \sqrt{\frac{Ek_v}{F_y}} \quad V_n = 0.60F_ybt \quad (5.8a)$$

$$\text{Case (b) for } 0.96 \sqrt{\frac{Ek_v}{F_y}} < \frac{b}{t} \leq 1.1415 \sqrt{\frac{Ek_v}{F_y}} \quad V_n = 0.64t^2 \sqrt{k_v} F_y E \quad (5.8b)$$

$$\text{Case (c) for } \frac{b}{t} > 1.415 \sqrt{\frac{Ek_v}{F_y}} \quad V_n = 0.905 \frac{Ek_v t^3}{b} \quad (5.8c)$$

where:

t = the web thickness;

b = depth of the flat portion of the web measured along the plane of the web;

k_v = the shear buckling coefficient, defined in Section C3.2 of the AISI Specification.

The safety factors which depend on the method of design are:

Case (a):

$$\begin{aligned}\Omega_b &= 1.50 && \text{for ASD method;} \\ \phi_b &= 1.00 && \text{for LRFD method.}\end{aligned}$$

Cases (b) and (c):

$$\begin{aligned}\Omega_b &= 1.67 && \text{for ASD method;} \\ \phi_b &= 0.90 && \text{for LRFD method.}\end{aligned}$$

5.5.6 Combined axial tension and bending

The required strengths T , M_x , M_y shall satisfy the following equations, respectively, using the ASD and LRFD methods:

$$\text{ASD: } \frac{M_x}{M_{nxt}/\Omega_b} + \frac{M_y}{M_{nyt}/\Omega_b} + \frac{T}{T_n/\Omega_t} \leq 1.0$$

$$\text{LRFD: } \frac{M_x}{\phi_b M_{nxt}} + \frac{M_y}{\phi_b M_{nyt}} + \frac{T}{\phi_t T_n} \leq 1.0$$

and

$$\text{ASD: } \frac{M_x}{M_{nx}/\Omega_b} + \frac{M_y}{M_{ny}/\Omega_b} - \frac{T}{T_n/\Omega_t} \leq 1.0$$

$$\text{LRFD: } \frac{M_x}{\phi_b M_{nx}} + \frac{M_y}{\phi_b M_{ny}} - \frac{T}{\phi_t T_n} \leq 1.0$$

where:

T =the required tensile axial strength;

T_n =the nominal tensile axial strength determined in accordance with Section 5.5.2;

M_x, M_y =the required flexural strengths about the centroidal axes of the section;

M_{nx}, M_{ny} =the nominal flexural strengths about the centroidal axes determined in accordance with Section 5.5.4;

$M_{nxt} = S_{fxt} F_y$

$M_{nyt} = S_{fyt} F_y$

S_{fxt} =the elastic section modulus of the full unreduced section for the extreme tension fibre about the x axis;

S_{fyt} =the elastic section modulus of the full unreduced section for the extreme tension fibre about the y axis;

$\Omega_b, \Omega_t, \phi_b, \phi_t$ =are the appropriate safety factors.

5.5.7 Combined axial compression and bending

If the member is not subject to the risk of axial buckling, the required strengths P, M_x, M_y shall satisfy the following equations, respectively, using the ASD and LRFD methods:

$$\text{ASD: } \frac{P}{P_n/\Omega_c} + \frac{M_x}{M_{nx}/\Omega_b} + \frac{M_y}{M_{ny}/\Omega_b} \leq 1.0 \quad (5.11)$$

$$\text{LRFD: } \frac{P}{\phi_c P_n} + \frac{M_x}{\phi_b M_{nx}} + \frac{M_y}{\phi_b M_{ny}} \leq 1.0$$

where:

P =the required compressive axial strength;

P_n =the nominal axial strength determined in accordance with Section 5.5.3;

M_x, M_y =the required flexural strengths with respect to the centroidal axes of the effective section determined for the required compressive axial strength alone;

M_{nx}, M_{ny} =the nominal flexural strengths about the centroidal axes determined in accordance with Section 5.5.4;

$\Omega_b, \Omega_c, \phi_b, \phi_c$ =the appropriate safety factors.

These expressions are obtained from more general ones provided by AISI which also take member buckling into account (see Section 5.6.2).

5.5.8 Combined shear force and bending moment

For beams with unreinforced webs, the required strengths M and V shall satisfy the following equations, respectively, using the ASD and LRFD methods:

$$\text{ASD:} \quad \left(\frac{M}{M_n/\Omega_b} \right)^2 + \left(\frac{V}{V_n/\Omega_v} \right)^2 \leq 1.0 \quad (5.12)$$

$$\text{LRFD:} \quad \left(\frac{M}{\phi_b M_n} \right)^2 + \left(\frac{V}{\phi_v V_n} \right)^2 \leq 1.0$$

where:

M =the required flexural strength;

M_n =the nominal flexural strength determined in accordance with Section 5.5.4;

V =the required shear strength;

V_n =the nominal shear force determined in accordance with Section 5.5.5;

$\Omega_b, \Omega_v, \phi_b, \phi_v$ =the appropriate safety factors.

For beams with transverse web stiffeners, both M and V shall not exceed the design value of the corresponding internal action (M_n/Ω_b and V_n/Ω_v for the ASD method, $\phi_b M_n$ and $\phi_v V_n$ for the LRFD method). When the ratio of required bending moment over design bending moment is larger than 0.5 and the ratio of required shear force over design shear force is larger than 0.7, M and V shall also satisfy the following equations, respectively, using the ASD and LRFD methods:

$$\text{ASD:} \quad 0.6 \left(\frac{M}{M_n/\Omega_b} \right) + \left(\frac{V}{V_n/\Omega_v} \right) \leq 1.3$$

$$\text{LRFD:} \quad 0.6 \left(\frac{M}{\phi_b M_n} \right) + \left(\frac{V}{\phi_v V_n} \right) \leq 1.3$$

5.6 BUCKLING RESISTANCE

5.6.1 Buckling resistance under axial compression

If the resultant of all loads acting on the member is an axial load passing through the centroid of the effective cross-section (i.e. if this coincides with the centroid of the gross cross-section), the nominal axial strength P_n shall be calculated as follows:

$$P_n = A_e F_n \tag{5.14}$$

where:

A_e = the effective area at the stress F_n ;

$$F_n = (0.658 \lambda_c^2) F_y \text{ for } \lambda_c \leq 1.5;$$

$$F_n = (0.877 / \lambda_c^2) F_y \text{ for } \lambda_c > 1.5 \text{ with } \lambda_c = \sqrt{F_y / F_e};$$

F_e = the smallest value for the elastic flexural, torsional and torsional-flexural buckling stress. If the section is not subjected to torsional or torsional-flexural buckling, the elastic flexural buckling stress is given by:

$$F_e = \frac{\pi^2 E}{(KL/r)^2}$$

where E is the modulus of elasticity, K is the effective length factor, L is the unbraced length of member, r is the radius of gyration of the full, unreduced section. Otherwise, F_e shall be determined according to the more detailed formulations given in Section C4.1–C4.3 of the AISI Specification.

The safety factors which depend on the method of design are:

$$\begin{aligned} \Omega_t &= 1.80 && \text{for ASD method;} \\ \phi_t &= 0.85 && \text{for LRFD method.} \end{aligned}$$

If the centroid of the effective cross-section does not coincide with the centroid of the gross cross-section, the cross-section shall be checked for axial compression and bending moment, in accordance with Section 5.6.2. For angle sections, a minimum value of $PL/1,000$ for the additional bending moment should always be considered.

5.6.2 Buckling resistance under axial compression and bending

The required strengths P , M_x , M_y shall satisfy the following equations, respectively, using the ASD and LRFD methods:

$$\text{ASD: } \frac{P}{P_n/\Omega_c} + \frac{C_{mx}M_x}{\alpha_x M_{nx}/\Omega_b} + \frac{C_{my}M_y}{\alpha_y M_{ny}/\Omega_b} \leq 1.0 \quad (5.15)$$

$$\text{LRFD: } \frac{P}{\phi_c P_n} + \frac{C_{mx}M_x}{\alpha_x \phi_b M_{nx}} + \frac{C_{my}M_y}{\alpha_y \phi_b M_{ny}} \leq 1.0$$

and

$$\text{ASD: } \frac{P}{P_{no}/\Omega_c} + \frac{M_x}{M_{nx}/\Omega_b} + \frac{M_y}{M_{ny}/\Omega_b} \leq 1.0 \quad (5.16)$$

$$\text{LRFD: } \frac{P}{\phi_c P_{no}} + \frac{M_x}{\phi_b M_{nx}} + \frac{M_y}{\phi_b M_{ny}} \leq 1.0$$

where:

P =the required compressive axial strength;

P_n =the nominal axial strength determined in accordance with Section 5.6.1;

P_{no} =the nominal axial strength determined in accordance with Section 5.5.3 (i.e. with $F_n=F_y$);

M_x, M_y =the required flexural strengths with respect to the centroidal axes of the effective section determined for the required compressive axial strength alone;

M_{nx}, M_{ny} =the nominal flexural strengths about the centroidal axes determined in accordance with Section 5.5.4;

$\Omega_b, \Omega_c, \phi_b, \phi_c$ =are the appropriate safety factors.

Buckled shape of column is shown by dashed line	(a)	(b)	(c)	(d)	(e)	(f)
Theoretical K value	0.5	0.7	1.0	1.0	2.0	2.0
Recommended K value when ideal conditions are approximated	0.65	0.80	1.2	1.0	2.10	2.0
End condition code						
	Rotation fixed, Translation fixed	Rotation free, Translation fixed	Rotation fixed, Translation free	Rotation free, Translation free		

Figure 5.8 (AISI, 1996).

The reduction coefficient α is given by:

$$\alpha_x = 1 - \frac{P}{P_{Ex}/\Omega_c} \text{ (ASD)} \quad \text{or} \quad \alpha_x = 1 - \frac{P}{\phi_c P_{Ex}} \text{ (LRFD)}$$

$$\alpha_y = 1 - \frac{P}{P_{Ey}/\Omega_c} \text{ (ASD)} \quad \text{or} \quad \alpha_y = 1 - \frac{P}{\phi_c P_{Ey}} \text{ (LRFD)}$$

with:

$$P_{Ex} = \frac{\pi^2 EI_x}{(K_x L_x)^2}$$

$$P_{Ey} = \frac{\pi^2 EI_y}{(K_y L_y)^2}$$

where:

I_x, I_y =the moments of inertia of the full unreduced section about the x axis and y axis, respectively;

L_x, L_y =the actual unbraced lengths for bending about the x axis and y axis, respectively;

K_x, K_y = the effective length factors for buckling about the x axis and y axis, respectively (Figure 5.8);

C_{mx}, C_{my} = coefficients defined as follows:

$C_m = 0.85$ for compression member in frames subject to joint translation (sideways);

$C_m = 0.6 - 0.4M_1/M_2$ for restrained compression members in frames braced against joint translation and not subjected to transverse loading between their supports in the plane of bending (M_1/M_2 is the ratio of the smaller to the larger moment at the end of the member);

$C_m = 0.85$ for compression members in frames braced against joint translation and subjected to transverse loading between their supports in the plane of bending, when their ends are restrained;

$C_m = 1.00$ for compression members in frames braced against joint translation and subjected to transverse loading between their supports in the plane of bending, when their ends are not restrained.

6

Comparison among codes

6.1 EXAMINED CODES

The know-how deriving both from the increased use of thin-gauge sections in structural applications and scientific research led to a progressive renewal of technical codes in this field. With this purpose in mind, the most recent European Codes—Eurocode 3 (EC3) (Part 1.3) (CEN, ENV 1993–1–3, 1996) and Eurocode 9 (EC9) (CEN, ENV 1999–1–1, 1998)—together with the American Code (AISI, 1996) aim at analysing the different problems of cold-formed thin-gauge members by means of a unified approach.

First, comparison between the two main codes for cold-formed steel structures—EC3 (Part 1.3) provision and the AISI Specification—has been done. For a wider overview, results from application of the Italian Code CNR 10022 (1984) are also reported and commented on. The comparison is not very easy both because of different notation and, mainly, the different approach to analysis (differing values of the safety factor, admissible stress or ultimate limit-state checks). The notation used here is predominantly that of EC3. Any differences to the general approach are partially overcome by using values which yield the most stressed fibre, with no safety factor.

Only in the case of members subjected to combined axial force and bending, is it necessary to explicitly use safety factors, because the AISI Specification gives distinct values for M and N . In this case, the difference due to the admissible stress versus limit-state approach was overcome by means of a coefficient equal to 1.5 (Gherzi and Landolfo, 1992).

The provisions used in the considered codes basically belong to three main methodologies, which are known as (Landolfo, 1992):

- a reduced thickness approach;
- b effective width approach;
- c reduced stress approach.

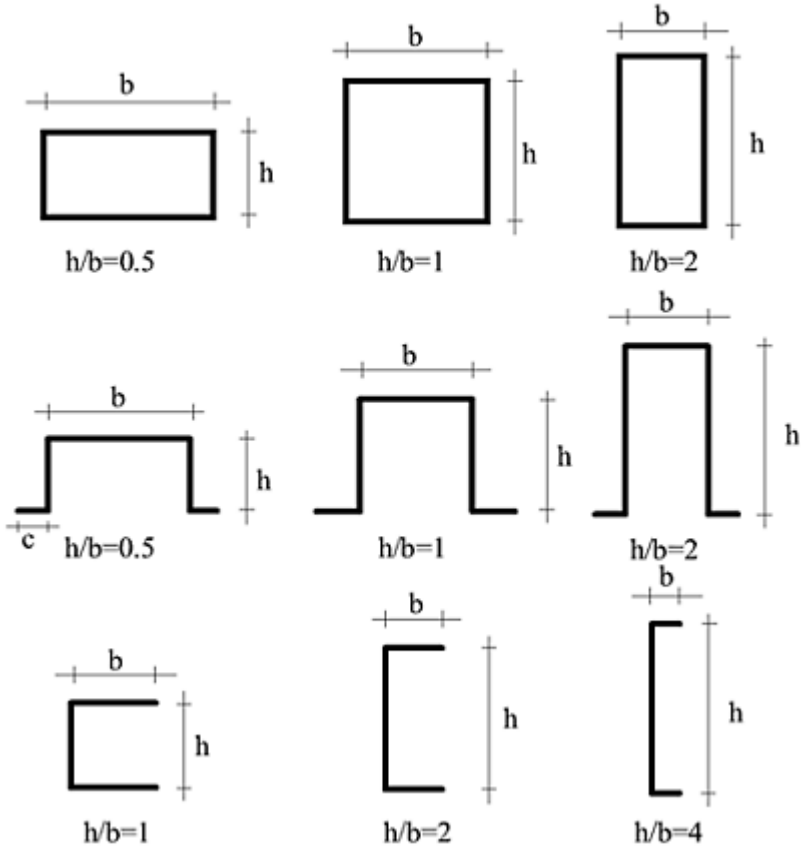


Figure 6.1 (Landolfo, 1992).

In particular, approach (a) has been followed for aluminium structures both by British Standard BS 8118 (1991) and by EC9 (CEN, ENV 1999–1–1, 1998). Approach (b) is typical for steel structures and is used in both EC3 (CEN, ENV 1993–1–3, 1998) and American Specification (AISI, 1996).

In order to compare the verification criteria provided by these codes, parametric analysis was carried out by applying the relevant provision to a set of sections which adequately represent the most important shapes obtained by means of cold forming. Three types of sections (box, omega and channel (C)) were selected, giving rise to three values of web-height-to-flange-width ratio (h/b) (see Figure 6.1). In particular:

a box sections: $h/b=0.5, 1, 2$;

b omega sections: $h/b=0.5, 1, 2$ and $c/b=0.2, 0.3, 0.4$;

c channel sections: $h/b=1, 2, 4$.

6.2 ELEMENTS SUBJECTED TO UNIFORM STRESS DISTRIBUTION

Every thin-gauge member can be considered as a set of straight and rounded walls. The local buckling of a section is, therefore, studied by evaluating the

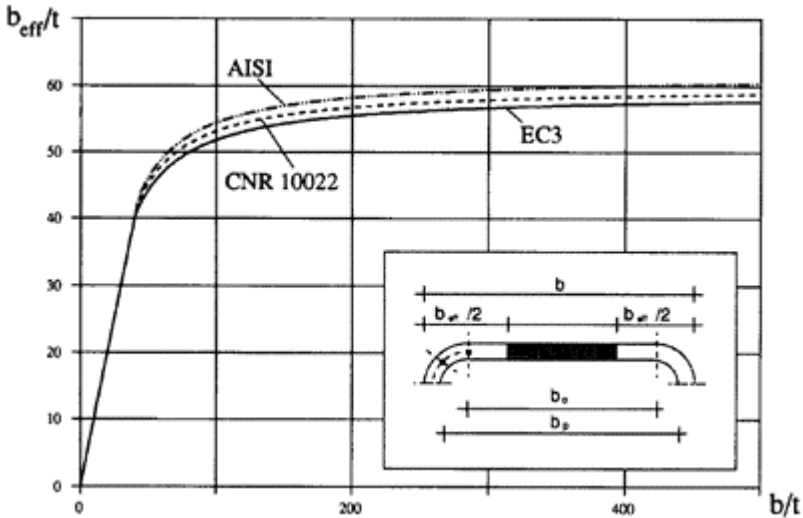


Figure 6.2 (Gherzi and Landolfo, 1992).

buckling of each straight element on the basis of the theory of compressed plate stability.

As is well known, the critical elastic load of a plate depends on the ratio of geometrical dimensions (width b to thickness t), the effectiveness of the restraints at the ends, the axial stress and its distribution, as well as the mechanical characteristics of the basic material. While modelling the actual section as a set of plates, the first two parameters can be evaluated in different ways.

Because each plane element is continuously connected to adjacent ones, the definition of the width b of the plate is simply conventional. EC3 also includes the corners, measuring a notational width b_p , starting at the middle of the corner. CNR and AISI, on the other hand, refer to the net width b_0 , which does not include corners (Figure 6.2).

The restraint mutually provided by adjacent elements is usually considered to be a simple support. Each code prescribes geometrical conditions to be fulfilled by the stiffening element in order to rely on the effectiveness of the restraint; if these are not satisfied, a reduced restraint must be considered.

The post-critical behaviour of a compressed plate is characterized by its capability of bearing increasing loads with a non-uniform distribution of stress. In numerical analyses, this can be modelled by considering alternatively:

- the maximum stress acting on a reduced part of the plate (effective width b_{eff});

- a reduced stress σ_{red} acting on the entire plate.

The Italian code CNR uses a mixed approach, following either the first or second method depending on the restraints of the element. The analysis of doubly supported (stiffened) elements should be carried out by means of the effective width approach and verified using effective cross-section properties.

A reduced admissible stress, on the other hand, together with the properties of the gross section, should be used in the case of singly supported (unstiffened) elements.

Many theoretical and experimental investigations have shown that the use of reduced stresses greatly penalizes sections with this latter type of element. For this reason, EC3 prescribes using a unified approach based only on the effective width criterion. The corresponding formulation, first proposed by Winter, is written in a non-dimensional form (see Sections 2.2 and 3.4.2):

$$b_{eff} = \rho b_p$$

with:

$$\rho = 1.0 \quad \text{for } \bar{\lambda}_p \leq 0.673 \quad (6.1)$$

$$\rho = \frac{1.0 - 0.22/\bar{\lambda}_p}{\bar{\lambda}_p} \quad \text{for } \bar{\lambda}_p > 0.673$$

and:

$$\bar{\lambda}_p = \sqrt{\frac{\sigma}{\sigma_{cr}}} = 1.052 \frac{b_p}{t} \sqrt{\frac{\sigma}{Ek_\sigma}}$$

The AISI Specification uses the same expression, but should be evaluated with reference to the net width b_0 rather than the notational width b_p . Although formally different, the CNR formulation for doubly supported elements is equivalent, but explicitly uses the yielding stress.

The values provided by the examined codes nearly coincide when $\sigma = f_y$, with minor differences due to the width considered (b_0 or b_p) and the numerical coefficients in the formulations. These values are substantially confirmed by experimental evidence. Figure 6.2, which displays the values of the ratio b_{eff}/t corresponding to the geometrical ratio b/t , shows that the difference is nearly constant with b/t , the maximum scatter being about 5% between AISI to EC3, while CNR gives intermediate values.

When $\sigma < f_y$ (e.g. in the serviceability state or in the final state of sections whose tension flange yields before the compression flange), equation (6.1) underestimates the effective width. For this reason, EC3 permits us to use equation (6.1) with the actual stress value,

but also provides a modified formulation for $\bar{\lambda}_p > 0.673$ (see Section 3.4.2):

$$\rho = \frac{1.0 - 0.22/\bar{\lambda}_{p,red}}{\bar{\lambda}_{p,red}} + 0.18 \frac{\bar{\lambda}_p - \bar{\lambda}_{p,red}}{\bar{\lambda}_p - 0.6}, \quad \text{with } \rho \leq 1.0 \quad (6.2)$$

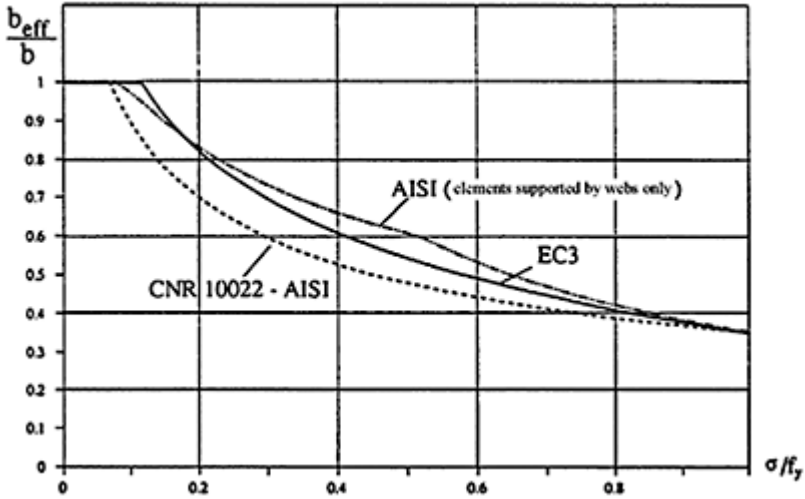


Figure 6.3 (Gherzi and Landolfo, 1992).

in which $\bar{\lambda}_{p,red}$ and $\bar{\lambda}_p$ are evaluated using the actual stress σ and yielding stress f_y respectively.

The AISI Specification gives an equivalent expression, which should be used only for checking the serviceability state of uniformly compressed elements supported by webs on both edges. Equation (6.1), with the actual stress value, should be used in any other case.

As for the serviceability state, the CNR code provides a formulation, obtained from equation (6.1), which relates to the actual stress. For evaluation of load-bearing capacity, equation (6.1), along with the yielding stress value, should be used even when $\sigma < f_y$.

Figure 6.3 displays the values of the b_{eff}/b ratio corresponding to the stress level for a given geometrical ratio ($b/t=150$), showing the progressive reduction in effectiveness of the section as the stress increases, confirming that CNR always provides safer values. The differences between the AISI and EC3 formulations and the substantial agreement of codes when are also pointed out.

6.3 MEMBERS IN BENDING

6.3.1 General

A section subjected to bending moment should be considered as a set of flanges (i.e. elements with a uniform stress distribution, under tension or compression) and webs (i.e. elements with a linear stress distribution).

The general criteria for elements subjected to pure compression are given in Chapter 2.

As for webs, different interpretations of general rules are provided by the codes. Some codes do not supply data, providing just a strong limit in geometrical slenderness (b/t ratio should remain below 150).

The AISI and EC3 codes, on the other hand, generalize basic formulations by providing values for the buckling coefficient k_σ that take the stress distribution in the web into account. EC3 provides a wider range of information, including simply supported elements with linear stress distribution. In the latter case, the AISI Specification more safely suggests evaluation of local buckling using a uniform distribution with the maximum value of stress. Nevertheless, the main difference between these codes does not stem from the k_σ values, but is connected to the expressions used to identify the effective parts in the element. In particular, note that the AISI formulation gives rise to web buckling for values of slenderness greater than those provided by EC3, but when this occurs the effective width of the web is suddenly greatly reduced.

6.3.2 Local buckling

Load-bearing capacity has been compared by evaluating the reduced yielding moment $M_{y,red}$ (on the basis of the effective width or reduced stress approach, according to code prescriptions) for many values of geometrical slenderness b/t . Figure (6.4a, b, c) plots the ratio of $M_{y,red}$ over the yielding moment of the gross section M_y , as a function of b/t for the three types of cross-sections selected in Section 6.1. The occurrence of web buckling (EC3, AISI) is marked by an arrow. Reaching the limit for web slenderness (CNR, AISI) is indicated by a star.

Comparison of the parts of Figure 6.4 just refers to local buckling of the cross-section; the bending behaviour of whole members is examined later in Section 6.3.3, where account is taken of the possibility of lateral torsional buckling. This analysis ignores plastic reverses of the section, which should be considered (according to EC3 and AISI) in just a few specific situations. Analysis of the numerical results leads to the following considerations.

Box sections (Figure 6.4a) The examined codes evaluate local buckling of compressed flanges by means of substantially coincident equations. Values for the reduced bending moment $M_{y,red}$ are therefore nearly the same up to the b/t ratio corresponding to the occurrence of web buckling. After this point, the AISI and EC3 codes provide values for the bending moment which are less than those given by CNR, with an increasing scatter of slenderness b/t . Despite different formulations used for web buckling, the AISI values match the CNR ones over a wider range, subsequently reaching the EC3 values after a discontinuous relationship. Note

a) box sections

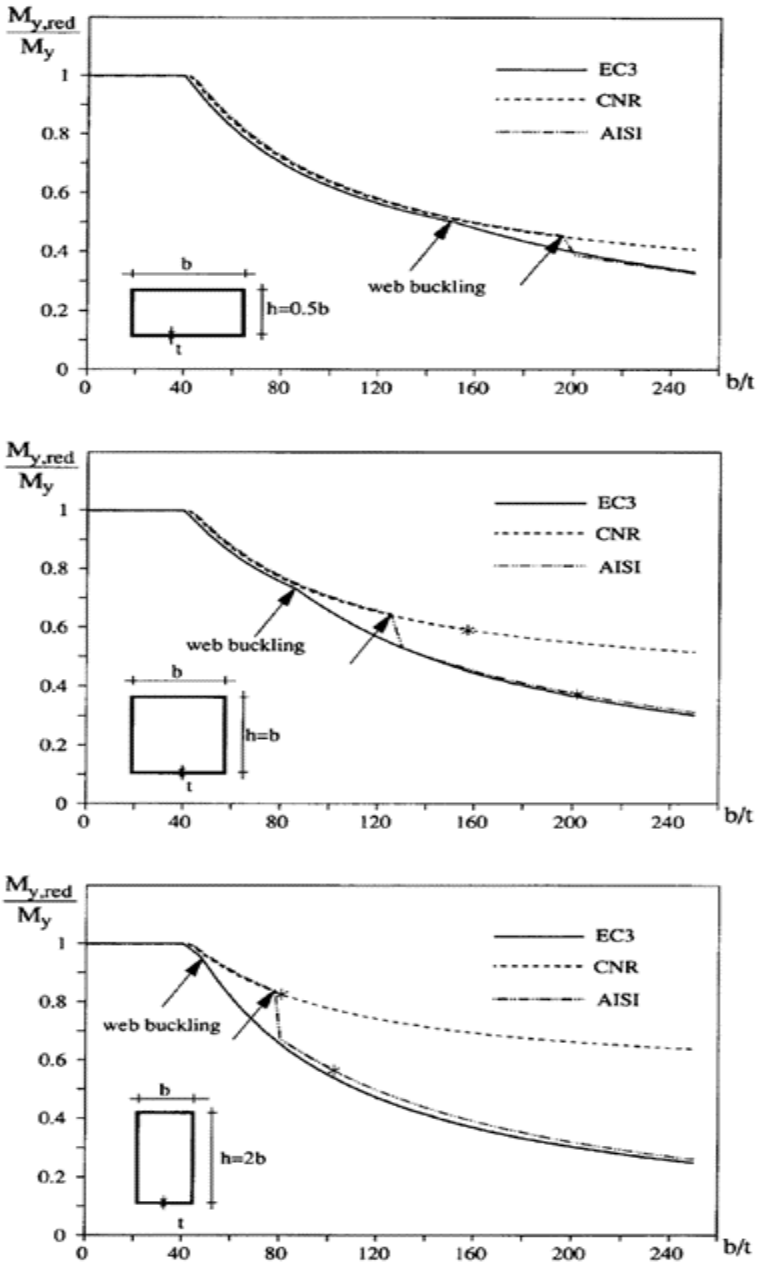


Figure 6.4(a) (Gherzi and Landolfo, 1992).

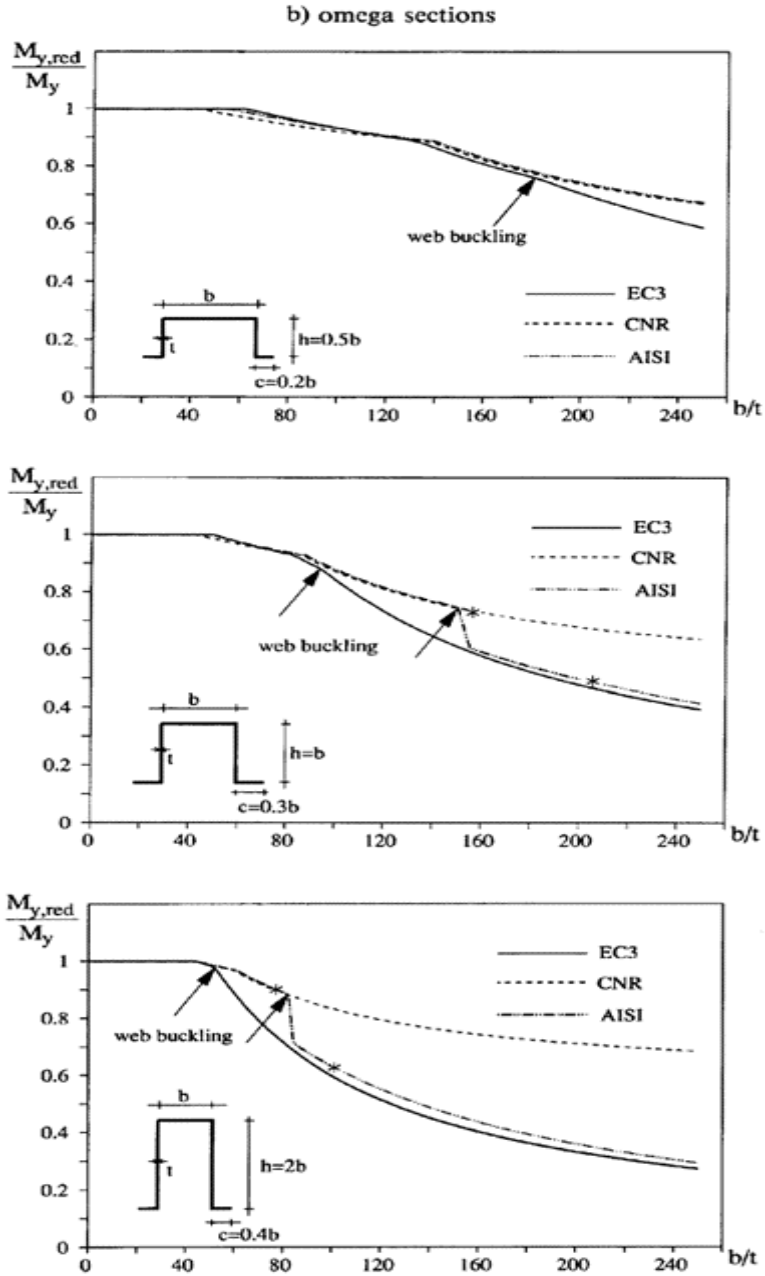


Figure 6.4(b) (Gherzi and Landolfo, 1992).

c) C sections

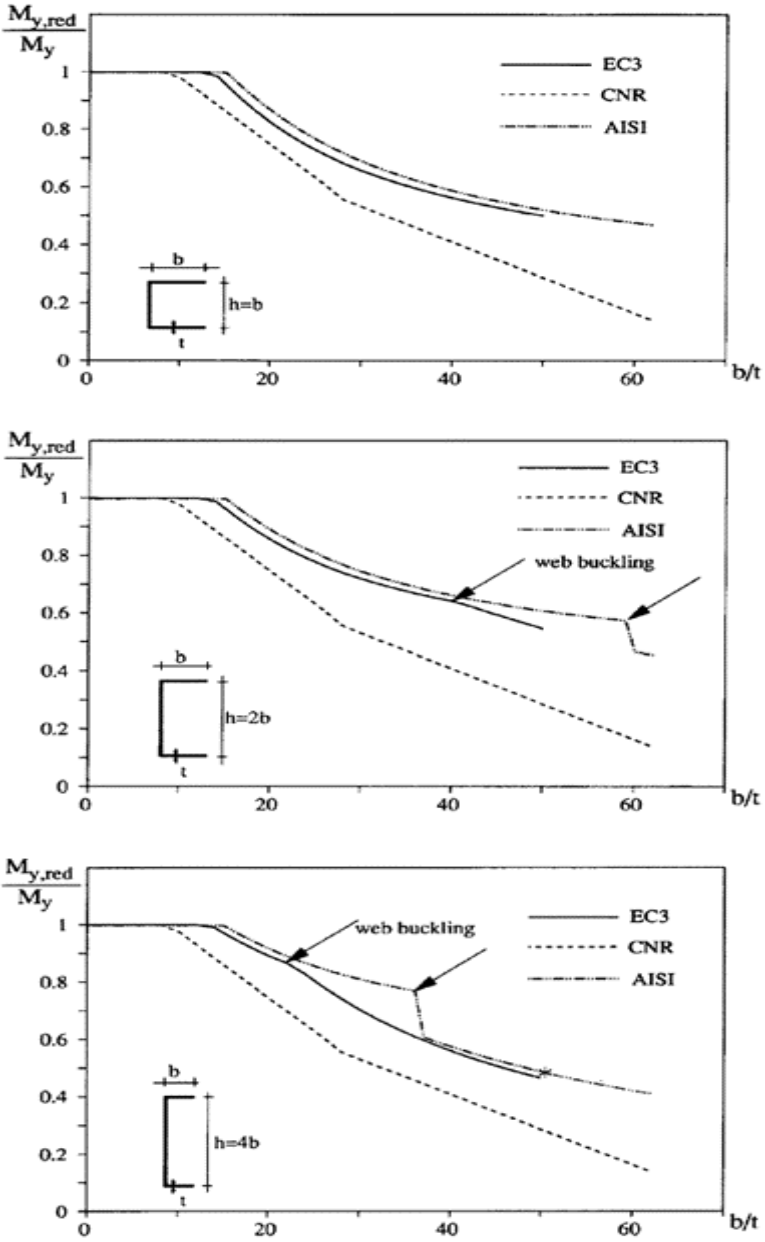


Figure 6.4(c) (Gherzi and Landolfo, 1992).

also that web buckling occurs for smaller values of the slenderness b/t ratio, when the relative height-to-width h/b ratio of the section is greater.

Omega sections (Figure 6.4b) In this kind of section, the centroid of the gross section is shifted towards the upper flange. For this reason, the yielding stress in the flange under tension is reached when $\sigma < f_y$ in the compressed flange. As the b/t ratio increases, the effective width of the flange decreases, with a corresponding lowering of the centroid, down to a limit value of b/t , which the yielding stress also simultaneously reaches in the compressed flange. In the first case ($\sigma < f_y$ in the compressed flange), the CNR values of $M_{y,red}$ are lower than those provided by the other codes, because the CNR formulation always uses the yielding stress to evaluate effective width. In the other cases, considerations related to box sections are also applicable to omega sections.

Channel sections (Figure 6.4c) The curves display the difference between the reduced stress (CNR) and effective width (AISI, EC3) approach to evaluation of the load-bearing capacity of an unlippped channel section. Contrary to the results of the previous two cross-sections, the Italian Code provides values notably lower than those of the other codes, with the gap increasing as does b/t . The AISI and EC3 values are similar, apart from the abovementioned difference in web-buckling occurrence.

6.3.3 Overall buckling

The overall buckling of a thin-gauge beam is a typical example of coupled buckling, in which the effect of local buckling of the compressed parts of the section is coupled to the global phenomenon, the so-called lateral torsional buckling. An approach to this problem might consist in the evaluation of the overall buckling load as the critical load of the effective section, calculated at the overall buckling stress. This should lead to an iterative procedure, because the buckling stress itself depends on the dimension of the effective section.

Nevertheless, a procedure based on the effective-section concept could give unreliable results for some types of section, such as the channels. We must remember that the hypothesis of constant stress acting on effective width is merely a simplification of the actual non-linear distribution of stress. Using this model, progressive elimination of the 'ineffective' end of a locally buckled unlippped flange greatly reduces the second moment of area about the minor axis and, therefore, a much greater lowering of the overall buckling load than experimental evidence shows.

For this reason, both AISI and EC3 codes provide a simplified approach which, first, requires evaluation of the elastic lateral buckling moment M_{cr} of the gross section.

EC3 calculates the limit moment of a beam, with respect to lateral torsional buckling $M_{b,red}$, by means of a coefficient χ_{LT} given by a general formulation widely used in codification to join elastic-buckling and yielding values:

$$M_{b,red} = \chi_{LT} M_{y,red}$$

being:

$$\chi_{LT} = \frac{1}{\phi_{LT} + \sqrt{\phi_{LT}^2 - \bar{\lambda}_{LT}^2}} \quad \text{with} \quad \chi_{LT} \leq 1 \quad (6.3)$$

where:

$$\phi_{LT} = 0.5[1 + \alpha_{LT}(\bar{\lambda}_{LT} - 0.2) + \bar{\lambda}_{LT}^2], \quad \bar{\lambda}_{LT} = \frac{\lambda_{LT}}{\lambda_1} \sqrt{\beta_w}$$

and:

$$\alpha_{LT} = 0.21, \quad \lambda_{LT} = \sqrt{\frac{\pi^2 E W_{pl}}{M_{cr}}}, \quad \lambda_1 = \pi \sqrt{\frac{E}{f_y}}$$

The approach proposed by the AISI Specification is slightly different. The stress σ_{cr} induced on the gross section by the global collapse moment (i.e. by the bending moment which takes both the yielding and the critical moments of the gross section into account) is first evaluated. The limit moment is then given as the yielding moment corresponding to the effective section determined for the critical stress σ_{cr} .

Finally, no prescription is given by the Italian Code CNR for analysis of the lateral buckling of thin-gauge sections.

As an example, Figure 6.5 shows the limit moment given by EC3 and AISI as a function of the geometrical slenderness ratio λ_{LT} in the case of a typical double-channel cold-formed section, with $h/b=2$ and $b/t=40$. The values provided by EC3 appear to be safer, mainly in the range $40 < \lambda_{LT} < 100$. For λ_{LT} greater than 120, both curves are practically coincident.

6.3.4 Serviceability limit state

Referring to the previously selected sections (box, omega and C), each with three given b/t ratios, comparison related to the serviceability limit state can be carried out by evaluating the moment of inertia of the effective section I_{eff} corresponding to an increasing moment M . Figure 6.6 (a,b,c) shows the ratio of I_{eff} over the moment of inertia of the gross section I , as a function of the ratio M/M_y . The CNR formulation leads to a more continuous curve which always decreases as M approaches M_y . Web buckling causes a

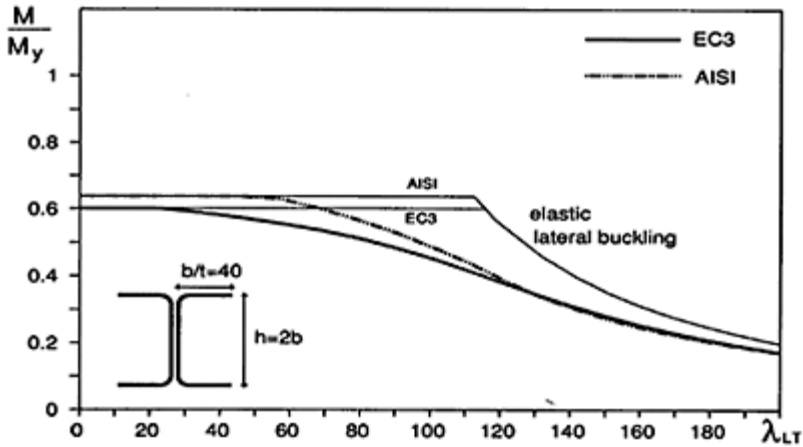


Figure 6.5 (Gherzi and Landolfo, 1992).

noticeable change of slope in EC3 curves, while sharp jumps and a decrease in M characterize the AISI curves. No comparison with CNR values is possible in the case of channel sections, because the Italian Code uses the reduced stress approach for simply supported elements, which is not consistent with the approaches used by the other two codes.

6.4 MEMBERS IN COMPRESSION

6.4.1 Local buckling

In this case, every element of the section is uniformly compressed. The effect of local buckling is, thus, taken into account by evaluating the effective width (or the reduced stress, for simply supported elements according to CNR Code) of each element. The effective area A_{eff} of the compressed section is, therefore, defined, based on the reduction of each element in width or stress. Comparative examination of the three codes is made by applying this criterion to the three types of sections defined in Section 6.1 (box, omega and C). Figure 6.7 (a, b, c) displays the parameter $\bar{A} = A_{eff}/A$, ratio of the effective over gross area, as a function of the slenderness b/t . The limit slenderness proposed by codes for lipped sections is marked by a star (Figure 6.7b).

In the case of box sections, which present only doubly supported elements, the values of \bar{A} given by all codes are comparable with very small scatters.

In the case of open sections (omega or channel) the reduced stress approach (CNR) appears once again to be too cautious, leading to values of \bar{A} lower than those given by the other codes. Numerical analysis points out the problem of the effectiveness of stiffening elements (i.e. bottom flanges in omega sections or both flanges in channels), which also exists

a) box sections

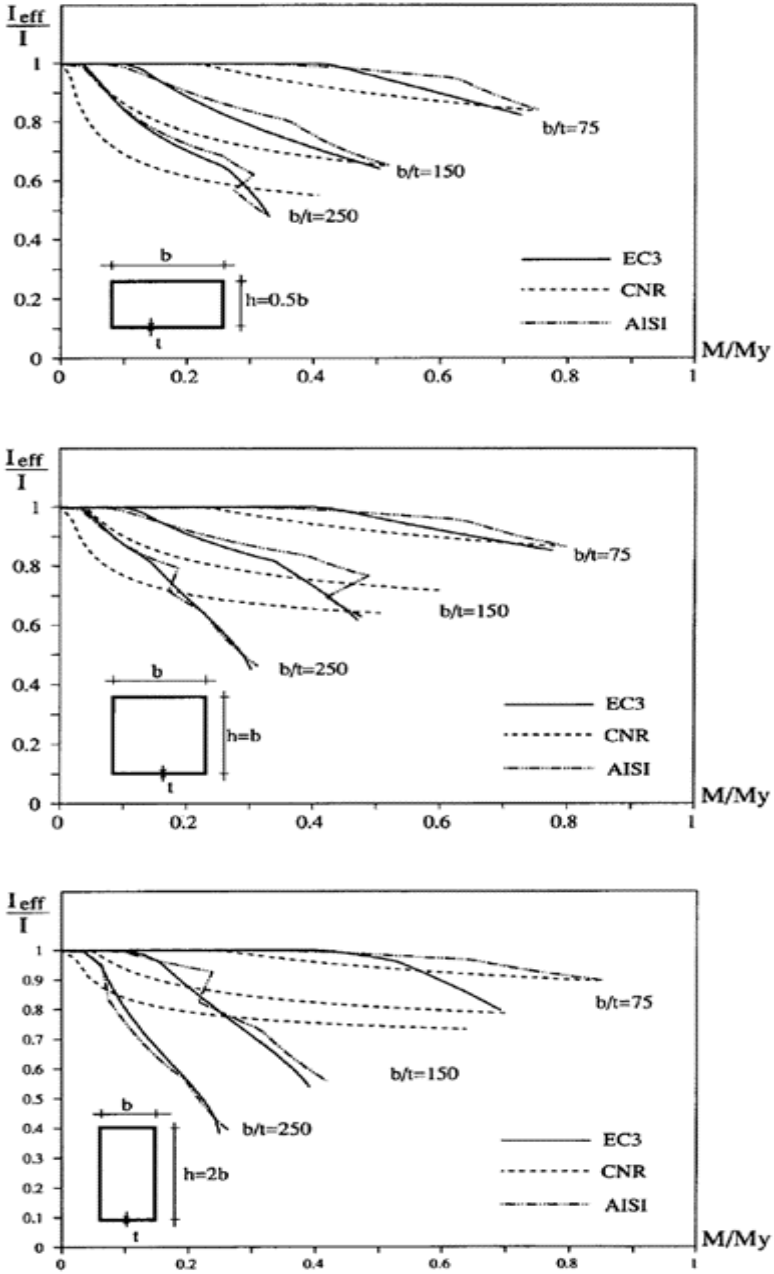


Figure 6.6(a) (Gherzi and Landolfo, 1992).

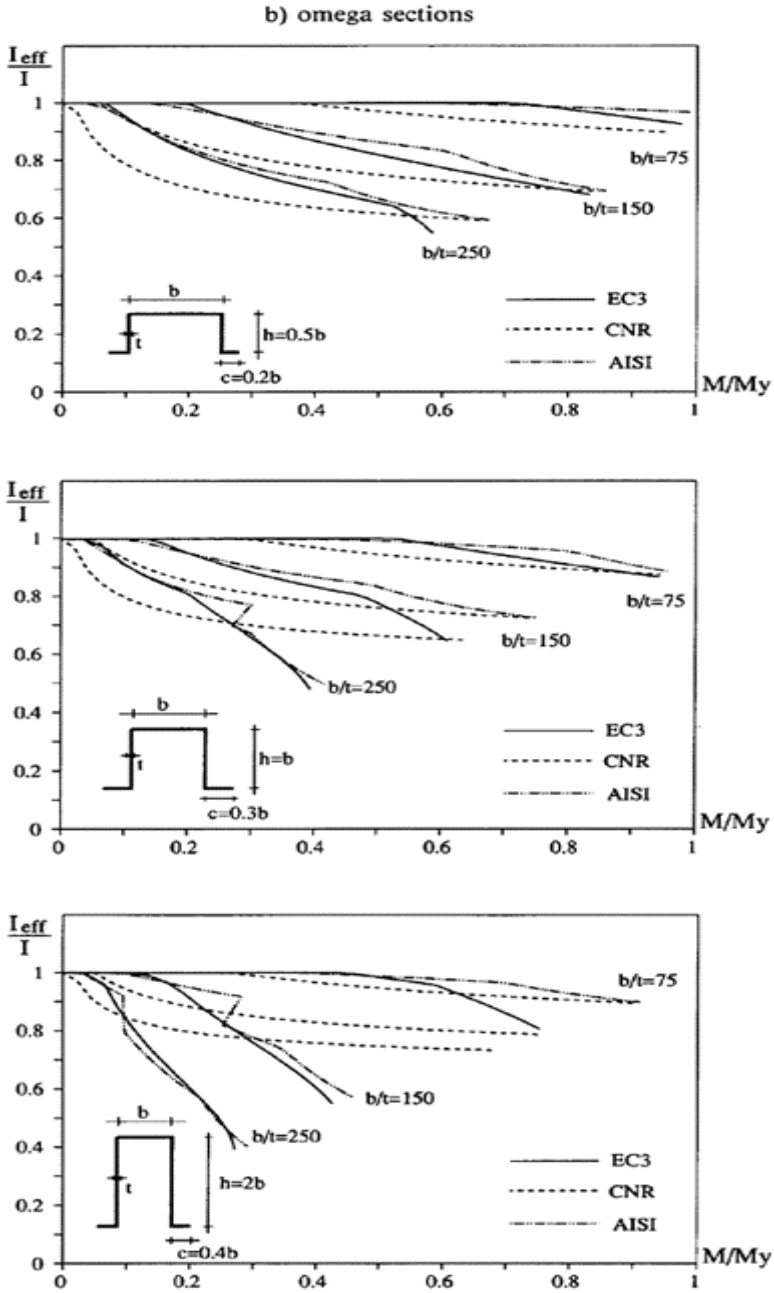


Figure 6.6(b) (Gherzi and Landolfo, 1992).

c) C sections

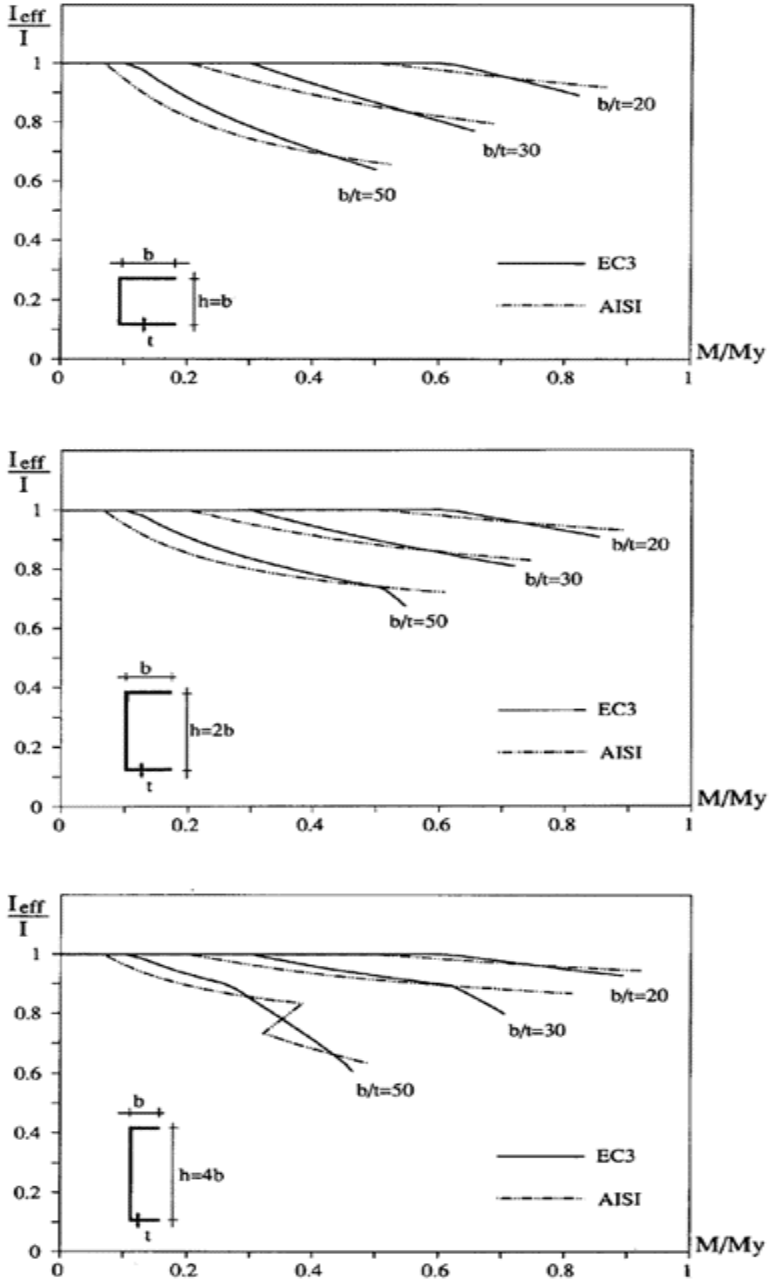


Figure 6.6(c) (Gherzi and Landolfo, 1992).

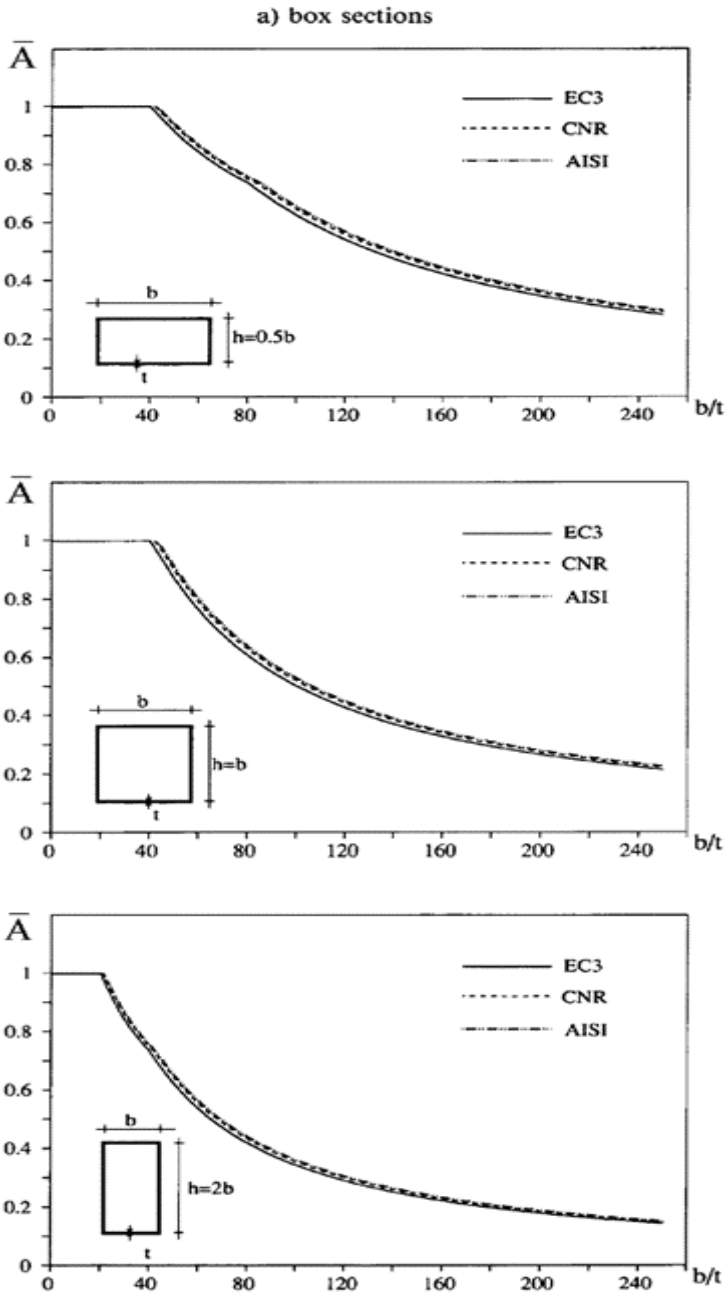


Figure 6.7(a) (Gherzi and Landolfo, 1992).

b) omega sections

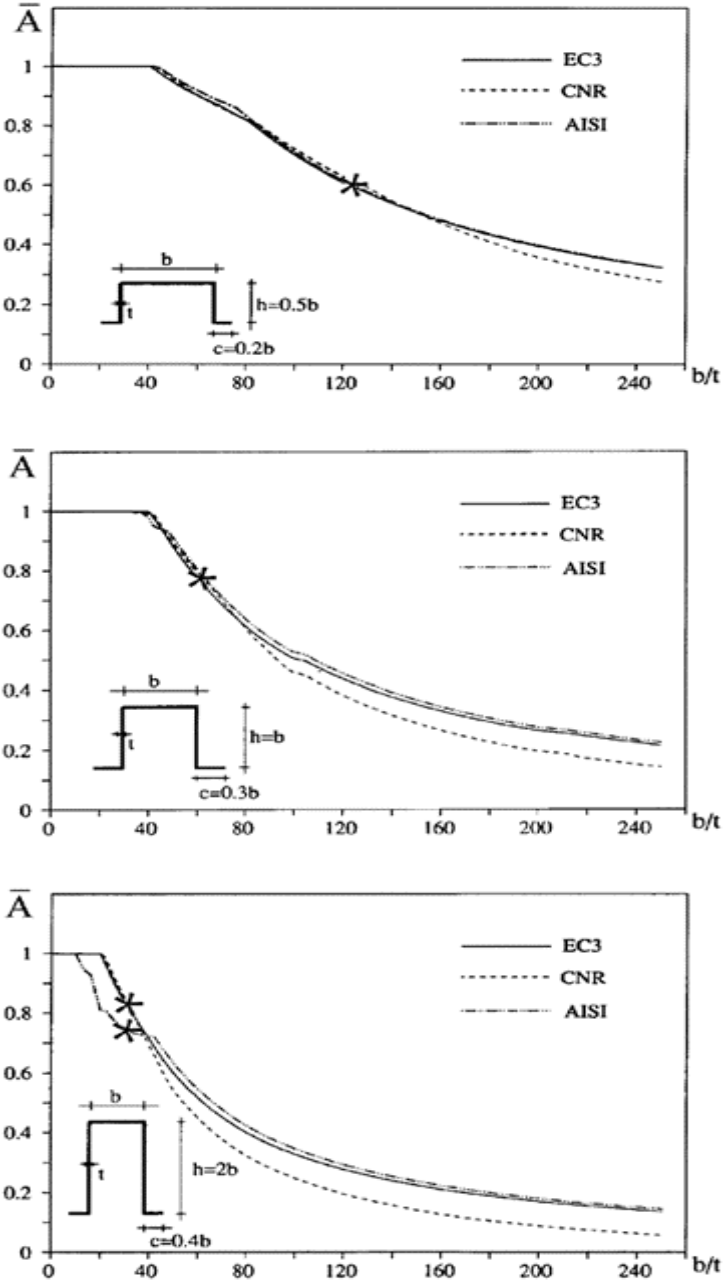


Figure 6.7(b) (Gherzi and Landolfo, 1992).

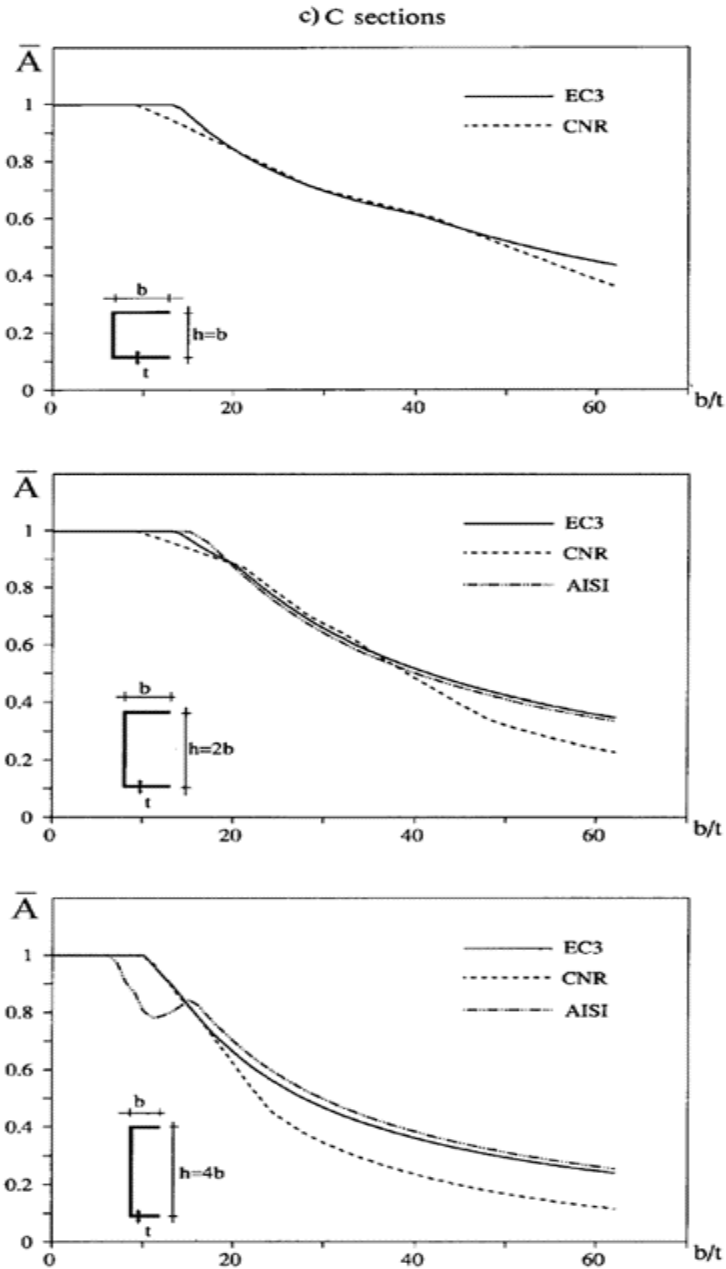


Figure 6.7(c) (Gherzi and Landolfo, 1992).

when members bend even though this is not manifested by the previously examined examples.

The Italian Code considers the restraining effect of a lip when its length is greater than a prescribed minimum value. This condition is fulfilled by the chosen sections. EC3 similarly limits the second moment of stiffener, but also proposes more careful analysis which models the lip as an elastic restraint. The AISI Specification supplies a minimum moment of inertia which a lip should have in order to be a fully effective restraint; in addition, the buckling coefficient k_σ should be reduced when the moment of inertia of the stiffener is lower than the limit and when its length is excessive (lips with a length greater than 80% the size of the stiffened element are not permitted).

The effect of these prescriptions is clearly depicted from the curves that relate to omega and channel sections with higher h/b ratios, which show a reduction in \bar{A} for low values of b/t .

6.4.2 Overall buckling

The interaction between local and global buckling plays a very important role in every member in compression. In order to verify a compression section, we have to evaluate a reduced axial force $N_{y,red}$ which takes both phenomena into account. The Italian Code reduces N by means of a coefficient ω , which may be determined from the member slenderness A (evaluated considering the gross section) and the coefficient \bar{A} (for the uniform stress distribution on the section). The 1990 preliminary version of EC3 used a coefficient X , analogous to XLT of equation (6.3), to connect $N_{y,red}$ to the slenderness λ and the \bar{A} factor, both determined for the effective section corresponding to The 1992 revised version substantially modified the approach, connecting $N_{y,red}$ to the slenderness of the gross section. The AISI Specification, using the same approach as for lateral torsional buckling of beams, seeks first to evaluate the reduced critical stress σ_n corresponding to slenderness of the gross section; $N_{y,red}$ is finally obtained multiplying σ_n by the value of the effective area evaluated for $\sigma = \sigma_n$.

Numerical comparison of the different approaches has been made with reference to the above box, omega and C sections with $h/b=0.5$ and three values of b/t ratio. The shape of the sections presents a symmetry axis corresponding to the weak direction along which the member may buckle. Figure 6.8 displays the ratio of $N_{y,red}$ over the axial force for the gross section needed to prevent buckling N_y , as a function of the slenderness A of the member.

The curves provided by the codes, in the cases of box and omega sections, show some differences, but are substantially analogous. It is only in the case of channel sections that the preliminary version of EC3 gives values which decrease too quickly with A , due to the strong difference between effective and gross section slenderness.

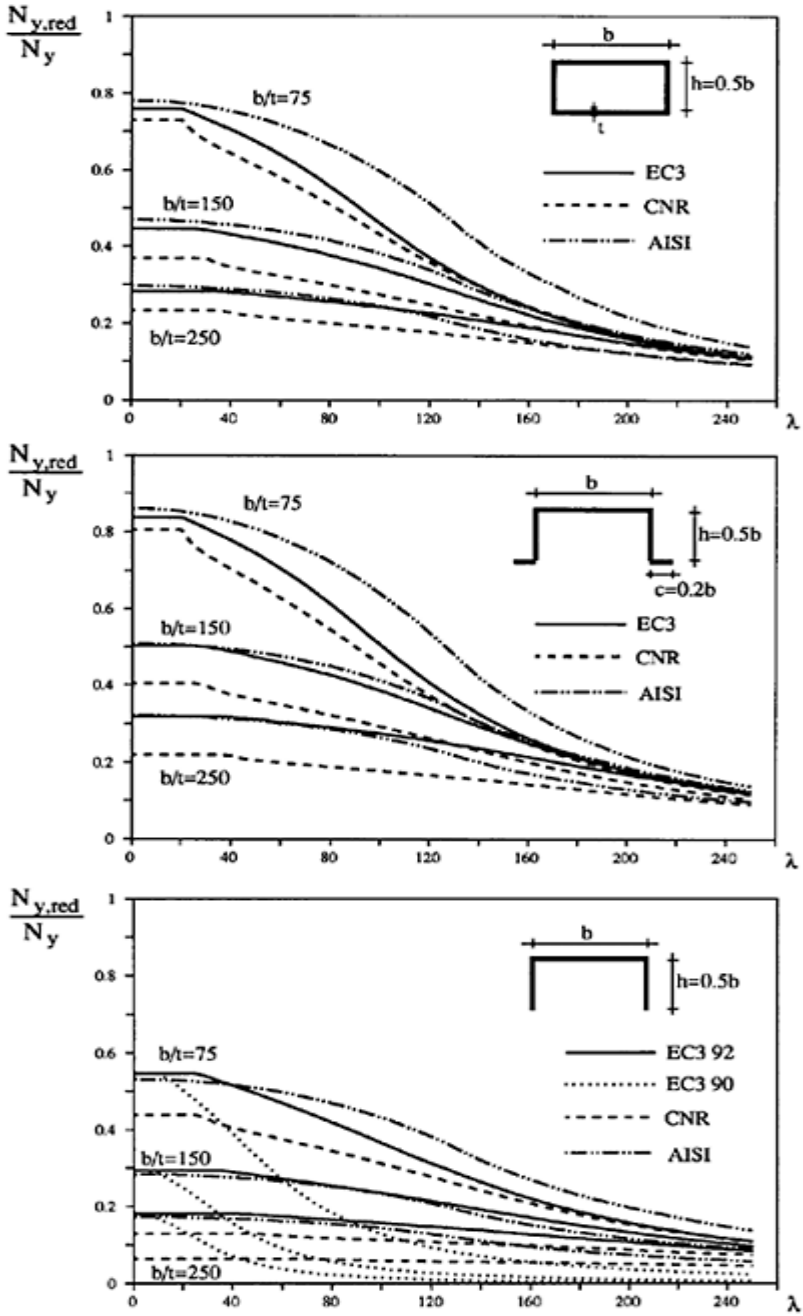


Figure 6.8 (Gherzi and Landolfo, 1992).

6.5 BEAM COLUMNS

In sections with a single axis of symmetry (e.g. omega and channel sections), the centroid of the effective section is shifted with respect to that of the gross cross-section. Therefore, the section is uniformly compressed only when the axial force is applied to the centroid of the effective section. Otherwise, the section should be checked for combined axial force and bending, this being evaluated with reference to the distance between the centres of the effective and gross sections. This important clarification is not present in the Italian Code, because in the case of open sections it uses the reduced stress approach, which does not permit identification of the centroid of the locally buckled section.

Analysis of a thin-gauge section having combined axial force and bending is very complex, even for evaluation of local buckling, because an iterative procedure should be followed to obtain the correct correspondence of stress distribution with the effective section. The intricacy of the problem is increased by the need to take both flexural and torsional buckling into account, together with the interaction between local and global buckling, as well as the distribution of bending moment along the longitudinal axis of the member. For these reasons, a conventional simplified approach should be followed in numerical applications. All codes determine the limit values for combined axial force and bending moment on the basis of the limit values for the single axial force ($N_{y,red}$) and bending moment ($M_{y,red}$), by means of equations which are similar, but may nevertheless lead to substantial differences.

Exhaustive analysis of this problem, which will require a very wide parametric investigation and comparison with experimental results, is beyond the scope of this book. Nevertheless, the $M-N$ limit curves plotted in Figure 6.9 provide interesting indications. They refer to three columns subjected to bi-triangular distribution of bending moment (a typical distribution in the case of horizontal action), made of box, omega and C sections with $b/t=75$ and $\lambda=100$. First, note the great difference in the shape of these curves, due to the peculiar formulation provided by each code.

The abovementioned shifting effect of the centroid (effective versus gross section) is clearly shown in the case of omega and channel sections. The axial force N , applied to the centre of the gross section, can reach its maximum value when added to the bending moment necessary to bring the resultant action to the centroid of the effective section and this bending moment is negative in the case of omega sections and, positive for channel sections, because of the different signs of eccentricity. Only the CNR values

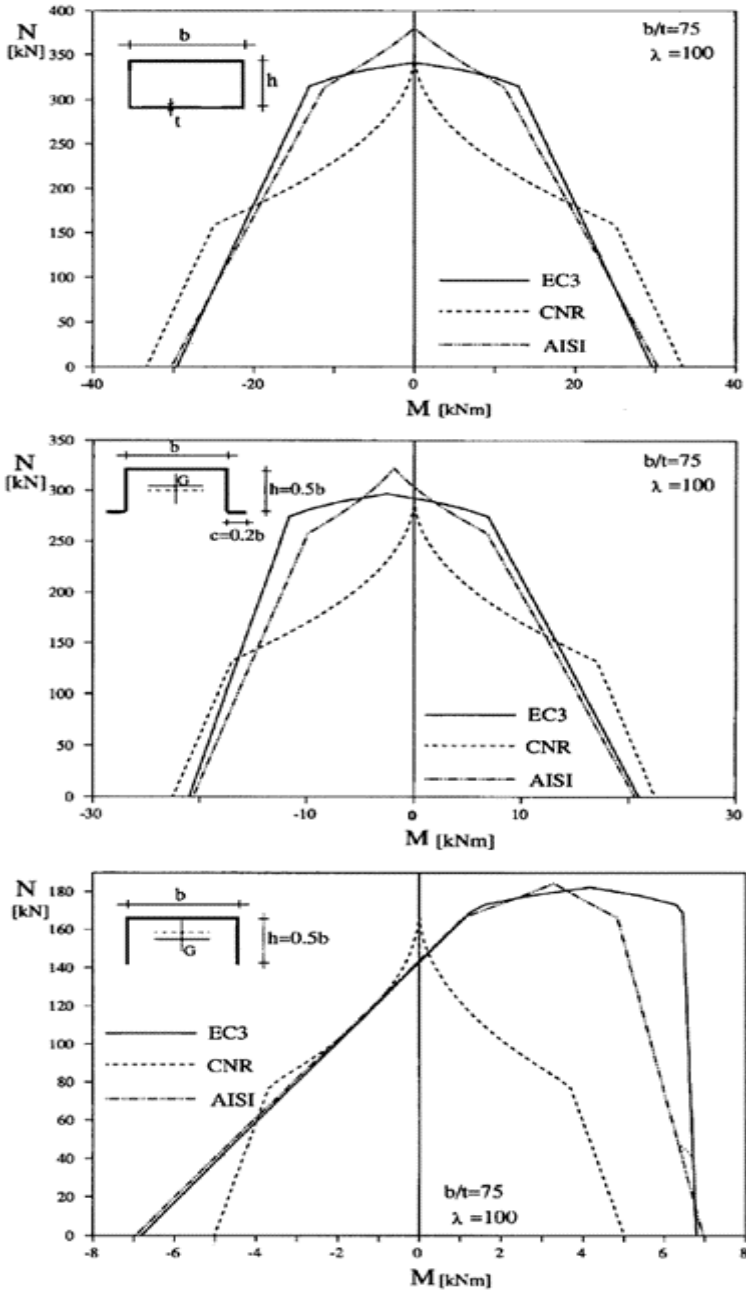


Figure 6.9 (Gherzi and Landolfo, 1992).

fail to show this effect, because of the reasons referred to above. The differences are enhanced in the case of channel sections, because of the greater value of the shift and the strong reduction of $N_{y,red}$ provided by the preliminary version of EC3, as discussed in Section 6.4.

6.6 APPLICATION OF DIFFERENT METHODOLOGIES

6.6.1 Design methodologies

Several approaches are available for predicting the ultimate strength of thin-walled sections, according to various specifications for steel and aluminium cold-formed profiles (Landolfo and Mazzolani, 1997).

As mentioned in Section 4.1, one method used for cold-formed aluminium alloy profiles is based on replacing the true section with an effective one obtained by reducing the actual thickness of the compressed parts. It has been adopted both in EC9 (CEN, ENV 1999-1-1, 1998) and British Standard BS 8118 (1991) for aluminium structures.

A second method, which is very popular in the field of cold-formed steel profiles, is based on the effective-width concept, which has been followed by both EC3 (CEN, ENV 1993-1-3, 1996) and AISI Specification (AISI, 1996). Finally, the reduced-stress approach evaluates the capacities of a slender section by considering a reduced value for the limiting stress acting on the full section. This route has been partially followed by the Italian code CNR for steel (CNR 10022, 1984).

As for sections subject to bending, the difference among the three approaches can be evaluated by comparing the corresponding design moment.

(a) *Reduced-thickness approach*

The load-carrying capacity in bending is given by:

$$M_{d,1} = W_{eff,t} f_d \quad (6.1)$$

where $W_{eff,t}$ is the section modulus of the effective cross-section obtained by reducing the thickness of any slender element which is wholly or partially in compression, by means of a factor k_L evaluated according to the code provision; f_d is the design value of the material strength.

(b) *Effective-width approach*

The load-carrying capacity in bending is given by:

$$M_{d,2} = W_{eff,b} f_d \quad (6.2)$$

where $W_{eff,b}$ is the section modulus of the effective cross-section obtained on the basis of the effective width of each individual element by applying the rules given in the codes; f_d is the design value of the material strength.

(c) Reduced-stress approach

Two different expressions of the ultimate design moment are available:

$$M_{d,3} = W_g f_d k_{L,min} \quad (6.3)$$

$$M_{d,4} = W_g f_d k_{L,av} \quad (6.4)$$

according to two definitions of the stress-reduction factor k_L , where W_g is the section modulus of the gross section and f_d is the design value of the material strength. The stress-reduction factor k_L can be defined in two ways:

- it can be equal to the smallest buckling coefficient kL provided by the code for a compressed flange ($k_{L,f}$) or web ($k_{L,w}$):

$$k_{L,min} = \min \begin{cases} k_{L,f} \\ k_{L,w} \end{cases} \quad (6.5)$$

- it can be a weighted average factor, evaluated as follows:

$$k_{L,av} = k_{L,av} \frac{bt_f k_{L,f} + ht_w k_{L,w}/3}{bt_f + ht_w/3} \quad (6.6)$$

where b and h are the actual widths of the flange and web, respectively.

The above design methodologies have been applied to predict the load-bearing capacity of a set of typical unwelded sections in bending. In order to emphasize just the influence of the design approach, the same local buckling curve [namely the one provided by EC3 (Part 1.3)] has been considered to evaluate the factor-reducing thickness, width or stress.

In particular, the three shapes of steel sections (box, omega and C) with three values of the ratio of web height h to flange width b have been used (see Figure 6.1).

The load-bearing capacity has been compared by evaluating the design moment M_d on the basis of different models and for many values of the geometrical slenderness ratio b/t . The M_d values are normalized by the yielding moment of the gross section $M_{y=}W_g f_d$, where f_d is the design strength which can be taken equal to f_y for steel and $f_{0.2}$ for aluminium alloys divided by the corresponding γ_m . In the application of the EC3 (Part 1.3) provision, the plastic reserves of the section have been ignored (i.e. the shape factor of the cross-section is taken equal to 1).

As design moments, equations (6.1)–(6.4) have been used.

6.6.2 Comparison

Box sections (Figure 6.10)

This kind of section is composed only of flat internal elements, for which the BS 8118 and EC3 (Part 1.3) approaches evaluate local buckling of the compressed part by means of similar relationships.

In all cases, the reduced-stress approach with $k_{L,min}$ is the most conservative, while the reduced thickness approach is the most optimistic.

Omega sections (Figure 6.11)

This profile is characterized by a mono-symmetrical gross section, whose centroid is located towards the upper flange. Due to this, in absence of local buckling phenomena, the yielding stress in the flange under tension is reached when in the compressed flange $\sigma < f_d$. As b/t increases, the upper flange partialization due to local buckling involves the centroid moving up to a limit value of b/t for which the yielding stress, evaluated on the effective section, is simultaneously reached in both flanges (point A in Figure 6.11).

Before point A is reached, the bending strength reduction due to local buckling in the flange is less strong. In fact, the reduction in terms of inertia moment of effective area is partially compensated by the reduction of distance between neutral axis and the most stressed flange (tensile flange). After this situation, the behaviour of the section becomes the same as a symmetrical one. Following the effective-width approach, as stated in EC3 (Part 1.3), such behavioural aspects are accounted for by considering the effective-width ratio related to the actual stress on the compressed flange, evaluated by means of an interactive procedure. On the contrary, BS 8118 for 'understressed flange elements' prescribes a more favourable classification based on a modified value of $\varepsilon = (250y_1/f_d y_2)^{0.5}$, where y_1 and y_2 are the distances from the neutral axis of the gross section to the most severely stressed fibres and to the element, respectively. In this way, the element slenderness is reduced by a factor exclusively connected to the gross section, which could also be much different from the effective one. For these reasons, this methodology always leads to unconservative values for the ultimate design moment, with respect to those provided by EC3 (Part 1.3).

For the two methods based on the reduced-thickness and reduced-strength approach, the trend in design moment curves confirms considerations related to the box section, with these methods representing the upper and lower bounds of all curves, respectively.

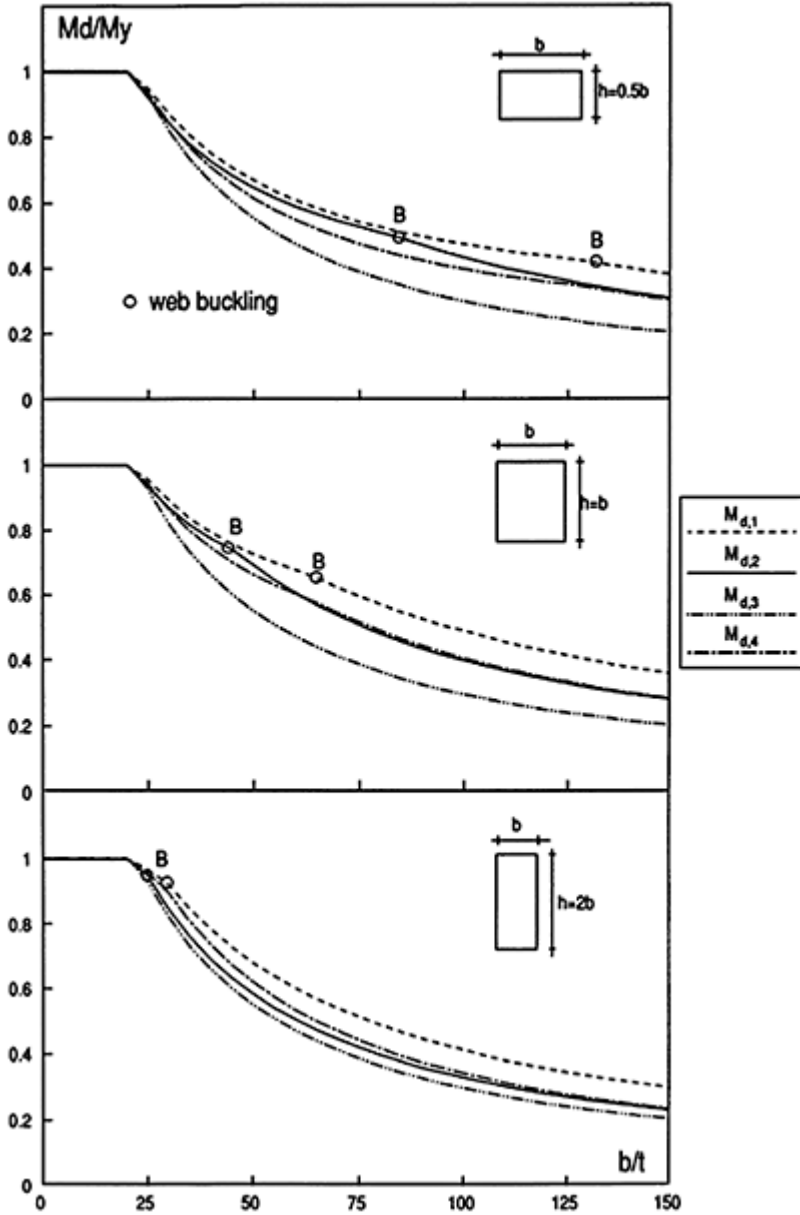


Figure 6.10 (Landolfo and Mazzolani, 1997).

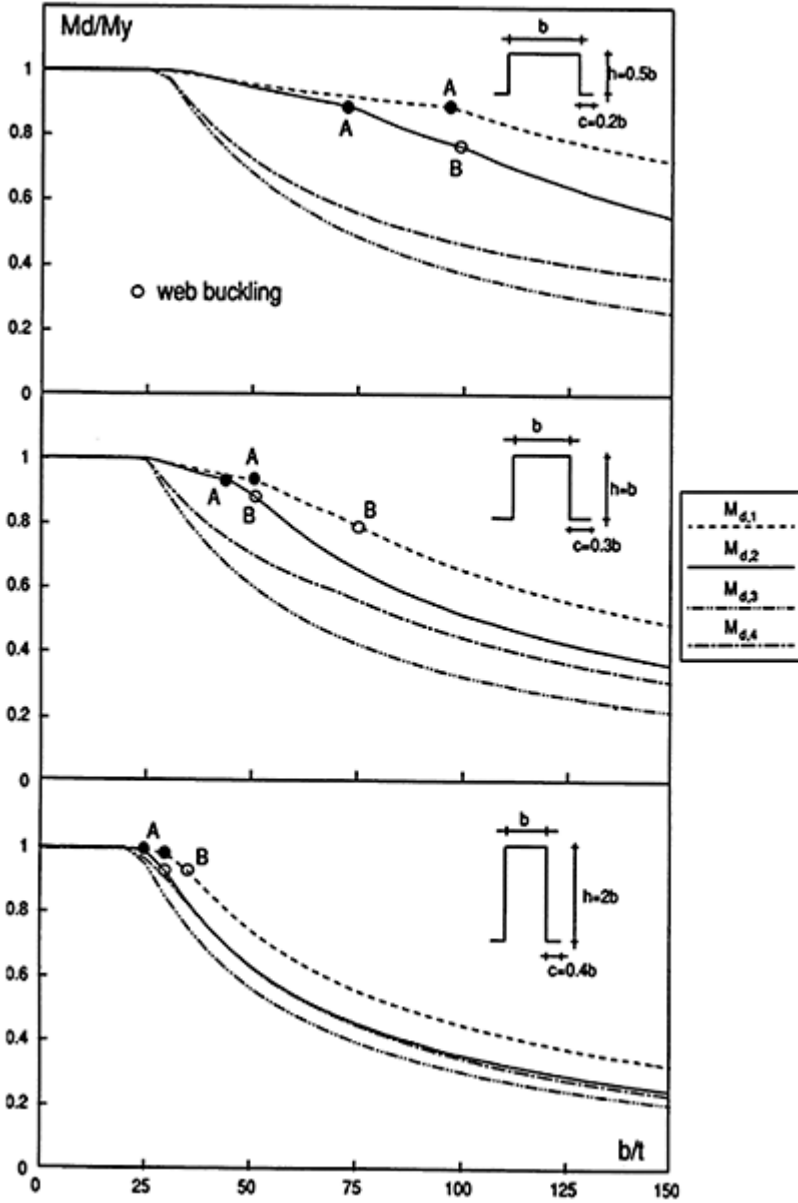


Figure 6.11 (Landolfo and Mazzolani, 1997).

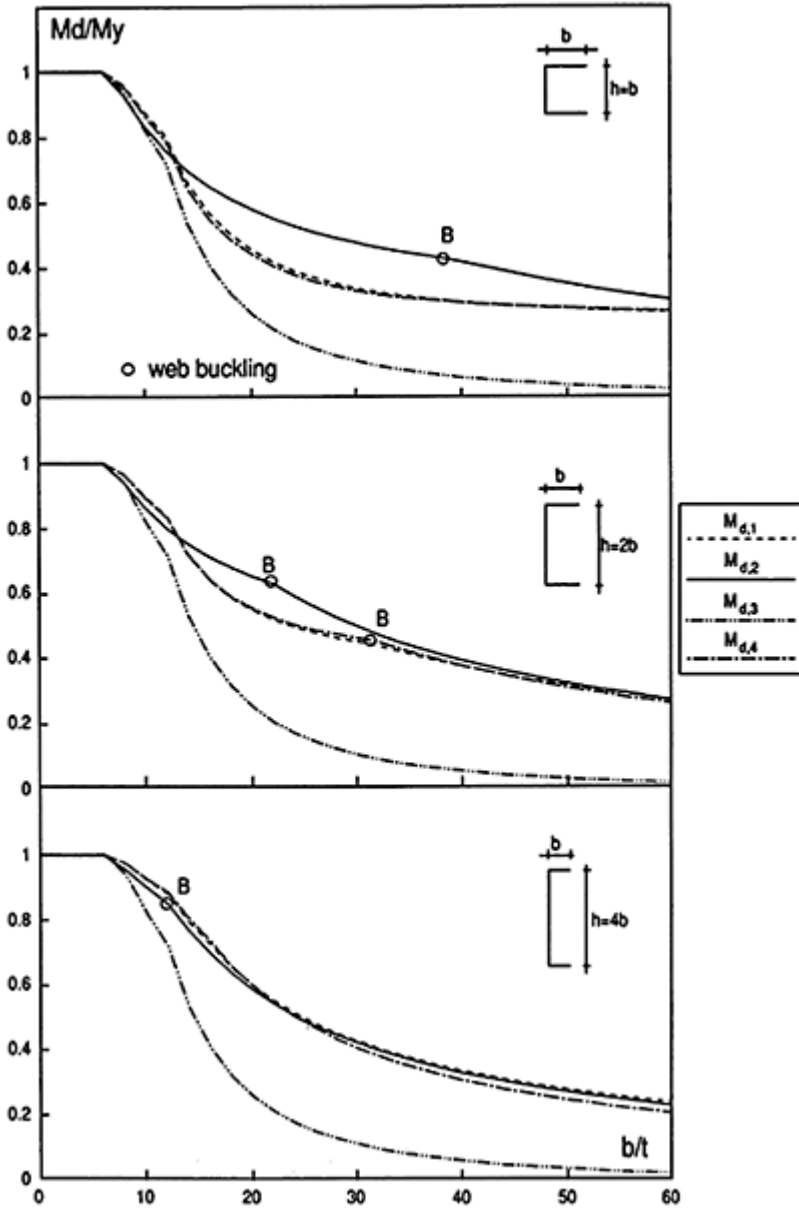


Figure 6.12 (Landolfo and Mazzolani, 1997).

Channel (C) sections (Figure 6.12)

In this case, the section is composed both by outstand (flanges) and internal (web) elements. Prior to web buckling, the comparison between $M_{d,1}$ and $M_{d,2}$ curves emphasizes how these approaches differ in accounting for local buckling in the outstand element. In particular, following the BS 8118 method, the reduction factor of flange thickness is proportional to the Euler buckling load starting from $b/t > 12.1$. As a consequence, the $M_{d,1}$ value is significantly lower than $M_{d,2}$, which is calculated on the basis of the effective width related to the postbuckling strength of the flange. However, when web buckling occurs (point B in Figure 6.12), such scatter tends to reduce and the design moments become practically coincident, especially for high values of the h/b ratio.

This happens for b/t values which decrease as the section height increases. As far as reduced-stress approaches are concerned, both $M_{d,3}$ and $M_{d,4}$ curves show a discontinuity for $b/t = 12.1$, corresponding to the change of the k_L law in the flange. The results obtained by using $k_{L,min}$ are very conservative, as in all the section cases examined, while the $M_{d,4}$ values are practically coincident with those provided by the reduced-thickness method. In the case of high sections, note that the b/t ratio corresponding to web buckling tends to approach that of the buckling load of flanges and the design moment becomes practically coincident, except for $M_{d,3}$ which is always the most conservative.

7

The ColdForm computer program

7.1 INTRODUCTION

The ColdForm computer program was created in the late 1980s at the University of Naples, Italy, as a research tool for comparing the provisions about thin-walled steel cross-sections given by Italian code (CNR 10022), European code (Eurocode 3 (Part 1.3)) and American code (AISI Specification).

Its first commercial version (ColdForm 2.0) was developed in 1993 with the sponsorship of CTA (Collegio dei Tecnici dell'Acciaio, i.e. College of Steel Technicians) and commercialized by ACAI (Associazione Costruttori in Acciaio Italiani, i.e. Association of Italian Steel Constructors). It was a Quick Basic version with a Windows-like appearance, which only allowed checking thin-walled steel cross-sections according to Eurocode 3 provisions.

The present release (ColdForm 3.0 or ColdForm 2001) is a Visual Basic version fully complying with Windows standards, which allows analysis of both steel members (according to Eurocode 3 and AISI Specification) and aluminium members (according to Eurocode 9 provisions).

7.1.1 Installing ColdForm 2001

ColdForm 2001 is equipped with a standard Setup program that checks the system and asks questions about how the user wants to install the product. The Setup program also decompresses the files on the program disks and copies them in the user-specified directory or in the system directory of the hard disk. Standard system requirements (Windows 95 or later, few megabytes of disk space) are necessary to perform installation and to run ColdForm 2001.

Please remember that the program disks include many .DLL files, which as in any Windows installation may overwrite previous versions in the system directory. According to Microsoft statements, this should give no problem to the system, but we all know how stable (or unstable) Windows is and what can happen because of inconsistent releases of .DLL files.

The README file on the program disks lists any changes to the ColdForm 2001 documentation since the publication date of this book and contains troubleshooting information for SETUP.EXE.

7.1.1 The graphic interface of ColdForm

Like most Windows programs, the ColdForm window (Figure 7.1) contains a menu bar, a tool bar and a status bar. Its working area contains the data window and output window.

The data window, non-resizeable and always placed to the right of the ColdForm window, outlines in brief the data in use (cross-section and load plane, member geometry, material) and allows the user to quickly modify them by double-clicking the corresponding portion of the window. Further information (code in use, option on corner thickness reduction) is given in the status bar and may be modified in the same way. The output window is usually filled with the results of the performed checks, which may be edited, added with remarks and reorganised using Notepad.

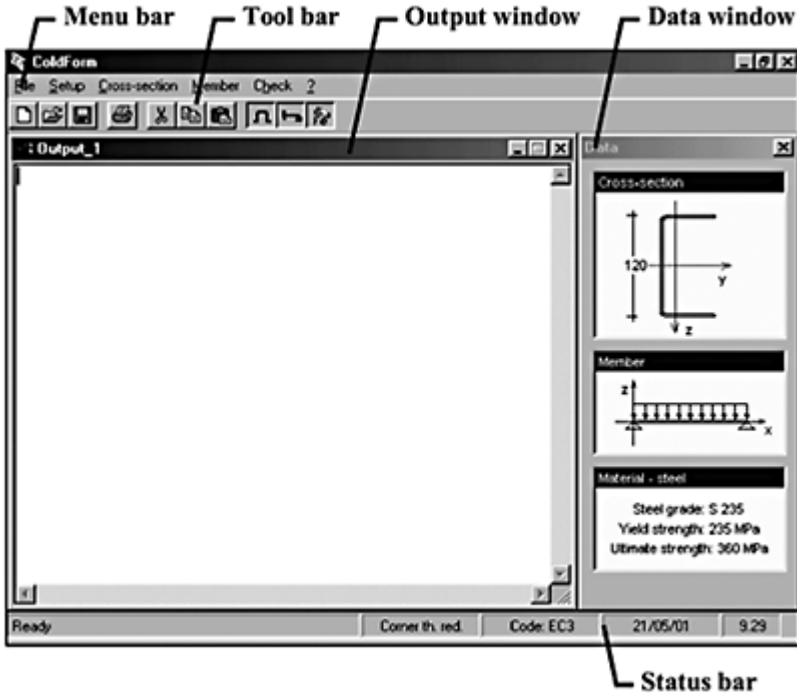


Figure 7.1 The ColdForm window.



Figure 7.2 Arrows, ellipses and check marks in menu commands.

7.2 MENU BAR

The menu bar (Figure 7.2), which allows selection of all ColdForm commands, has six menus: **File**, **Setup**, **Cross-section**, **Member**, **Check** and **?** (i.e. Information). As usual in Windows programs, each menu is popped down by clicking on its name (or by the shortcut Alt+underlined letter). In each menu, the active commands are drawn in black, while those which cannot be used at the moment are faded (e.g. **Check member** when member geometry or loads are not defined). An arrow (▶) following a menu command points out the presence of a submenu, while the ellipsis (...) announces a dialog box. A check mark (✓) individuates an active option (e.g. **Corner thickness reduction**) or a current selection (e.g. the type of cross-section).

7.2.1 File menu

Most commands of the File menu are related to the output window (Figure 7.3). **New output** closes the output window (after asking us for confirmation, if it contains unsaved data) and opens a new window with a default name (**Output_1**, **Output_2** and so on). **Open output** allows the user to search for a file to open, by means of the standard Open dialog box. **Close output** closes the output window (after asking us for confirmation, if it contains unsaved data). **Save output** saves the data in the output window as a text file, having the name displayed in the title bar of the window (with the default extension .CLF, if no other extension has been expressly defined). **Save output as** allows us to give a new name to the output window and to save its data, by means of the standard **Save as** dialog box. **Print output** sends the text in the output window to the system printer.

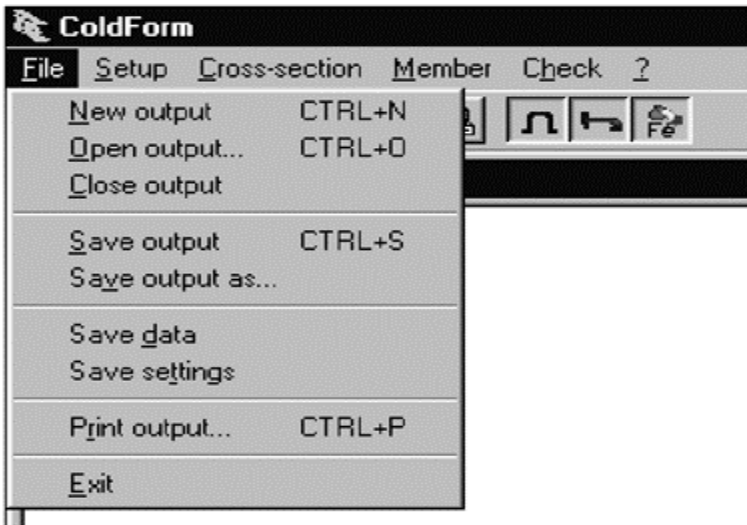


Figure 7.3 The File menu.

Two commands allow us to save the actual values of data and program settings. **Save data** keeps it all in a text file named COLDFORM.DAT in the Windows directory, including items such as the last type of cross-section used, data describing the last values used for each type of cross-section, geometry and loads of the member. **Save settings** writes to a text file, named COLDFORM.INI also in the Windows directory, information describing the material and code in use, and also the size and position of the program windows. These files are updated only when we expressly use the **Save data** and **Save settings** commands and should be manually deleted if we want to return to the defaults of the program.

Finally, the **Exit** command ends the program execution, after asking us if we want to save the data contained in the output window, if they have not yet been saved.

7.2.2 Setup menu

A setup menu usually contains commands which govern the options and characteristics of the program and which, in most cases, are used just once, after installation, to modify the program defaults. The **Setup** menu of ColdForm 2001 (Figure 7.4) also includes a command to define the type of material (steel or aluminium), its characteristics and the code according to which structural checks should be performed (i.e. information which should not be frequently varied, unless comparative analyses are requested). Material and code are strictly connected, because each code deals with a specific material; the **Material and code** command is discussed in detail in Section 7.2.3.

The **Safety factors** dialog box (Figure 7.5) contains of four tabs, which

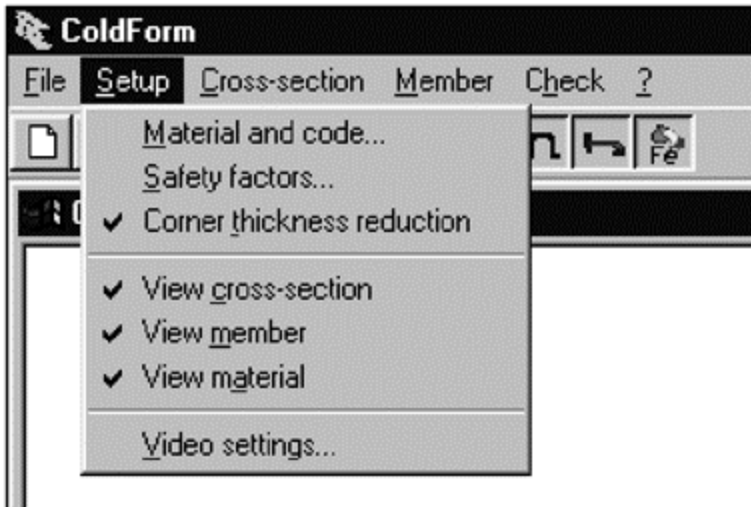


Figure 7.4 The **Setup** menu.



Figure 7.5 Two tabs of the **Safety factors** dialog box.

allows us to modify the partial safety factors γ used by Eurocodes 3 and 9 and the coefficients ω and ϕ used by AISI, so that permissible strengths in the case of allowable stress design (ASD) or factored resistances in the case of load and resistance factor design (LRFD) can be obtained. The option of modifying these factors is expressly considered by the Eurocodes, which leave final definition of their values to national application documents (NADs); in the computer program such an option has been extended to AISI values for the sake of generality.

Thinning of corners because of cold-forming was discussed in Section 1.6. It can be taken into account, for determining cross-section properties, by activating the **Corner thickness reduction** option. This option may be switched (activated or deactivated) by clicking on the corresponding command in the setup menu or by double-clicking the indication provided in the status bar. When the option is active the words **Cornerth. red.** in the status bar are drawn in black and a check mark appears in the **Corner thickness reduction** menu command.

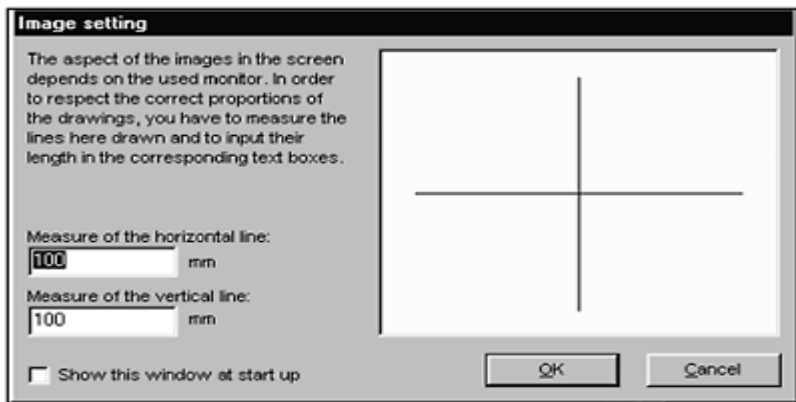


Figure 7.6 **Image setting** dialog box.

The View options (**View cross-section**, **View member**, **View material**) refer to three boxes in the data window; when an option is active the corresponding box is filled with graphic or textual information, which recalls the data in use. Furthermore, a double click on a box in the data window is a handy shortcut to open the corresponding dialog box and to modify the data.

Finally, the **Video settings** command (Figure 7.6) allows us to properly scale the horizontal and vertical size of the images shown in the screen, so as to faithfully present the correct proportion of the drawings. The dialog box shows two lines, the length of which should be measured and put in the text boxes.

7.2.3 Material and code

The **Material and code** dialog box (Figures 7.7 and 7.8) can be opened either by using the **Material and code** command in the setup menu or by double-clicking the material box in the data window or the code indication in the status bar. The window allows, first, the choice of code to be used (and, for AISI Specification, the allowable stress design and load and resistance factor design). It is then possible to reconcile the type of steel and its grade, or the aluminium alloy and its temper. When Eurocode 3 is used, it is also possible to characterize the type of forming (i.e. cold rolling, heat treated).

The computer program also allows generation of user-defined materials. In order to do this, it is necessary to select **User defined material** within the material types, thus showing the list of already-created user materials together with the word **New...** When this word is double-clicked, the grade (or temper) text box appears, where it is possible to assign values in the strength text boxes. A click in the window, outside the interactive area,



Figure 7.7 **Material and code** dialog box.



Figure 7.8 Creating a user-defined material.

Table 7.1 Characteristics of materials defined inside the program

	<i>Steel</i>	<i>Aluminium</i>
Modulus of elasticity	$E=210,000$ MPa	$E=70,000$ MPa
Poisson's ratio	$\nu=0.3$	$\nu=0.3$
Unit mass	$\rho=7850$ kg/m ³	$\rho=2700$ kg/m ³

closes the definition phase. By double-clicking a user-defined material it is possible to modify its data. By clicking it once and then pressing the **Del** key it is possible to delete it. The program retains three different sets of user-defined materials, one for each code. Remember that the material data (including user-defined materials) should be saved using the **Save settings** command in the file menu.

Finally, note that some characteristics of materials, shown in Table 7.1, are defined inside the program and cannot be modified by the user.

7.2.4 Cross-section menu

The commands of the **Cross-section** menu (Figure 7.9) allow us to choose the type of cross-section to be used and the definition of its geometrical



Figure 7.9 The **Cross-section** menu; a check mark indicates the type in use.

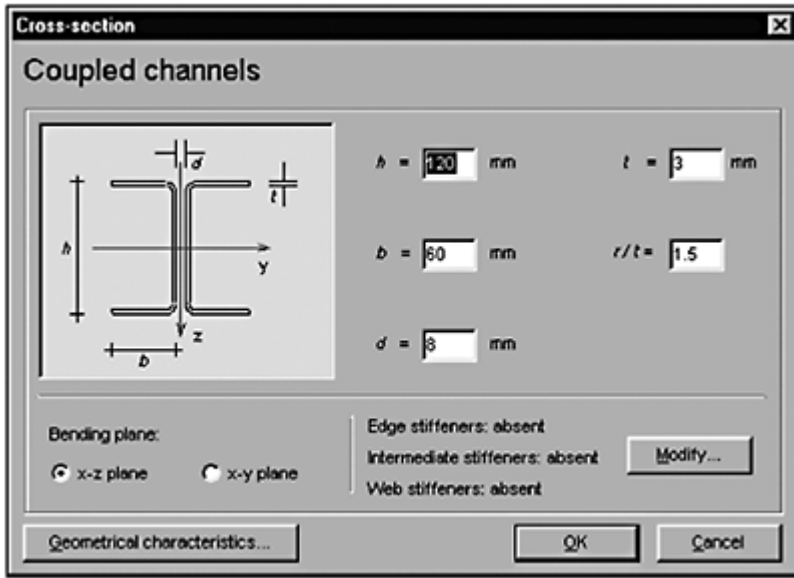


Figure 7.10 **Cross-section** dialog box.

characteristics. ColdForm 2001 has a large number of predefined cross-section shapes, divided in four categories: open sections (channel, angle, zed and omega), coupled open sections (i.e. sections made with two joined open sections—back-to-back channels and angles), hollow sections (circular and box) and trapezoidal sheeting. It, furthermore, allows description of a generic hollow or open cross-section made of plane elements connected in nodes, by assigning their coordinates. Every type of cross-section, apart from the circular one, can be provided with stiffeners.

The **Cross-section** dialog box (Figure 7.10), opened by commands in the **Cross-section** menu, contains an image of the cross-section describing its shape and the data necessary to define its geometry, text boxes for data input, an option button to select the bending plane and a button to modify the stiffeners (the latter are discussed in detail in Section 7.2.5).

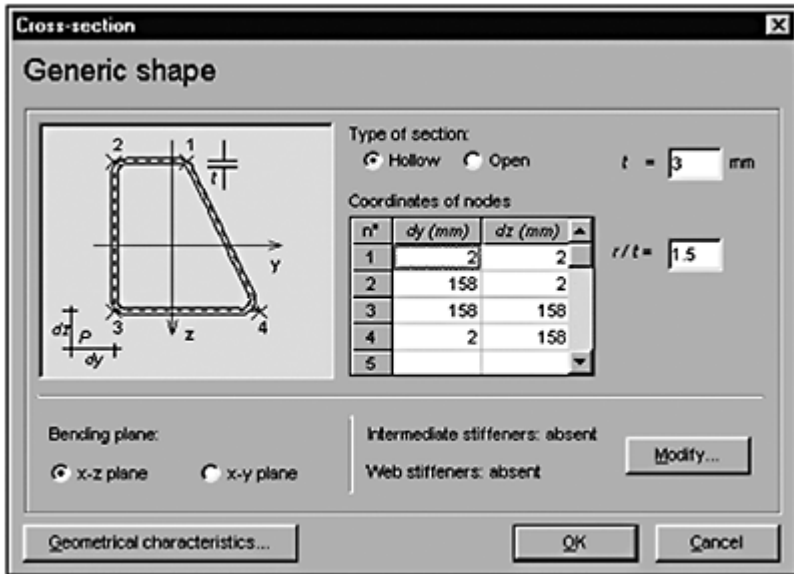


Figure 7.11 Dialog box for a **Generic shape** cross-section.

For the **Generic shape** cross-section (Figure 7.11) a grid with scroll bar is used instead of text boxes for inputting node coordinates. Note that in this case a node is defined as the intersection of the midlines of two adjacent plane elements, ignoring rounded corners (which are afterwards automatically added by the computer program with the given radius of curvature r).

The node coordinates are referred to as a set of y - z axes, oriented as shown in Figure 7.11, the origin of which can be placed anywhere in the plane of the cross-section.

ColdForm 2001 checks the correspondence of the geometrical characteristics of the cross-section to the provisions of the code (thickness, b/t ratio and so on). When necessary, it warns us by showing the code limits and points out which code provision is not being respected (Figure 7.12). However, we are allowed to confirm values that do not conform with the code and to use them for structural checks, while meaningless or inconsistent values (like a negative or null length) are not permitted at all.

The dialog box for the type of cross-section in use can also be opened by double-clicking the **Cross-section** box of the data window. This is probably the quickest way to modify the geometrical data of the cross-section in use. However, it is necessary to use the **Cross-section** menu commands to change the type of cross-section.

The last command in the **Cross-section** menu, **Geometrical characteristics**, is used to evaluate the location of the centroid together with the area, unit weight, moments of inertia and section moduli of the cross-section (Figure 7.13). The **Geometrical characteristics** button in the **Cross-section** dialog box serves the same purpose. The results shown in the

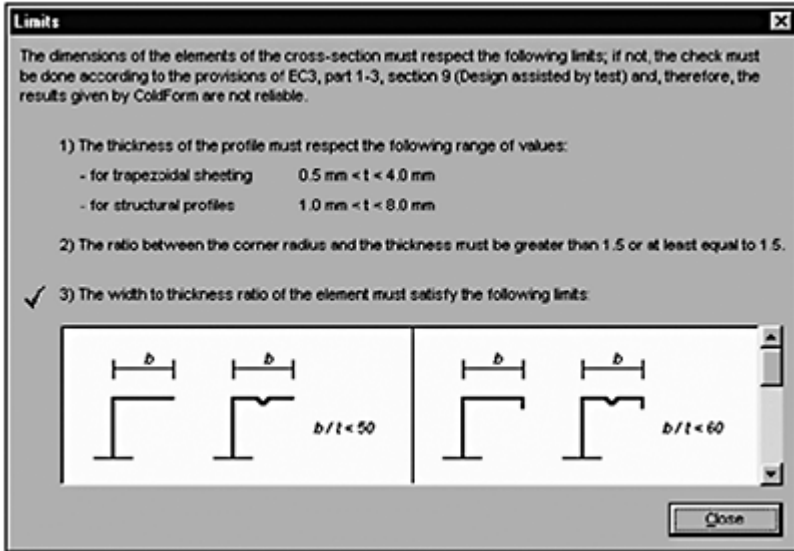


Figure 7.12 Code provisions (the check mark points out non-respected limits).

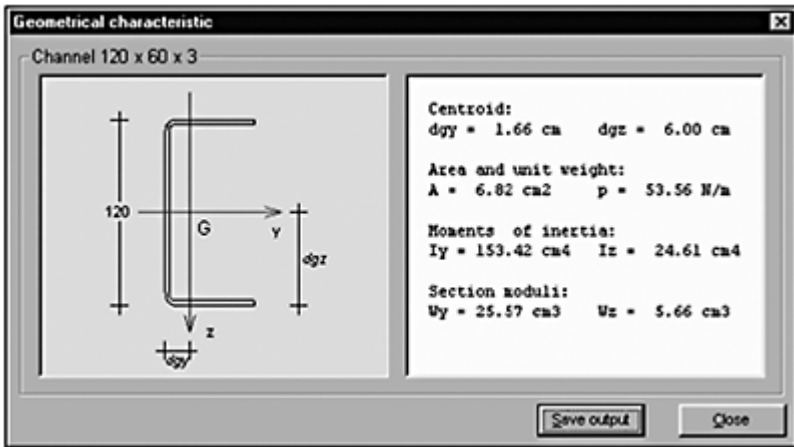


Figure 7.13 Geometrical characteristics output box.

Geometrical characteristics output box are sent to the output window by clicking the **Save output** button.

7.2.5 Stiffeners

The cross-section is often provided with stiffeners for reducing the effect of local buckling. Information in the **Cross-section** dialog box indicates the presence of stiffeners; the nearby **Modify** button opens the **Stiffeners** dialog box, which manages their type, number and location. In order to identify a

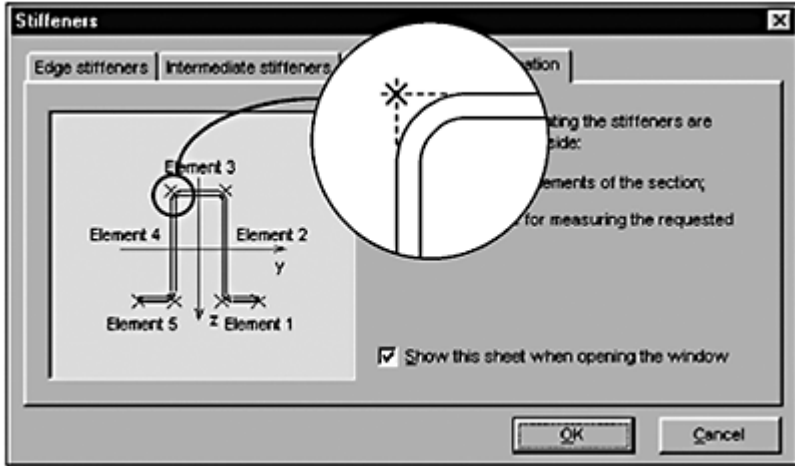


Figure 7.14 Information tab in **Stiffeners** dialog box.

stiffener, we need to define its type, the plane element it belongs to and its distance from a reference point (individuated as the intersection of the external sides—or the midlines in the case of generic-shape cross-sections—of two adjacent plane elements). Information about the number of elements in the section and their reference points are shown in the **Information tab** of the **Stiffeners** dialog box (Figure 7.14). It is possible to insert an edge stiffener at the free edge of the first and the last element of an open cross-section and one or two intermediate or web stiffeners in any element of the section. Intermediate and web stiffeners differ in shape, being intended to prevent buckling by compression (or bending moment) and shear force, respectively. The computer program does not allow intermediate and web stiffeners placed together in the same element.

Another tab in the **Stiffeners** dialog box manages each type of stiffener (edge, intermediate and web). A check box in the tab allows us to choose which kind of stiffeners are to be taken into account, separately for each type. This may be used to compare the strength of stiffened versus non-stiffened cross-sections. However, the main reason for introducing this check box was the need to avoid problems when modifying cross-section data. For example, changing the length of one element of the cross-section might make the location of previously defined stiffeners inconsistent. In such a case, the stiffeners are deactivated, but their data are not eliminated and we can easily modify them, before activating stiffeners once again.

Edge stiffeners consist either in a single edge fold or in a double edge fold, described by means of lengths d_1 and d_2 and angle α (Figures 7.15 and 7.16). When d_2 is not provided, or it is zero, the computer assumes the stiffener has a single edge fold. The check box **Equal stiffeners at both edges** is used to force the data of the two edge stiffeners to be equal.

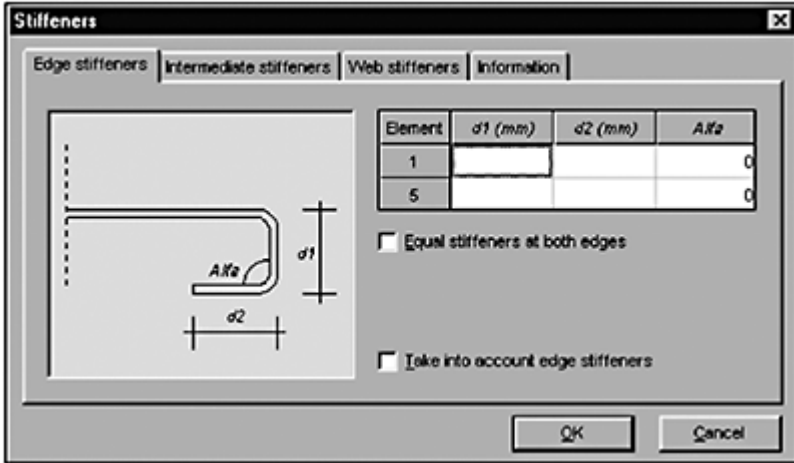


Figure 7.15 Edge stiffeners tab in Stiffeners dialog box.

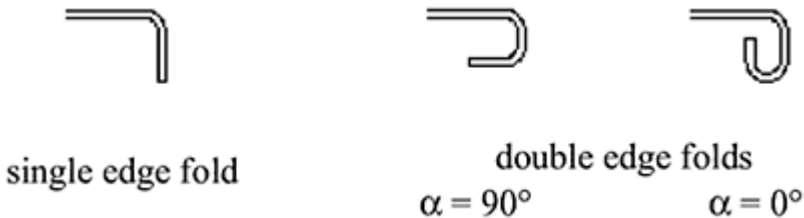


Figure 7.16 Edge stiffeners.

Intermediate stiffeners consist in a 180° fold having external diameter d connected to the element by means of rounded corners with the same internal radius r used to connect adjacent plane elements (Figure 7.17). Each element can contain up to two intermediate stiffeners, the locations of which are indicated by distances b_1 and b_2 from the fold centres to the reference points at the opposite edges of the element. The check box **Equal edge distance** is used to force distances b_1 and b_2 to be equal (or, if no value is allocated to b_1 and b_2 , to locate only one stiffener in the middle of the element).

Web stiffeners consist in a plane element having slope a with respect to the stiffened element and length s , connected to the element by means of rounded corners with the same internal radius r used in connecting adjacent plane elements (Figure 7.18). Each

element may contain up to two intermediate stiffeners, the locations of which are indicated by distances b_1 and b_2 from the edges of the rounded corners to the reference points at the opposite edges of the element. The default values of the angles α_1 and α_2 are $+45^\circ$ and -45° , respectively; we can modify them by clicking the button **Angles alfa** in the **Web stiffeners** tab. The check box **Equal edge distance**

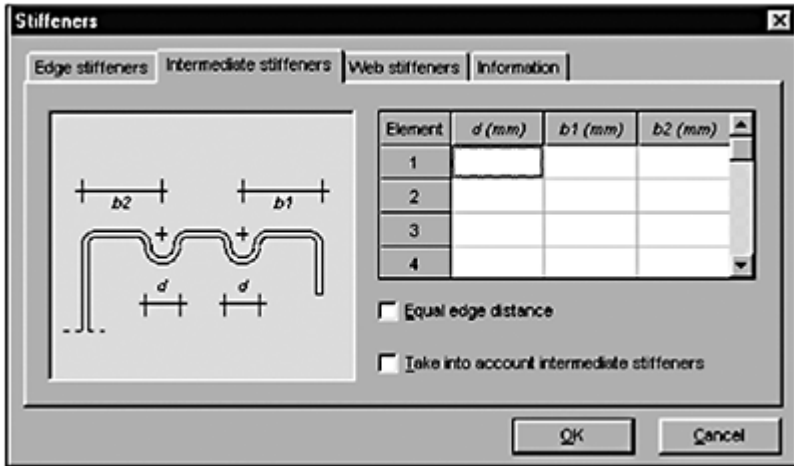


Figure 7.17 Intermediate stiffeners tab in Stiffeners dialog box.

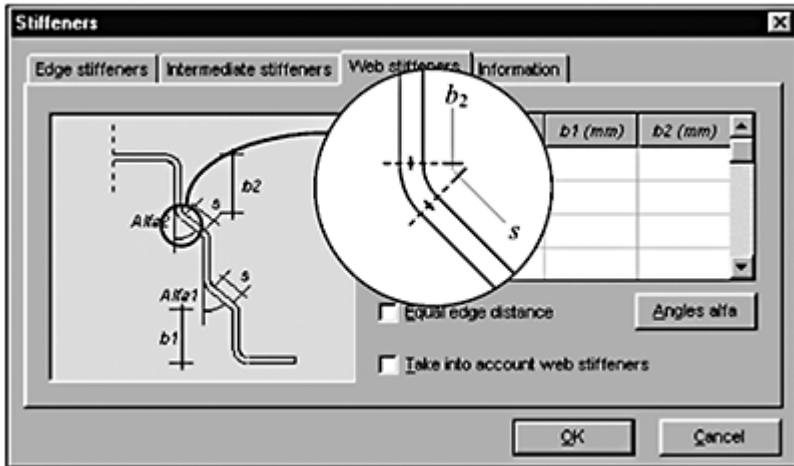


Figure 7.18 Web stiffeners tab in Stiffeners dialog box.

is used to force distances b_1 and b_2 to be equal (or, if no value is allocated to b_1 and b_2 , to locate only one stiffener in the middle of the element).

7.2.6 Member menu

ColdForm 2001 allows us to check a single cross-section excluding global buckling), a cross-section belonging to a given member (thus including global buckling) or a set of cross-sections belonging to the

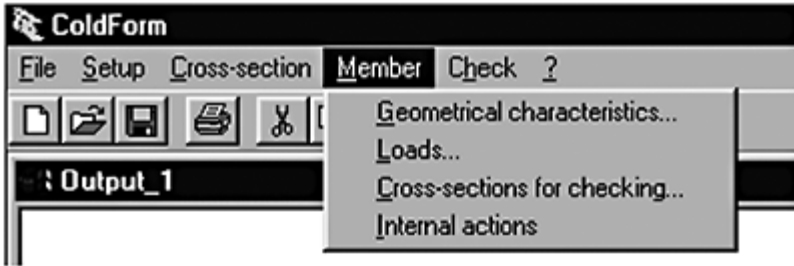


Figure 7.19 The **Member** menu.

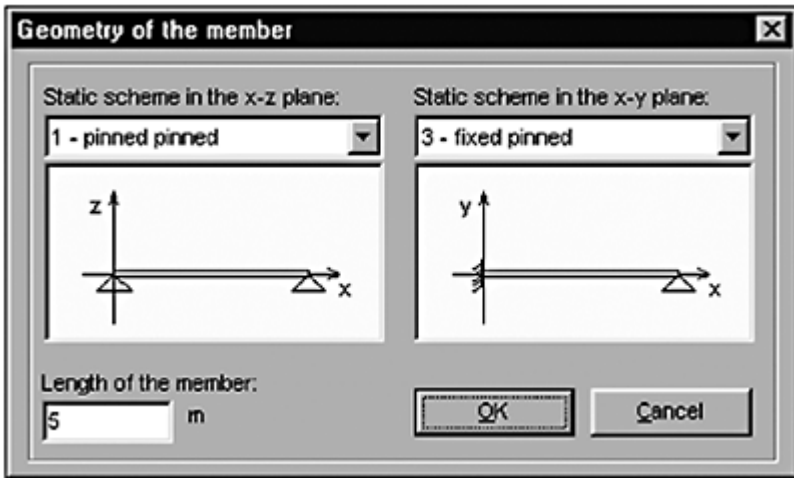


Figure 7.20 **Geometrical characteristics** dialog box.

member. In the second case, it is necessary to describe to geometry and restraints of the member, while in the third case it is also necessary to define member loads and the cross-sections in which checks have to be carried out (Figure 7.19).

The **Geometrical characteristics** command of the **Member** menu opens the corresponding dialog box, and is used to define the length of the member and its static

scheme in the $x-z$ and $x-y$ planes (Figure 7.20). Accurate definition of the restraints is of capital importance for correct evaluation of the buckling strength of the member. A shortcut to help us modify these data is available by double-clicking the **load plane box** of the data window, which shows the restraints in the load plane.

The **Loads** dialog box contains four tabs, which define load plane, concentrated loads, distributed loads (either equally distributed along the whole member or linearly variable and applied to a portion of the member) and end actions. The sign convention for loads is shown in the tabs (Figure 7.21).

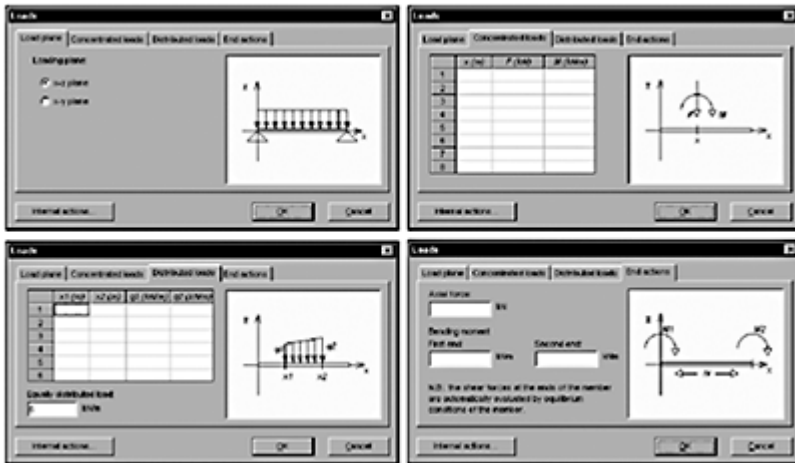


Figure 7.21 The tabs of the **Loads** dialog box.

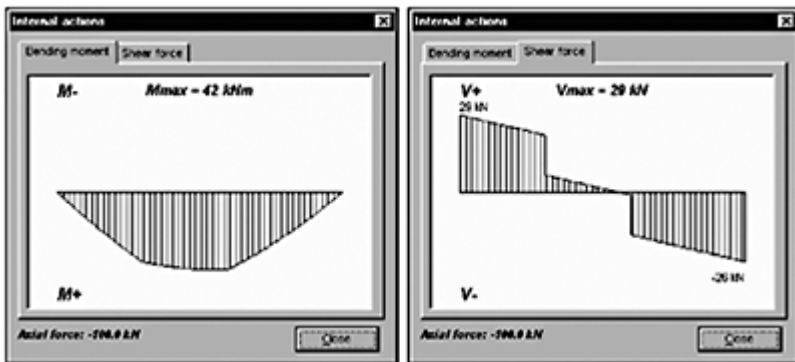


Figure 7.22 The tabs in the **Internal actions** window.

The bending moment and shear force diagrams, corresponding to the assigned loads, are shown in the **Internal actions** window (Figure 7.22), which can be opened either by the

corresponding command in the **Member** menu or by the **Internal actions** button in the **Load** dialog box.

Finally, the number and location of the cross-sections that have to be checked by the program are defined by the **Cross-sections for checking** dialog box (Figure 7.23). Using the **Insert cross-sections with a constant step** check box, we can define the location of the cross-sections automatically, but we can also choose to assign their coordinates manually one by one. A maximum number of thirty cross-sections for checking are allowed by the program.

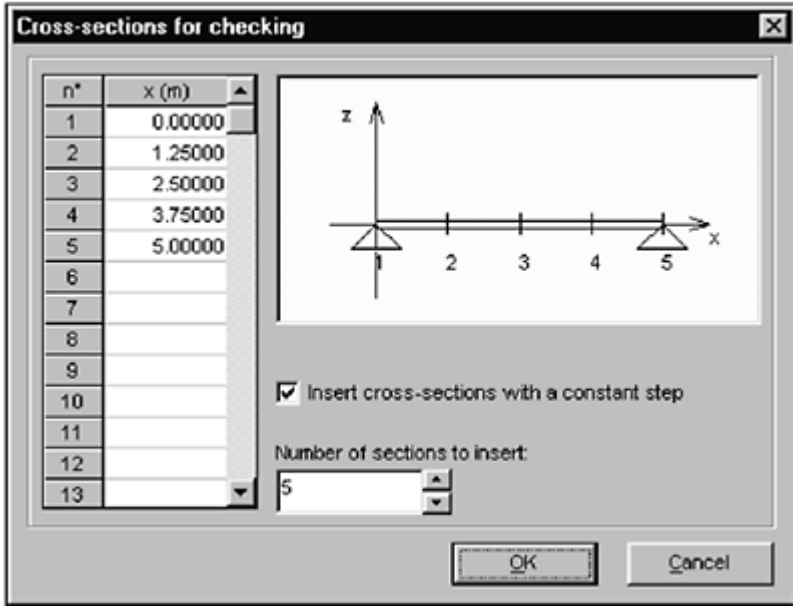


Figure 7.23 **Cross-sections for checking** dialog box.



Figure 7.24 The Check menu and its submenus.

7.2.7 Check menu

Regarding single cross-sections, ColdForm 2001 distinguishes between strength checks and buckling strength checks (Figure 7.24). The former relate exclusively to the cross-section and only take local buckling into account. The latter require definition of the geometry and end restraints of the member and can thus also account for global buckling (only flexural buckling is considered in the present version of the program; torsional and flexural-torsional buckling should be manually checked).

The program also allows a whole member to be checked. In this case, it is necessary to fully describe the geometry and loads and to define the set of cross-sections in which checks have to be performed.

Cross-section—single internal action

When the cross-section is checked against a single internal action (axial tension, axial compression, bending moment, shear force, compression including flexural buckling) the program gives the value of the design resistance (tension, compression, bending, shear and flexural buckling resistance, respectively; in the case of bending moment, both the positive and negative moment resistance are provided). We can thus perform the check simply by comparing the design value of an internal action with the corresponding design resistance provided by the program.

As an example, let us consider a $180 \times 100 \times 40 \times 2$ omega cross-section (Figure 7.25) made with S 235 hot-rolled steel sheet ($f_y = 235$ MPa, $f_u = 360$ MPa) and let us use

Eurocode 3. The program gives a compression resistance $N_{c,Rd}=144.4$ kN (Figure 7.26). Note that the program warns that, in this case, the centroid of the effective cross-section does not coincide

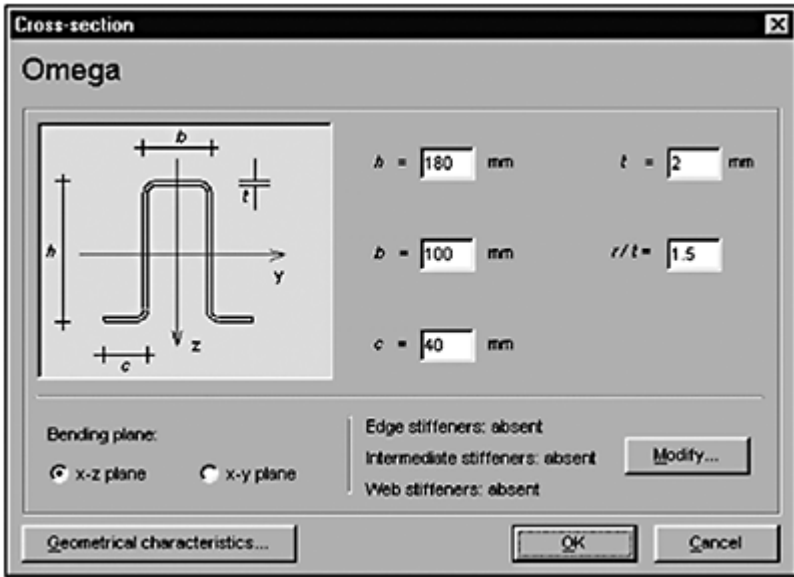


Figure 7.25 Geometrical data of the example cross-section.

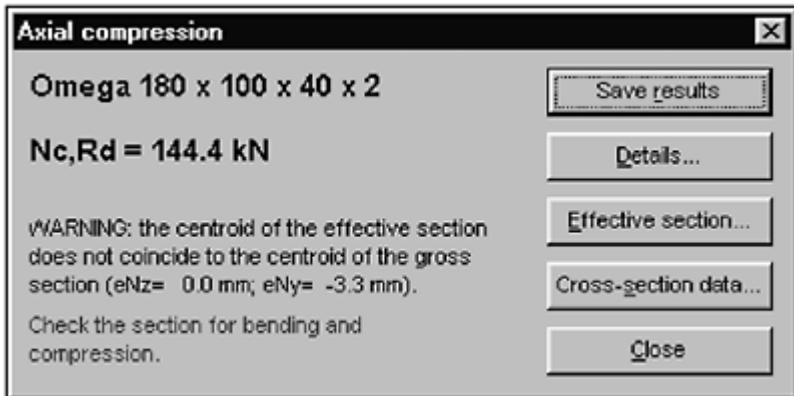


Figure 7.26 The evaluated resistance window.


```

                                rho = 0.7716
                                beff = 29.19 mm
Element 2 doubly supported element
  geometrical data: bP = 175.66 mm t = 2.00 mm bP/t =
87.83
                                end 1 - fr=2.83 mm
                                end 2 - fr=2.83 mm
  axial stresses: end 1 - sigma=213.64 MPa
                                end 2 - sigma=213.64 MPa
  coefficients: k sigma = 4.0000
                                lambdaP = 1.5454 lambdaP red =
1.5454
                                rho = 0.5550
                                beff = 97.48 mm be1 = 48.74 mm
be2=48.74 mm
Element 3 doubly supported element
  geometrical data: bP = 95.66 mm t = 2.00 mm bP/t =
47.83
                                end 1 - fr = 2.83 mm
                                end 2 - fr = 2.83 mm
  end 1 - sigma = 213.64 MPa
                                end 2 - sigma = 213.64 MPa
  k sigma = 4.00 00
                                lambdaP = 0.8416 lambdaP red =
0.8416
                                rho = 0.8776
                                beff = 83.95 mm be1 = 41.98 mm be2
= 41.98 mm
Element 4 doubly supported element
  geometrical data: bP = 175.66 mm t = 2.00 mm bP/t =
87.83
                                end 1 - fr = 2.83 mm
                                end 2 - fr = 2.83 mm
  axial stresses: end 1 - sigma = 213.64 MPa
                                end 2 - sigma = 213.64 MPa
  coefficients: k sigma = 4.0000
                                lambdaP = 1.5454 lambdaP red =
1.5454
                                rho = 0.5550
                                beff = 97.48 mm be1 = 48.74 mm be2
= 48.74 mm
Element 5 outstand element, supported at end 1
  geometrical data: bP = 37.83 mm t = 2.00 mm bP/t =
18.91
                                end 1 - fr = 2.83 mm
  axial stresses: end 1 - sigma = 213.64 MPa
                                end 2 - sigma = 213.64 MPa
  coefficients: k sigma = 0.4300
                                lambdaP = 1.0151 lambdaP red =
1.0151
                                rho = 0.7716
                                beff = 29.19 mm

```

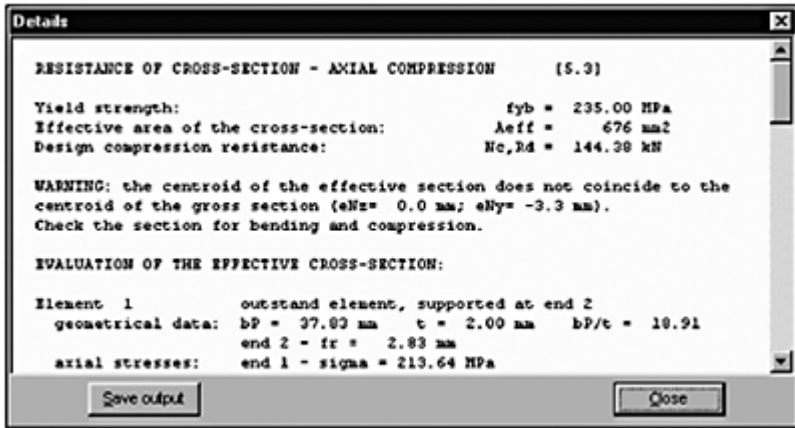


Figure 7.28 Details window.

As a further example, let us imagine that the same omega cross-section is made from a wrought aluminium alloy S 235 (ENAW-5083, H24/H34 temper, having $f_{0.2}=250$ MPa, $f_u=340$ MPa) and let us use Eurocode 9. In this case, the program gives a compression resistance $N_c, R_d=100.7$ kN. The results provided by the **Details** window, shown in the next listing, indicate that the difference is mainly due to the value of the plate slenderness

$\bar{\lambda}_p$, which is larger in the aluminium element because of the smaller value of the elastic modulus E .

```
Omega 180 x 100 x 40 x 2
RESISTANCE OF CROSS-SECTION - AXIAL COMPRESSION [5.3]
Limiting strength: f0 = 250.00 MPa
Effective area of the cross-section: Aeff = 443 mm2
Design compression resistance: Nc, Rd = 100.73 kN
WARNING: the centroid of the effective section does not
coincide to the centroid of the gross section (eNz =
0.0 mm; eNy = -3.5 mm).
Check the section for bending and compression.
EVALUATION OF THE EFFECTIVE CROSS-SECTION:
Element 1 outstand element, supported at end 2
  geometrical data: bp = 37.83 mm t = 2.00 mm bp/t =
18.91
                    end 2 - fr = 2.83 mm
  axial stresses: end 1 - sigma = 227.27 MPa
end 2 - sigma = 227.27 MPa
  coefficients: k sigma = 0.4300
                lambdaP = 1.7581 lambdaP red = 1.8134
                rho = 0.4846
                teff = 0.97 mm
Element 2 doubly supported element
  geometrical data: bp = 175.66 mm t = 2.00 mm bp/t =
87.83
```



```

                end 1 - fr = 2.83 mm
                end 2 - fr = 2.83 mm
    axial stresses: end 1 - sigma = 227.27 MPa
                   end 2 - sigma = 227.27 MPa
    coefficients: k sigma = 4.0000
                  lambdaP = 2.6767 lambdaP red =
2.7608
                rho = 0.3333
                teff = 0.67 mm
Element 3 doubly supported element
    geometrical data: bP = 95.66 mm t = 2.00 mm bP/t =
47.83
                end 1 - fr = 2.83 mm
                end 2 - fr = 2.83 mm
    axial stresses: end 1 - sigma = 227.27 MPa
                   end 2 - sigma = 227.27 MPa
    coefficients: k sigma = 4.0000
                  lambdaP = 1.4577 lambdaP red =
1.5035
                rho = 0.5678
                teff = 1.14 mm
Element 4 doubly supported element
    geometrical data: bP = 175.66 mm t = 2.00 mm bP/t =
87.83
                end 1 - fr = 2.83 mm
                end 2 - fr = 2.83 mm
    axial stresses: end 1 - sigma = 227.27 MPa
                   end 2 - sigma = 227.27 MPa
    coefficients: k sigma=4.0000
                  lambdaP = 2.6767 lambdaP red =
2.7608
                rho = 0.3333
                teff = 0.67 mm
Element 5 outstand element, supported at end 1
    geometrical data: bP = 37.83 mm t = 2.00 mm bP/t =
18.91
                end 1 - fr = 2.83 mm
                end 1 - sigma = 227.27 MPa
                end 2 - sigma = 227.27 MPa
    coefficients: k sigma=0.4300
                  lambdaP = 1.7581 lambdaP red =
1.8134
                rho = 0.4846
                teff = 0.97 mm

```

Cross-section—combined internal actions

When the cross-section is checked against the contemporary presence of two internal actions (combined tension and bending, combined compression and bending, combined shear and bending, bending and compression including flexural buckling) the program gives the value of the design resistance for both internal actions, separately evaluated,

and asks us for the design values of the actions, in order to carry out the combined check. As an example, let us once again consider the 180×100×40×2 omega cross-section made with S 235 hot-rolled steel sheet. The program

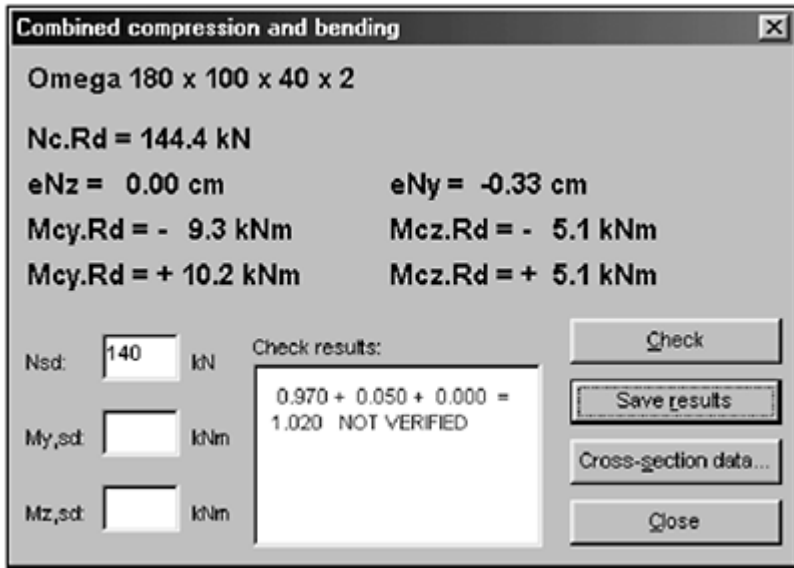


Figure 7.29 The check for **Combined compression and bending** window.

(Figure 7.29) gives the compression resistance ($N_{c,Rd}=144.4$ kN) and the bending resistances about the y - y axis ($M_{cy,Rd}=-9.3$ kNm; $+10.2$ kNm) and the z - z axis ($M_{cz,Rd}=\pm 5.1$ kNm). When the design actions are given ($N_{sd}=140$ kN; $M_{y,sd}=M_{z,sd}=0$), the **Check** button starts evaluation of the ratios of design actions over resistances, the sum of which should be less than or equal to unity (equation 3.25). The results are reported in the **Check results** box and can be sent to the output window by means of the **Save results** button along with some more details (see next listing). Note that the program automatically includes the additional bending moment due to the non-coincidence of the centroid of effective and gross cross-sections (in the example, $e_{Ny}=-0.33$ cm, $\Delta M_y=140\times 0.0033=-0.46$ kNm).

```
Omega 180 x 100 x 40 x 2
COMBINED COMPRESSION AND BENDING
Nsd 140.0 kN Nc, Rd = 144.4 kN NSd/Nc. Rd = 0.970
MySd = 0.0-0.5 kNm Mcy.Rd = -9.3 kNm MySd/Mcy. Rd =
0.050
MzSd = 0.0 kNm Mcz.Rd = -5.1 kNm MzSd/Mcz. Rd = 0.000
0.970 + 0.050 + 0.000 = 1.020 NOT VERIFIED
```

The computer program follows the same approach, whichever code is used. In all instances, the symbols which define design actions and resistances conform to the code, as is shown (see listing) in the results obtained for the same check when the Load and Resistance Factor Design method of AISI Specification is used.

```
Omega 180 x 100 x 40 x 2
COMBINED COMPRESSION AND BENDING
P = 140.0 kN Pmax = 142.3 kN P/Pmax=0.984
My = 0.0-0.4 kNm Mmax y = -9.5 kNm My/Mmax y = 0.042
Mz = 0.0 kNm Mmax z = -4 . 9 kNm Mz/Mmax z = 0.000
0.984 + 0.042 + 0.000 = 1.026 NOT VERIFIED
```

Member checks

When we require a strength (or buckling strength) member check, the computer program repeats the abovedescribed checks for the given set of cross-sections, providing the design actions and resistances and their ratio for each section.

In the case of deflection checks, the program evaluates the displacement of the member in each section. In order to do this, it determines the effective cross-section along the member, depending on internal action diagrams, and analyses the member as subdivided into a set of short elements having constant cross-section (different from each other).

Remember that according to all codes, apart from the Allowable Stress Design method of the AISI Specification, different loads must be considered for ultimate limit-state checks and service-state checks. As the user, it is our responsibility to provide ColdForm 2001 with the proper value of loads for strength checks and deflection checks.

As an example, let us consider a 100×50×50×20×3 trapezoidal sheeting (Figure 7.30) made with S 235 hot-rolled steel sheet ($f_y=235$ MPa, $f_u=360$ MPa) and let us use the ASD method of the AISI Specification. The member has a 3m span and is fixed pinned (Figure 7.31). The **bending**

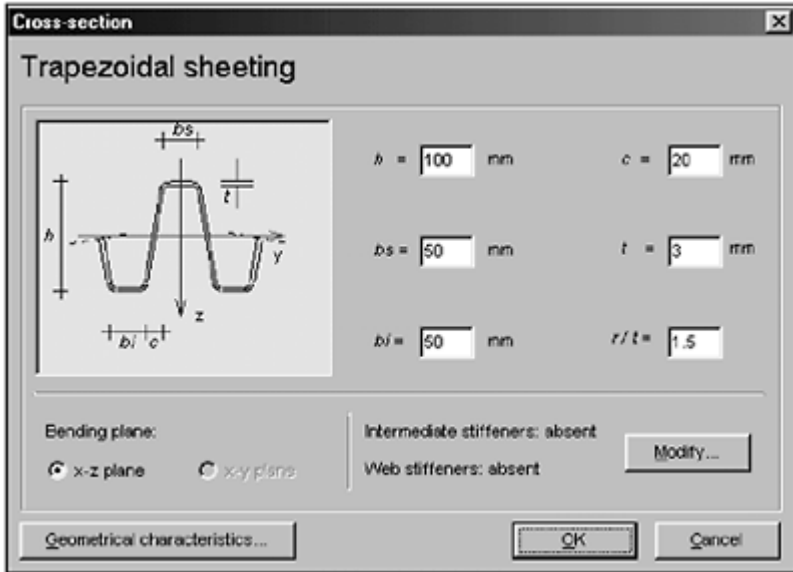


Figure 7.30 Geometrical data of the Trapezoidal sheeting.

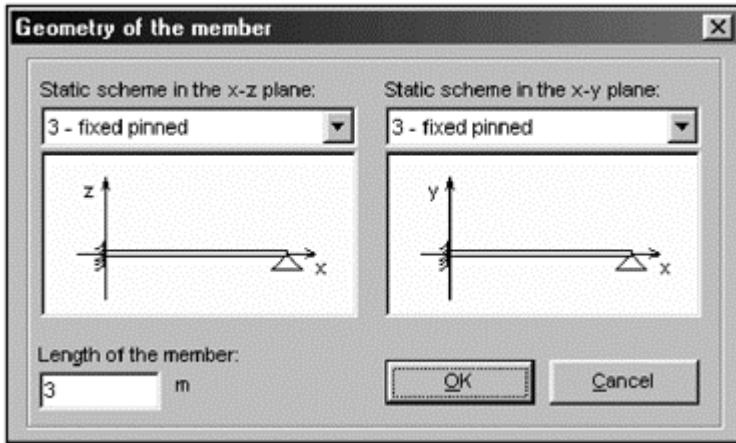


Figure 7.31 Geometry of the member.

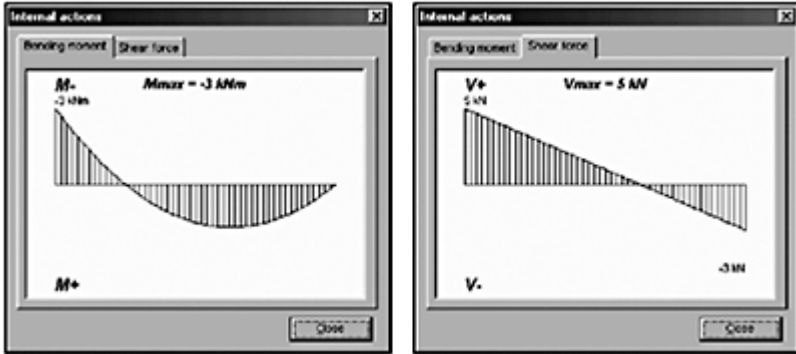


Figure 7.32 **Bending moment and Shear force** diagrams along the member.

moment and shear force diagrams caused by the uniformly distributed load acting on it (2.5 kN/m) are shown in Figure 7.32. The check has to be carried out in five uniformly spaced cross-sections, including both ends of the member, plus the cross-section where the positive bending moment is maximum, located at $x=1.875$ m. The results provided by the program are shown in this listing:

```

Trapezoidal sheeting 100 x 50 x 50 x 20 x 3
x = 0.00 N = 0.00 kN M = -2.81 kNm V = 4.69 kN
Combined shear and bending
V = 4.7 kN Vmax = 45.2 kN (V/Vmax)^2 = 0.011
M = -2.8 kNm Mmax = -3.4 kNm (M/Mmax)^2 = 0.686
0.011 + 0.686 = 0.697 OK
x = 0.75 N = 0.00 kN M = 0.00 kNm V = 2.81 kN
Shear force
V = 2.8 kN Vmax = 45.2 kN
Check result: OK
x = 1.50 N = 0.00 kN M = 1.41 kNm V = 0.94 kN
Combined shear and bending
V = 0.9 kN Vmax = 45.2 kN (V/Vmax)^2 = 0.000
M = 1.4 kNm Mmax = 3.4 kNm (M/Mmax)^2 = 0.172
0.000 + 0.172 = 0.172 OK
x = 1.88 N = 0.00 kN M = 1.58 kNm V = 0.00 kN
Bending moment
M = 1.6 kNm Mmax = -3.4 kNm Mmax = + 3.4 kNm
Check result: OK
x = 2.25 N=0.00 kN M=1.41 kNm V = - 0.94 kN
Combined shear and bending
V = 0.9 kN Vmax = 45.2 kN (V/Vmax)^2 = 0.000
M=1.4 kNm Mmax=3.4 kNm (M/Mmax)^2=0.172
0.000+0.172=0.172 OK
x = 3.00 N = 0.00 kN M = 0.00 kNm V = -2.81 kN
Shear force
    
```

$V = 2.8 \text{ kN}$ $V_{\max} = 45.2 \text{ kN}$
 Check result: OK



Figure 7.33 The information menu.

7.2.8 Information menu

By means of commands from the information menu ? (Figure 7.33) it is possible to have information about the trading licence (i.e. the conditions under which it is possible to use the program) and the version of the program. In most Windows programs this menu also contains a Help command but the present version of the ColdForm 2001 does not include any help on line.

7.3 TOOLBAR

The toolbar (Figure 7.34) is a shortcut for executing commands, which are otherwise selected from pull-down menus. Seven buttons relate to management of the Output window; their use is well understood, being standard in



Figure 7.34 The toolbar.

all Windows programs. The remaining three buttons are used for opening and closing boxes in the Data window:



The button **New output** closes the Output window (after asking us to confirm whether, it contains unsaved data) and opens a new window with a default name (**Output_1**, **Output_2** and so on).



The button **Open output** allows the user to search for a file to open, by means of the standard Open dialog box.



The button **Save output** saves the data in the Output window as a text file, having the name displayed in the title bar of the window (with the default extension .CLF, if no other extension has been expressly defined).



The button **Print output** sends the text in the Output window to the system printer.



The button **Cut** deletes the selected text in the Output window and puts it in the computer memory.



The button **Copy** copies the selected text from the Output window into the computer memory.



The button **Paste** copies the memorized text from the computer memory into the Output window, in the current cursor position.



The button **View cross-section** opens or closes the Cross-section box in the Data window.



The button **View member** opens or closes the Member box in the Data window.



The button **View material** opens or closes the Material box in the Data window.

7.4 DATA WINDOW

The Data window (Figure 7.35) is a non-resizeable window always placed to the right of the ColdForm window. It contains three boxes, which can individually be opened or closed by means of buttons in the toolbar or commands in the Setup menu.

The Cross-section box shows a scale drawing of the cross-section, which includes all the stiffeners (if the image is not correctly scaled, use the **Video settings** command in the Setup menu to adjust it). The axis that indicates the load plane is drawn in red. When this box is double-clicked the program opens the Cross-section dialog box, thus allowing fast resizing of the cross-

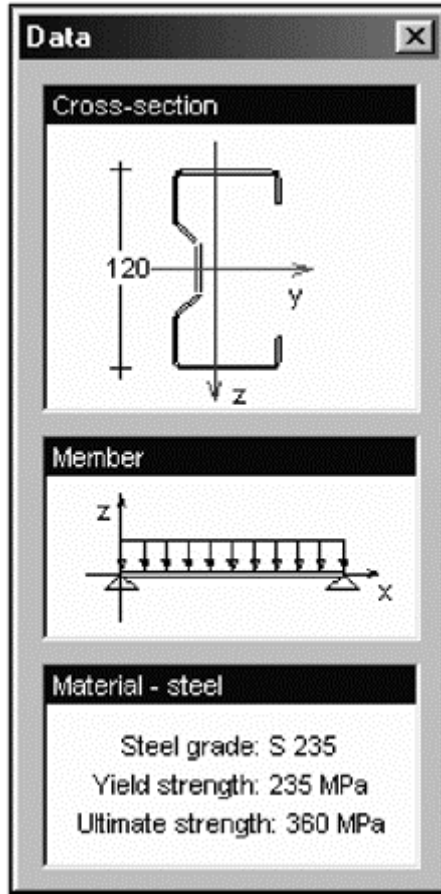


Figure 7.35 The Data window.

section and redefinition of the load plane. In order to select a different cross-section shape, we should instead use commands from the Cross-section menu.

The Member box shows a scheme of the member, pointing out the restraints in the load plane. When this box is double-clicked the program opens the Geometrical characteristics dialog box, thus allowing modification of restraints and member length. In order to assign new loads or cross-sections for checking, we should instead use commands from the Member menu.

The Material box indicates the type of material in use (steel or aluminium alloy) and its mechanical characteristics. Double-clicking it, the program opens the Material and code dialog box.

7.5 OUTPUT WINDOW

The Output window (Figure 7.36) is usually filled with the results of all the checks carried out, along with notes by the user. The **Save results** or **Save output** commands in the check windows put the results of the check at the end of the text displayed in the Output window. This window is, as a matter of fact, a text window that can be used in exactly the same way as a Notepad window. We can write and also edit in it, cut or move text with the

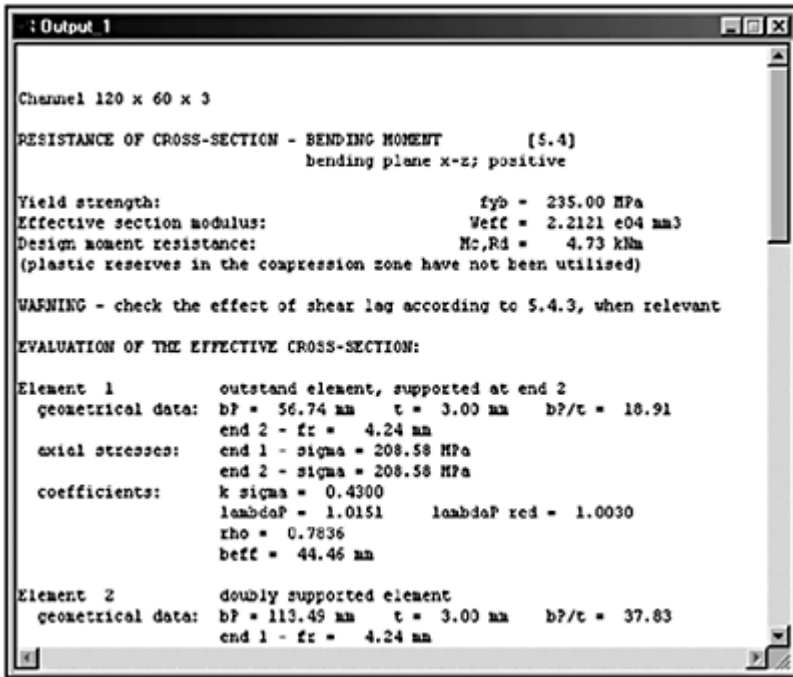


Figure 7.36 The **Output** window.



Figure 7.37 The **Message** area.

same commands (**Cut**, **Copy**, **Paste**) and shortcuts (**Ctrl-X**, **Ctrl-C**, **Ctrl-V**), used in the Notepad program.

7.6 MESSAGE AREA

The message area (Figure 7.37), situated at the bottom of the ColdForm window, is divided into five parts. The first contains information about the command in use. The second shows whether the Corner thickness reduction option is active or not; double-clicking it changes the status of the option (i.e. activates or deactivates it). The third part indicates the code being presently used; double-clicking it opens the Material and code dialog box. The last two parts contain the date and time.

References

- AISI (1996) *Cold-formed Steel Design Manual*, American Iron and Steel Institute.
- Baldacci, F. (1984) 'Metasistema per l'edilizia industrializzata residenziale in acciaio', *Costruzioni Metalliche*, 6.
- Ballio, G. and Mazzolani, F.M. (1983) *Theory and Design of Steel Structures*, London: Chapman & Hall.
- Bijlaard, P.P. (1949) 'Theory and tests on the plastic stability of plates and shells', *Journal of the Aeronautical Sciences*.
- Bleich, F. (1952) *Buckling Strength of Metal Structures*, New York: McGraw-hill Book Co., Inc.
- BS 8118 (1991) *The Structural Use of Aluminium*, London: British Standards Institute.
- Calderoni, B., De Martino, A. and Landolfo, R. (1999) 'Il comportamento sismico di telai in profili sottili: Limiti di servizio e definizione del fattore di struttura', *Costruzioni Metalliche*, 2.
- Calderoni, B., De Martino, A., Ghersi, A. and Landolfo, R. (1995) 'On the seismic resistance of light gauge steel frames', in *Behaviour of Steel Structures in Seismic Areas* (eds Mazzolani, F.M. and Gioncu, V.), London: E. & F.N. Spon (Proc. of STESSA '97, Kyoto).
- Calderoni, B., De Martino, A., Ghersi, A. and Landolfo, R. (1997) 'Influence of local buckling on the global seismic performance of light gauge portal frames', in *Behaviour of Steel Structures in Seismic Areas* (eds Mazzolani, F.M. and Akiyama, H.), Salerno: Edizioni 10/17 (Proc. of STESSA '97, Kyoto).
- CEN, EN 1993-1-1 (1992) *Eurocode 3: Design of steel structures—Part 1-1: General rules and rules for buildings*.
- CEN, ENV 1993-1-3 (1996) *Eurocode 3: Design of steel structures—Part 1-3: General rules—Supplementary rules for cold formed thin gauge members and sheeting*.
- CEN, ENV 1999-1-1 (1998) *Eurocode 9: Design of aluminium structures—Part 1-1: General rules*.
- CEN, prENV 1999-1-3 (1999) *Eurocode 9: Design of aluminium structures—Part 1-3: General rules—Supplementary rules for thin-walled aluminium sheeting* (internal document).
- CNR, 10022 (1984) *Profilati di acciaio formati a freddo. Istruzioni per l'impiego nelle costruzioni*.
- Davies, J.M. (1998) 'Light gauge steel framing for house constructions', in *Thin Walled Structures, Research and Developments* (eds Shanmugam, N.E., Liew, J.Y.R. and Thevendran, V.), London: Elsevier (Proc. of 2nd International Conference on Thin-Walled Structures, Singapore).
- Davies, J.M. (2000) 'Recent research advances in cold-formed steel structure', *Journal of Constructional Steel Research*, 55.
- Davies, J.M. and Bryan, E.R. (1982) *Manual on Stressed Skin Design*, London: Granada Publishing.
- De Martino, A., Ghersi, A., Landolfo, R. and Mazzolani, F.M. (1991) 'Bending behaviour of long-span steel sheeting: Test and simulation', in *Steel Structures: Recent Research and Developments* (eds Lee, S.L. and Shanmugam, N.E.), London: Elsevier (Proc. of ICSAS '91, Singapore).
- De Martino, A., Ghersi, A., Landolfo, R. and Mazzolani, F.M. (1992) 'Calibration of a bending model for cold-formed sections', Proc. of 11th International Specialty Conference on Cold-Formed Steel Structures, University of Missouri-Rolla.
- De Matteis, G. and Landolfo, R. (1999a) Structural behaviour of sandwich panel shear wall: An experimental analysis, *Material and Structures*, 32.

- De Matteis, G. and Landolfo, R. (1999b) Mechanical fasteners for cladding sandwich panels: Interpretative models for shear behaviour, *Thin-Walled Structures*, 35(1).
- De Matteis, G. and Landolfo, R. (2000a) Modelling of lightweight shear diaphragms for dynamic analysis, *Journal of Constructional Steel Research*, 53.
- De Matteis, G. and Landolfo, R. (2000b) 'Diaphragm action of sandwich panels in pin-jointed steel structures: A seismic study', *Journal of Earthquake Engineering*, 4(3).
- De Matteis, G., Landolfo, R. and Mazzolani, F.M. (1998) 'Dynamic response of infilled multistorey steel frames', in *XI European Conference on Earthquake Engineering* (eds Bisch, P., Labbè, P. and Pecker, A.), Rotterdam: Balkema (Proc. of ECEE '98, Paris).
- Dubina, D. and Vayas, I. (eds) (1995) Proc. of the *Seminar on Eurocode 3—Part 1.3: Cold-formed gauge members and sheeting*, Tempus 4502–94, Timisoara, Romania.
- Dubina, D., Fülöp, L. and Zaharia, R. (1999) 'Floor and wall bracing systems for steel framed houses', in *Stability and Ductility of Steel Structures* (eds Dubina, D. and Ivanyi, M.), London: Elsevier (Proc. of 6th International Colloquium, Timisoara, Romania).
- Dwight, J.B. and Moffin, D.D. (1982) 'Local buckling of aluminium: Preliminary proposal', *ECCS Committee T2 Document*, Cambridge.
- Dwight, J.B. and Moffin, D.S. (1984) 'Buckling of aluminium plates in compression', in *Behaviour of Thin-walled Structures* (eds Rhodes, J. and Spence, J.), London: Elsevier.
- ECCS (1978) *European Recommendations for Aluminium Alloy Structures*.
- ESDEP (1994) *Thin-walled Construction*, European Steel Design Education Programme, Working Group 9.
- Galambos, T. (ed.) (1998) *Guide to Stability Design Criteria for Metal Structures*, New York: John Wiley & Sons.
- Gerard, G. (1957) 'Plastic stability theory of thin shells', *Journal of the Aeronautical Sciences*.
- Gerard, G. (1962) 'Plastic stability theory of geometrically orthotropic plates and cylindrical shells', *Journal of the Aeronautical Sciences*.
- Gerard, G. and Becker, H. (1957) 'Handbook of structural stability. Part 1—Buckling of plates', Technical Note 3781, Natl Advisory Committee for Aeronautics (presently NASA), Washington D.C.
- Ghersi, A. and Landolfo, R. (1992) Innovative aspects of EC3 for the check of cold-formed thin gauge members, *Costruzioni Metalliche*, 5.
- Ghersi, A. and Landolfo, R. (1996) Thin-walled sections in round-house type material: A simulation model, *Costruzioni Metalliche*, 6.
- Ghersi, A., Landolfo, R. and Mazzolani, F.M. (1994) 'Buckling modes of double-channel cold-formed beams', *Thin-Walled Structures*, 19(2–4).
- Giannattasio, G., Pagano, M. and Palumbo, N. (1988) 'Il mattone d'acciaio: Teorie e applicazioni', *Acciaio*, 1.
- Gioncu, V. (1994) 'General theory of coupled instabilities', *Thin-Walled Structures*, 19(2–4).
- Hancock, G.J. (1997) 'Light gauge construction', *Progress in Structural Engineering and Materials*, 1.
- Jombock, J.R. and Clark, J.W. (1968) 'Bending strength of aluminium formed sheet members', *Journal Structural Division ASCE*, 94(ST2).
- Kaehler, R.C. and Seaburg, P.A. (1996) 'A new AISI cold-formed steel design manual', in *13th International Specialty Conference on Cold-formed Steel Design and Construction*, St Louis, Missouri.
- La Boube, R.A., Yu, W.W. and Langon, J.E. et al. (1997) 'Cold-formed steel webs with openings: Summary report', *Thin-walled Structures*, 27(1).
- Landolfo, R. (1992) 'On the bending behaviour of thin-walled cold-formed members and sheeting' (in Italian), Ph.D. Thesis, University of Naples 'Federico II'.
- Landolfo, R. (2000) 'Coupled instabilities in non-linear materials', in *Coupled Instabilities in Metal Structures* (eds Comotim, D., Dubina, D. and Rondal, J.) London: Imperial College Press (Proc. of CISM '2000, Lisbon).

- Landolfo, R. and Mazzolani, F.M. (1990a) 'Behaviour of 3rd generation trapezoidal steel sheetings', in *Testing of Metals for Structures* (ed. Mazzolani, F.M.), London: E. & F.N.Spon, Proc. of *International Workshop 'Needs in Testing Metals' held by RILEM, Naples*.
- Landolfo, R. and Mazzolani, F.M. (1990b) 'Sistemi misti acciaio calcestruzzo con l'impiego di lamiere grecate di terza generazione: Indagine sperimentale, *Acciaio*, 1.
- Landolfo, R. and Mazzolani, F.M. (1994) 'Ultimate behaviour of trapezoidal steel sheets in bending', Proc. of *12th International Specialty Conference on Cold-Formed Steel Structures*, University of Missouri-Rolla.
- Landolfo, R. and Mazzolani, F.M. (1995a) 'Comportamento flessionale di lamiere grecate in acciaio: Analisi sperimentale', *Costruzioni Metalliche*, 1.
- Landolfo, R. and Mazzolani, F.M. (1995b) 'Different approaches in the design of slender aluminium alloy sections', Proc. of *3rd International Conference on Steel and Aluminium Structures, ICSAS '95*, Istanbul.
- Landolfo, R. and Mazzolani, F.M. (1997) Different approaches in the design of slender aluminium alloy sections, *Thin-Walled Structures*, 17(1).
- Landolfo, R. and Mazzolani, F.M. (1998) 'The background of EC9 design curves for slender sections', Volume *In honour of Prof. J.Lindner*, Berlin.
- Landolfo, R., Mazzolani, F.M. and Piluso, V. (1999a) 'Local buckling of aluminium channels: Tests and simulation', in *Stability and Ductility of Steel Structures* (eds Dubina, D. and Ivanyi, M.), London: Elsevier (Proc. of *6th International Colloquium, Timisoara, Romania*).
- Landolfo, R., Piluso, V., Hopperstad, O.S. and Langseth, M. (1999b) 'EC9 provisions for flat internal elements: Comparison with experimental results', in *Light-weight Steel and Aluminium Structures* (eds Mäkeläinen, P. and Hassinen, P.), London: Elsevier (Proc. of *ICSAS '99, Espoo, Finland*).
- Lawson, R.M. and Ogden, R.G. (2001) 'Recent developments in light steel housing in the UK', Proc. of *9th Nordic Steel Construction Conference*, Helsinki.
- Mäkeläinen, P. and Kesti, J. (1999) 'Advanced method for light weight steel joining', *Journal of Constructional Steel Research*, 49.
- Mandara, A. and Mazzolani, F.M. (1995) 'Behavioural aspects and ductility demand of aluminium alloy structures', Proc. of *3rd International Conference on Steel and Aluminium Structures, ICSAS '95*, Istanbul.
- Mazzolani, F.M. (1994) 'Thin-walled metal constructions: Research, design and codification', *50th Anniversary Conference of SSRC*, Lehigh University, Bethlehem.
- Mazzolani, F.M. (1995a) 'Cold-formed thin-walled constructions: Recent developments', in *Steel Structures* (ed. Kounads, A.), Rotterdam: Balkema (Proc. of *EuroSteel '95, Atene*).
- Mazzolani, F.M. (1995b) *Aluminium Alloy Structures*, 2nd edn, London: Chapman & Hall.
- Mazzolani, F.M. and Piluso, V. (1995) 'Prediction of rotation capacity of aluminium alloy beams', Proc. of *3rd International Conference on Steel and Aluminium Structures, ICSAS '95*, Istanbul.
- Mazzolani, F.M., De Matteis, G. and Mandara, A. (1996a) 'Classification system for aluminium alloy connections', Proc. of *IABSE Colloquium on Semi-rigid Structural Connections*, Istanbul.
- Mazzolani, F.M., Faella, C., Piluso, V. and Rizzano, G. (1996b) 'Experimental analysis of aluminium alloy SHS-members subjected to local buckling under uniform compression', Proc. of *5th Int. Colloquium on Structural Stability, SSRC, Brazilian Session*, Rio de Janeiro.
- Mazzolani, F.M., Landolfo, R. and De Matteis, G. (1996c) *Analysis of the Contributing Effect of Building Panels on Steel Structures' Resistance to Seismic and Aeolian Phenomena*, Technical Final Report, ECSC Executive Committee F6 'Steel Structures', Agreement No. 7210-SA/421.
- Mazzolani, F.M., Landolfo, R. and De Matteis, G. (1998) 'Influence of welding on the stability of aluminium thin plates', in *Stability and Ductility of Steel Structures* (eds Usami, T. and Itoh, Y.), London: Pergamon.
- Mazzolani, F.M., Piluso, V. and Rizzano, G. (1997) 'Numerical simulation of aluminium stocky hollow members under uniform compression', Proc. of *5th Int. Colloquium on Stability and Ductility of Steel Structures, SDSS '97*, Nagoya.

- Pearson, C.E. (1950) 'Bifurcation criterion and plastic buckling of plates and shells', *Journal of the Aeronautical Sciences*.
- Pedreschi, R.F., Sinha, B.P. and Davies, R. (1997) 'Advanced connection techniques for cold-formed steel structures', in *Journal of Structural Engineering ASCE*, 123(2).
- Peköz, T. (1987) *Development of a Unified Approach to the Design of Cold-formed Steel Members*, Research Report CF 87-1, American Iron and Steel Institute.
- Radhakrishnan, S. (1956) 'Plastic buckling of circular cylinders', *Journal of the Aeronautical Sciences*.
- Ramberg, W. and Osgood, W.R. (1943) 'Description of stress-strain curves by three parameters', NACA Technical Note 902.
- Rhodes, J. (1992) *Cold Formed Members*, in *Constructional Steel Design: An International Guide*, London: Elsevier.
- Rhodes, J. (ed.) (1990) *Design of Cold-formed Steel Structural Members*, London: Elsevier.
- Rondal, J. (2000) 'Cold-formed steel members and structures—General Report', *Journal of Constructional Steel Research*, 55.
- Schafer, B.W. and Peköz, T. (1998) 'Direct strength prediction of cold-formed steel members using numerical elastic buckling solution', in *Thin-Walled Structures, Research and Developments* (eds Shanmugam, N.E., Liew, J.Y.R. and Thevendran, V.), London: Elsevier (Proc. of 2nd International Conference on Thin-Walled Structures, Singapore).
- Sharp, M.L. (1993) *Behavior and Design of Aluminium Structures*, New York: McGraw-Hill.
- Stowell, E.Z. (1946) 'A unified theory of plastic buckling of columns and plates', Technical Note 1556, Natl Advisory Committee for Aeronautics (presently NASA), Washington, DC.
- Vol' Mir, A.S. (1965) 'Stability of elastic system', Foreign Technology Division, Wright Patterson Air Force Base, Ohio.
- Walker, A.C. (ed.) (1975) *Design and Analysis of Cold-formed Sections*, London: Intertext Books.
- Weingarten, V.I, Morgan, E.J. and Seide, P. (1960) 'Final report of design criteria for elastic stability of thin shell structures', Space Tech. Labs.
- Winter, G. (1949) Light gage steel—A new technique in building construction, *The Cornell Engineer*, 14(6).
- Yu, W.W. (1992) *Cold-formed Steel Design*, New York: John Wiley.
- Yu, W.W., Wolford D.S. and Johnson, A.L. (1996) 'Golden anniversary of the AISI Specification', in *13th International Specialty Conference on Cold-formed Steel Design and Construction*, St Louis, Missouri.

Index

- AISI Specification 75–76
 - buckling resistance
 - under axial compression 90–91
 - under axial compression and bending 91–93
 - local buckling 80–81
 - uniformly compressed elements with an edge stiffener 84–85
 - uniformly compressed elements with one intermediate stiffener 83–84
 - uniformly compressed unstiffened/ stiffened elements 81–82
 - unstiffened elements and edge stiffened with stress gradient 82
 - webs/stiffened elements with stress gradient 82
 - material properties 76–79
 - resistance of cross-sections 85
 - axial compression and bending 89
 - axial tension and bending 88–89
 - shear force and bending moment 89–90
 - under axial compression 86
 - under axial tension 85
 - under bending moment 86
 - under shear 87
 - section properties 77
- Aluminium structures, *see* Eurocode 9
- Applications of cold-formed members 12–19

- BS 8118 (British Standards code) 95

- CNR 10022 (Italian code) 94
- Code comparison 94
 - application of different methodologies 116
 - comparison of methodologies 118–122
 - design methodologies 116–118
 - for beam columns 114–116
 - for members in bending 98–99
 - local buckling 99–103
 - overall buckling 103–104
 - serviceability limit state 104–108
 - for members in compression 105
 - local buckling 105, 109–112
 - overall buckling 112–114
 - for uniform stress distribution 95–98
- ColdForm computer program 123–150
- Critical stress (Euler formula) 22
 - see also* Structural analysis

Cross-sectional properties 10–11

Effects of cold-forming 8

geometrical imperfections 9–10

residual stresses 8

strain-hardening effect 8–10

Eurocode 3 39

buckling resistance 55

bending and axial compression 57

flexural buckling 55–56

cross-section classification 39

see also Limit states

compact 39

ductile 39

semi-compact 39

slender 39

local buckling 43–44

plane elements with edge stiffeners 47–50

plane elements without stiffeners 44–47

Material properties 40–41

Part 1.1 40

Part 1.3 40

resistance of cross-sections 50

axial force and bending 54

shear force and bending 55

under axial compression 50

under axial tension 50

under bending moment 51–53

under shear 53–54

section properties 41–43

Eurocode 9 58–59

buckling resistance 73

bending and axial compression 73–74

flexural buckling 73

cross-section classification, *see* Eurocode 3

curved internal element 59

flat internal element 59

flat outstand element 59

element classification 61–62

local buckling 63–64

plane elements with intermediate stiffeners 65–68

plane elements without stiffeners 65

material properties 61–63

resistance of cross-sections 68

axial force and bending 71–72

shear force and bending 72

under axial compression 68–69

under axial tension 68

under bending moment 69–70

under shear 70–71

section properties 62–63

slenderness of reinforced flat elements 61
slenderness of unreinforced flat elements 59–61

Limit states 20
collapse 20
elastic 20
elastic buckling 20
plastic 20

Manufacture methods 5
cold rolling 5–6
comparative costs 7
press-braking 6–7

Materials 7
aluminium alloys 7–8
galvanized steels 7
mechanical properties 7
zinc protection 7

Sheeting 3
trapezoidal stiffened longitudinally 3
trapezoidal stiffened longitudinally/ transversally 4
trapezoidal without stiffeners 3

Steel structures, *see* Eurocode 3

Structural analysis 20–21
aluminium plate buckling 26–38
linear theory 21
non-linear analysis 21
steel plate buckling 22–23, 25

Structural behaviour 5
factors influencing 5

Structural members 3

CD-ROM Single-User Licence Agreement

We welcome you as a user of this Spon Press CD-ROM and hope that you find it a useful and valuable tool. Please read this document carefully. This is a legal agreement between you (hereinafter referred to as the 'Licensee') and Taylor and Francis Books Ltd., under the imprint of Spon Press (the 'Publisher'), which defines the terms under which you may use the Product. By breaking the seal and opening the package containing the CD-ROM you agree to these terms and conditions outlined herein. If you do not agree to these terms you must return the Product to your supplier intact, with the seal on the CD case unbroken.

1. Definition of the Product

The product which is the subject of this Agreement, *Cold Form software and worked examples on CD-ROM* (the 'Product') consists of:

- 1.1 Underlying data comprised in the product (the 'Data')
- 1.2 A compilation of the Data (the 'Database')
- 1.3 Software (the 'Software') for accessing and using the Database
- 1.4 A CD-ROM disk (the 'CD-ROM')

2. Commencement and licence

- 2.1 This Agreement commences upon the breaking open of the package containing the CD-ROM by the Licensee (the 'Commencement Date').
- 2.2 This is a licence agreement (the 'Agreement') for the use of the Product by the Licensee, and not an agreement for sale.
- 2.3 The Publisher licenses the Licensee on a non-exclusive and non-transferable basis to use the Product on condition that the Licensee complies with this Agreement. The Licensee acknowledges that it is only permitted to use the Product in accordance with this Agreement.

3. Installation and Use

- 3.1 The Licensee may provide access to the Product for individual study in the following manner: The Licensee may install the Product on a secure local area network on a single site for use by one user.
- 3.2 The Licensee shall be responsible for installing the Product and for the effectiveness of such installation.

4. Permitted Activities

4.1 The Licensee shall be entitled:

- 4.1.1 to use the Product for its own internal purposes;
- 4.1.2 to download onto electronic, magnetic, optical or similar storage medium reasonable portions of the Database provided that the purpose of the Licensee is to undertake internal research or study and provided that such storage is temporary;
- 4.1.3 to make a copy of the Database and/or the Software for backup/archival/disaster recovery purposes.

4.2 The Licensee acknowledges that its rights to use the Product are strictly set out in this Agreement, and all other uses (whether expressly mentioned in Clause 5 below or not) are prohibited.

5. Prohibited Activities

The following are prohibited without the express permission of the Publisher:

- 5.1 The commercial exploitation of any part of the Product.
- 5.2 The rental, loan, (free or for money or money's worth) or hire purchase of this product, save with the express consent of the Publisher.
- 5.3 Any activity which raises the reasonable prospect of impeding the Publisher's ability or opportunities to market the Product.
- 5.4 Any networking, physical or electronic distribution or dissemination of the product save as expressly permitted by this Agreement.
- 5.5 Any reverse engineering, decompilation, disassembly or other alteration of the Product save in accordance with applicable national laws.
- 5.6 The right to create any derivative product or service from the Product save as expressly provided for in this Agreement.
- 5.7 Any alteration, amendment, modification or deletion from the Product, whether for the purposes of error correction or otherwise.

6. General Responsibilities of the License

- 6.1 The Licensee will take all reasonable steps to ensure that the Product is used in accordance with the terms and conditions of this Agreement.
- 6.2 The Licensee acknowledges that damages may not be a sufficient remedy for the Publisher in the event of breach of this Agreement by the Licensee, and that an injunction may be appropriate.
- 6.3 The Licensee undertakes to keep the Product safe and to use its best endeavours to ensure that the product does not fall into the hands of third parties, whether as a result of theft or otherwise.
- 6.4 Where information of a confidential nature relating to the product of the business affairs of the Publisher comes into the possession of the Licensee pursuant to this Agreement (or otherwise), the Licensee agrees to use such information solely for the purposes of this Agreement, and under no circumstances to disclose any element of the information to any third party save strictly as permitted under this Agreement. For

the avoidance of doubt, the Licensee's obligations under this sub-clause 6.4 shall survive the termination of this Agreement.

7. Warrant and Liability

- 7.1 The Publisher warrants that it has the authority to enter into this agreement and the Authors warrant that they have secured all rights and permissions necessary to enable the Licensee to use the Product in accordance with this Agreement.
- 7.2 The Publisher and the Licensee acknowledge that the Publisher supplies the Product on an 'as is' basis. The Publisher gives no warranties:
- 7.2.1 that the Product satisfies the individual requirements of the Licensee; or
 - 7.2.2 that the Product is otherwise fit for the Licensee's purpose; or
 - 7.2.3 that the Data are accurate or complete or free of errors or omissions; or
 - 7.2.4 that the Product is compatible with the Licensee's hardware equipment and software operating environment.
- 7.3 The Publisher hereby disclaims all warranties and conditions, express or implied, which are not stated above.
- 7.4 Nothing in this Clause 7 limits the Publisher's liability to the Licensee in the event of death or personal injury resulting from the Publisher's negligence.
- 7.5 The Publisher hereby excludes liability for loss of revenue, reputation, business, profits, or for indirect or consequential losses, irrespective of whether the Publisher was advised by the Licensee of the potential of such losses.
- 7.6 The Licensee acknowledges the merit of independently verifying Data prior to taking any decisions of material significance (commercial or otherwise) based on such data. It is agreed that the Publisher shall not be liable for any losses which result from the Licensee placing reliance on the Data or on the Database, under any circumstances.
- 7.7 Subject to sub-clause 7.4 above, the Publisher's liability under this Agreement shall be limited to the purchase price.

8. Intellectual Property Rights

- 8.1 Nothing in this Agreement affects the ownership of copyright or other intellectual property rights in the Data, the Database of the Software.
- 8.2 The Licensee agrees to display the Authors copyright notice in the manner described in the Product.
- 8.3 The Licensee hereby agrees to abide by copyright and similar notice requirements required by the Authors, details of which are as follows: '© 2002 A.Gherzi, R.Landolfo, F.M.Mazzolani. All rights reserved. All materials in *ColdForm software and worked examples on CD-ROM* are copyright protected. No such materials may be used, displayed, modified, adapted, distributed, transmitted, transferred, published or otherwise reproduced in any form or by any means now or hereafter developed other than strictly in accordance with the terms of the licence agreement enclosed with the CD-ROM. However, text and images may be printed and copied for research and private study within the preset program limitations. Please note the copyright notice above, and that any text or images printed or copied must credit the source.'

8.4 This Product contains material proprietary to and copyedited by the Publisher, Authors and others. Except for the licence granted herein, all rights, title and interest in the Product, in all languages, formats and media throughout the world, including copyrights therein, are and remain the property of the Publisher or other copyright holders identified in the Product.

9. Non-assignment

This Agreement and the licence contained within it may not be assigned to any other person or entity without the written consent of the Publisher.

10. Termination and Consequences of Termination

10.1 The Publisher shall have the right to terminate this Agreement if:

- 10.1.1 the Licensee is in material breach of this Agreement and fails to remedy such breach (where capable of remedy) within 14 days of a written notice from the Publisher requiring it to do so; or
- 10.1.2 the Licensee becomes insolvent, becomes subject to receivership, liquidation or similar external administration; or
- 10.1.3 the Licensee ceases to operate in business.

10.2 The Licensee shall have the right to terminate this Agreement for any reason upon two month's written notice. The Licensee shall not be entitled to any refund for payments made under this Agreement prior to termination under this sub-clause 10.2.

10.3 Termination by either of the parties is without prejudice to any other rights or remedies under the general law to which they may be entitled, or which survive such termination (including rights of the Publisher under sub-clause 6.4 above).

10.4 Upon termination of this Agreement, or expiry of its terms, the Licensee must:

- 10.4.1 destroy all back up copies of the product; and
- 10.4.2 return the Product to the Publisher.

11. General

11.1 Compliance with export provisions

The Publisher hereby agrees to comply fully with all relevant export laws and regulations of the United Kingdom to ensure that the Product is not exported, directly or indirectly, in violation of English law.

11.2 Force majeure

The parties accept no responsibility for breaches of this Agreement occurring as a result of circumstances beyond their control.

11.3 No waiver

Any failure or delay by either party to exercise or enforce any right conferred by this Agreement shall not be deemed to be a waiver of such right.

11.4 Entire agreement

This Agreement represents the entire agreement between the Publisher and the Licensee concerning the Product. The terms of this Agreement supersede all prior purchase orders, written terms and conditions, written or verbal representations, advertising or statements relating in any way to the Product.

11.5 Severability

If any provision of this Agreement is found to be invalid or unenforceable by a court of law of competent jurisdiction, such a finding shall not affect the other provisions of this Agreement and all provisions of this Agreement unaffected by such a finding shall remain in full force and effect.

11.6 Variations

This agreement may only be varied in writing by means of variation signed in writing by both parties.

11.7 Notices

All notices to be delivered to: aghersi@dica.unict.it

11.8 Governing law

This Agreement is governed by English law and the parties hereby agree that any dispute arising under this Agreement shall be subject to the jurisdiction of the English courts.

CD-ROM Information

Minimum System Requirements for PCs

Pentium Processor Windows 95 or later operating system (Designed for Windows 95/98/Me and Windows NT/2000)

16MB of RAM

10MB of available hard disk space

CD-ROM drive

Mouse

Double-click on *Startup.htm* to start and follow on-screen instructions.